The Late Inhibition of IκB Kinase Attenuates Acute Kidney Injury and the Subsequent Development of Renal Fibrosis in Animal Models of Ischaemia-Reperfusion Injury and Unilateral Ureteral Obstruction

A thesis presented by

Florence Lilian Johnson

Registered at

Barts and the London School of Medicine and Dentistry

Queen Mary University of London

For the degree of

Doctor of Philosophy

Translational Medicine and Therapeutics

The William Harvey Research Institute

John Vane Science Centre

Charterhouse Square

London

EC1M 6BQ

Statement of Originality

I, Florence Lilian Johnson, confirm that the research included within this thesis is my own work or that where it has been carried out in collaboration with, or supported by others, that this is duly acknowledged below and my contribution indicated. Previously published material is also acknowledged below.

I attest that I have exercised reasonable care to ensure that the work is original, and does not to the best of my knowledge break any UK law, infringe any third party's copyright or other Intellectual Property Right, or contain any confidential material.

I accept that the College has the right to use plagiarism detection software to check the electronic version of the thesis.

I confirm that this thesis has not been previously submitted for the award of a degree by this or any other university.

Signature:

Date: 12/04/2016

Details of Collaboration: Collaboration with Prof Massimo Collino and Fausto Chiazza, who kindly performed the western blots in chapter II of this thesis, and for assisting me with the blots in chapters III and IV. Guillaume Hache who helped me with the formulation of the correlation data in chapter III. George Elia and Emily Austin for the wax blocking and section cutting of my samples.

For Martin and Linda

Abstract

Acute kidney injury (AKI) is a major risk factor for chronic kidney disease (CKD). For patients who recover from AKI, there is a 25% increase in the risk of CKD, and a mortality rate of up to 50% after 10 years. Nuclear factor kappa-B (NF-κB) is a family of transcription factors that regulates the transcription of many proteins that play a key role in inflammation. Inhibitor of IκB kinase (IKK) is directly upstream of NF-κB. My aim was to investigate a) the role of IKK in the progression of AKI to CKD, and b) whether its inhibition attenuates renal fibrosis. In this thesis I used a model of unilateral renal ischaemia-reperfusion injury with contralateral nephrectomy, to firstly map the acute time course of AKI. From the data generated from the time course, I decided to treat the animals at 24 h post reperfusion with the IKK inhibitor, IKK16, as i) this was at the peak of renal dysfunction (24 h post reperfusion), and ii) prior to the activation of NF-κB (48 h post reperfusion). The inhibition of IKK at 24 hours post reperfusion, as a delayed treatment, successfully attenuated renal dysfunction, NF-κB activation and renal structural damage. I subsequently increased the recovery time after ischaemia-reperfusion in my rat model to 28 days to study the development of fibrosis post AKI. The inhibition of IKK at 24 hours post reperfusion successfully attenuated the development of fibrosis, formation of myofibroblasts, macrophage infiltration, the expression of pro-fibrotic markers and the deposition of extracellular matrix components at 28 days post reperfusion.

In addition, the delayed inhibition of IKK at days 7-13 post unilateral ureteral obstruction in a rat model, successfully attenuated the development of fibrosis, formation of myofibroblasts, macrophage infiltration, the expression of pro-fibrotic markers and the deposition of extracellular matrix components. These data indicate that the activation of the IKK complex drives tubulointerstitial fibrosis, and suggests that the inhibition of IKK could be a useful pharmacological tool for the creation of therapies to combat AKI and the subsequent development of fibrosis, via the reduction of both inflammation and the prevention of the expression of pro-fibrotic markers.

Acknowledgements

Firstly, thank you to the British Pharmacological Society for funding my PhD via the AJ Clarke studentship, I am eternally grateful. I would like to express sincere gratitude to Professor Christoph Thiemermann for the opportunities presented to me during both my extra-mural year and my PhD at the William Harvey Research Institute. I have had a fulfilling, interesting experience at the WHRI and I have Prof Thiemermann to thank for the resources and supervision I have received. Secondly, a massive thank you to Dr. Nimesh Patel, who has been such an encouraging mentor and has taught me a great deal, I wish you all the best in your future Nim. Thanks also to Prof Massimo Collino and Fausto Chiazza, who have taught me everything I know about western blots (but more about gelato!), my trip to your lab in Turin was so special. G – thank you for your enthusiasm, help with the correlation graphs and open mic nights! I would also like to thank George Elia and Emily Austin from BCI pathology for your patience whilst endless wax blocking and section cutting. Special mentions to the terrible trio (and their endless larries), Jianmin for her friendship and her special talent of certificate losing (!), Gareth for being Gareth and being the best drinking buddy and confidant a girl could ask for, and Will for beatboxing swag and lotus biscuit pranks. To the team at TMT: thank you every single one of you. Gareth, Jianmin, Rachel, Regina, Amy, Will, Vicky, G, Noriaki, Kiran, Sura, Lukas, it has been so much fun because of you guys.

Finally, thank you Dad, Mum, Peter, Henry and Cameron: for listening, encouraging and supporting me throughout my PhD. It would not have been possible without your constant love and laughter.

Publications

The following abstracts and papers have been submitted in support of this thesis:

Abstracts

1. **Johnson FL**, Patel NSA, Chiazza F, Sordi R, Collino M, Yaqoob MM, Thiemermann C. The Late Inhibition of Inhibitor of IκB Kinase Attenuates Acute Kidney Injury and the Subsequent Development of Fibrosis in a Rat Model of Ischaemia-Reperfusion Injury. Oral presentation at the William Harvey Annual Research Review, London, UK (June 2015)

2. **Johnson FL**, Patel NSA, Chiazza F, Sordi R, Collino M, Yaqoob MM, Thiemermann C. The Late Inhibition of Inhibitor of IκB Kinase Attenuates Acute Kidney Injury and the Subsequent Development of Fibrosis in a Rat Model of Ischaemia-Reperfusion Injury. Poster presentation at the XVI. Congress of The European Shock Society, Cologne, Germany (September 2015)

3. **Johnson FL**, Patel NSA, Chiazza F, Sordi R, Collino M, Yaqoob MM, Thiemermann C. The Late Inhibition of Inhibitor of IκB Kinase Attenuates Acute Kidney Injury and the Subsequent Development of Fibrosis in a Rat Model of Ischaemia-Reperfusion Injury. Poster presentation at Kidney Week 2015, The American Society of Nephrology, San Diego, California (November 2015)

4. **Johnson FL**, Patel NSA, Chiazza F, Sordi R, Collino M, Yaqoob MM, Thiemermann C. The Late Inhibition of Inhibitor of IκB Kinase Attenuates Acute Kidney Injury and the Subsequent Development of Fibrosis in a Rat Model of Ischaemia-Reperfusion Injury. Oral presentation at Pharmacology 2015, The British Pharmacological Society, London, UK (December 2015)

5. **Johnson FL**, Patel NSA, Chiazza F, Sordi R, Collino M, Yaqoob MM, Thiemermann C. The Late Inhibition of Inhibitor of IκB Kinase Attenuates Acute Kidney Injury and the Subsequent Development of Fibrosis in Animal Models of Acute Kidney Injury and Fibrosis. Oral presentation at The William Harvey New Year Review, London, UK (December 2016), and winner of the best PhD presentation: £250 travel award.

Full Papers

1. **Johnson FL**, Patel NSA, Collino M, Chiazza F, Sordi R, Yaqoob MM, Thiemermann C. The Late Inhibition of Inhibitor of IκB Kinase Attenuates Acute Kidney Injury and the Subsequent Development of Fibrosis. Submitted to *Scientific Reports*

The following papers have been published during the course of my PhD:

1. Patel NSA, Kerr-Peterson HL, Brines M, Collino M, Rogazzo M, Fantozzi R, Wood EG, **Johnson FL**, Yaqoob MM, Cerami A, Thiemermann C: Delayed Administration of Pyroglutamate Helix B Surface Peptide, a Novel Non-Erythropoietic Analogue of Erythropoietin, Attenuates Acute Kidney Injury (2012) *Molecular Medicine* **18**: 719-727

2. Sordi R, Chiazza F, **Johnson FL**, Patel NSA, Brohi K, Collino M, Thiemermann C: Inhibition of IκB Kinase Attenuates the Organ Injury and Dysfunction Associated with Hemorrhagic Shock (2015) *Molecular Medicine* **21(1)** 563-575

3. Sordi R, Nandra KK, Chiazza F, **Johnson FL**, Cabrera CP, Torrance HD, Patel NSA, Barnes MR, Brohi K, Collino M, Thiemermann C: Artesunate Protects Against the Organ Injury and Dysfunction Induced by Severe Hemorrhage and Resuscitation (2015) *Annals of Surgery* {EPub ahead of print)

Contents

Page

Abbreviations

AAN	aristolochic acid nephropathy
ACE	angiotensin converting enzyme
Ach	acetylcholine
AKI	acute kidney injury
AKIN	acute kidney injury network
ARF	acute renal failure
ATN	acute tubular necrosis
ATP	adenosine triphosphate
BAFF	B-cell activating factor
BCA	bicinchoninic assay
BH4	tetrahydrobiopterin
b.i.d.	bis in die (twice daily)
BLC	B lymphocyte chemoattractant
Ca^{2+}	calcium
CD11b	cluster of differentiation molecule 11B
CKD	chronic kidney disease
Cl^-	chloride
CMJ	corticomedullary junction
cNOS	constitutive nitric oxide synthase
COX	cyclooxygenase
Cr	creatinine
CTGF	connective tissue growth factor
DMSO	dimethyl sulfoxide
eCCL	estimated creatinine clearance
ECL	enhanced chemiluminescence
ECM	extracellular matrix
EMT	epithelial-mesenchymal transition
EndoMT	endothelial-mesenchymal transition
eNOS	endothelial nitric oxide synthase
EPO	erythropoietin
ESRD	end-stage renal disease
FAD	flavin adenine dinucleotide

Fe^{2+}	iron
FE_{Na+}	fractional excretion of sodium
FGF	fibroblast growth factor
FMN	flavin mononucleotide
GADPH	glyceraldehyde 3-phosphate dehydrogenase
GFR	glomerular filtration rate
H^+	proton
H_2O_2	hydrogen peroxide
H&E	haematoxylin and eosin
Hsp90	heat shock protein 90
i.p.	intraperitoneally
i.v.	intravenously
IRI	ischaemia-reperfusion injury
IC_{50}	the half maximal inhibitory concentration
ICAM	intercellular adhesion molecule
IKK	IκB kinase
IL-	interleukin
iNOS	inducible nitric oxide synthase
JNK	c-Jun N-terminal kinase
K^+	potassium
KIM-1	kidney injury molecule-1
LAP	latency associated peptide
LPS	lipopolysaccharide
MCP-1	monocyte chemoattractant protein-1
MRI	magnetic resonance imaging
Na^+	sodium
NaCl	sodium chloride
NADP+	nicotinamide adenine dinucleotide phosphate
NADPH	nicotinamide adenine dinucleotide phosphate-oxidase
NEMO	nuclear factor kappa-B essential modulator
NF-κB	nuclear factor kappa-B
NGAL	neutrophil gelatinase-associated lipocalin
nNOS	neuronal nitric oxide synthase
NO	nitric oxide

NSAIDs	non-steroidal anti-inflammatory drugs
OD	optical density
$^{\bullet}$OH	hydroxyl radical
O_2	oxygen
$O_2^{\bullet-}$	superoxide radical
p.o.	per os (by mouth)
PBS	phosphate buffered saline
PDGF	platelet derived growth factor
PDTC	pyrrolidine dithiocarbamate
pO_2	partial pressure of oxygen
PPAR-γ	peroxisome proliferator-activated receptor-γ
q.a.d.	quaque altera die (every other day)
RIFLE	risk, injury, failure, loss, end-stage kidney disease
ROS	reactive oxygen species
RRT	renal replacement therapy
RVR	renal vascular resistance
s.c.	subcutaneously
SCr	serum creatinine
SDS-PAGE	sodium dodecyl sulphate polyacrylamide gel electrophoresis
SEM	standard error of the mean
Ser	serine
siRNA	small interfering ribonucleic acid
SLC	secondary lymphoid-tissue chemokine
SOD	superoxide dismutase
TGF-β	transforming growth factor-beta
Thr	threonine
TIMP	tissue inhibitor of metalloproteinases
TLR	toll-like receptor
TNF-α	tumour necrosis factor-alpha
UO	urine output
UUO	unilateral ureteral obstruction
VCAM	vascular cell adhesion protein
VEGF	vascular endothelial growth factor
α-SMA	alpha-smooth muscle actin

Units

C	Celsius
dl	decilitre
g	gram
g	gravitational acceleration
h	hours
kDa	kilodalton
kg	kilogram
L	litre
m	metre
mg	milligram
min	minute
ml	millilitre
mM	millimolar
mmol	millimole
v/v	volume/volume percent
µM	micromolar
µmol	micromoles

Chapter I

General Introduction

The Basic Structure and Function of the Kidney

The kidneys are vital organs, performing multiple functions necessary for life. Located at the rear of the abdominal space, the kidneys are positioned either side of the vertebral column. The main function of the kidney is excreting metabolic waste products such as urea, uric acid and creatinine (Rang et al., 2007), alongside maintaining sodium (Na^+), electrolyte levels, extracellular fluid volume and regulating the acid-base balance of the blood (Widmaier et al., 2007). In addition to these homeostatic roles, the kidneys produce the hormones erythropoietin (EPO), renin and vitamin D. The basic structure of both the kidney and its functional unit, the nephron, are shown in Figure 1.1.

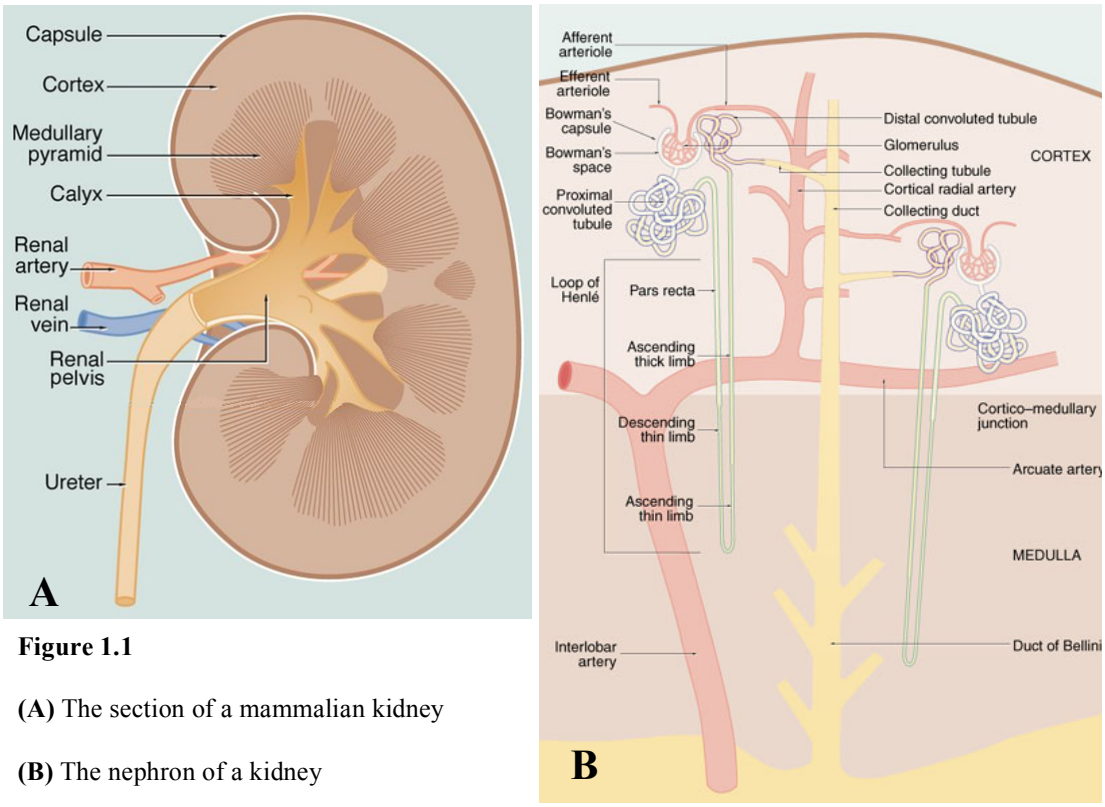

Figure 1.1

(A) The section of a mammalian kidney

(B) The nephron of a kidney

Adapted from Young and Heath (2000)

The nephron consists of two distinct sections; the first, named the renal corpuscle, consists of the Bowman's capsule and the glomerulus, and is responsible for the filtration of the plasma (Figure 1.1B). The kidneys receive approximately 20% of the total cardiac output, which arrives at the renal corpuscle via the afferent arteriole, feeding into the glomerular capillaries. The high hydrostatic pressure created by the small diameter of the efferent arteriole causes ultrafiltration: the movement of small molecules such as water, amino acids, glucose, urea and sodium chloride (NaCl) from the blood into the Bowman's capsule. This is called the filtrate, and is practically isotonic to the plasma (Widmaier et al., 2007). Larger molecules such as cells and proteins remain in the blood. The remainder of the blood (approximately 80%) then re-enters the circulation from the glomerulus via the efferent arteriole (Rang et al., 2007).

From here, the filtrate then enters the second section of the nephron, the renal tubule. This section spans from the proximal convoluted tubule through to the collecting duct (Figure 1.1B) and it is here the filtrate is concentrated and finally excreted. The proximal tubule is divided into two portions – convoluted and straight, and from this is further subdivided into three further portions – S1, S2 and S3. S1 is present only in the convoluted portion, S2 is present in both convoluted and straight portions, and S3 in only the straight portion of the proximal tubule (Boron and Boulpaep, 2008). When the filtrate enters the proximal tubule, approximately two thirds of the NaCl in the tubular fluid is reabsorbed through Na^+ transporters (Atthe et al., 2009). From here, the remainder of the fluid moves into the loop of Henlé; consisting of the *pars recta*, the descending thin limb, the ascending thin limb and the ascending thick limb. The high osmolality generated in loop of Henlé causes the reabsorption of water. On passing through the loop of

Henlé the fluid passes into the distal convoluted tubule, and then to the collecting duct system, which empties out into the renal pelvis. From here the now concentrated fluid, or urine, passes through the ureter and into the bladder, ready for excretion.

Measurement of Renal Function

Accurate measurement of renal function is paramount in both clinical and research settings. Renal function is measured by the glomerular filtration rate (GFR); described as the volume of fluid filtered from the glomerular capillaries into the Bowman's capsule per unit time (Widmaier et al., 2007). An individual's GFR is dependent on a multitude of factors, including age, race, body size and gender, and, therefore, no universal figure for a 'normal' GFR exists. However, the National Kidney Foundation Guidelines suggest that without kidney damage or any other underlying disease, the GFR of a healthy young adult is around $\geq$90mL/min/1.73m^2 (K/DOQI 2002). GFR is most accurately measured by the infusion of inulin, a polymer of fructose commonly found in plants. Inulin is an exogenous compound that is freely filtered and is neither secreted nor reabsorbed by the renal tubules, nor metabolised, so is the 'ideal compound' to measure the GFR. Despite this, inulin is seldom used to measure GFR in the clinical setting, as i) it is expensive to purify, ii) it is difficult to measure iii) its measurement is invasive to the patient and iv) its measurement is time consuming (Traynor et al., 2006).

More commonly, creatinine is used clinically to measure renal function. Creatinine is an endogenous compound generated from the metabolism of the skeletal muscle

component creatine. Inulin and creatinine are both filtered at the glomerulus and do not undergo tubular reabsorption; but unlike inulin, creatinine undergoes a small amount of secretion (Widmaier et al., 2007). This proximal tubular secretion of creatinine causes the creatinine clearance (an indicator of glomerular function) to overestimate the GFR, but is close enough for clinical diagnosis (Traynor et al., 2006). Despite this, the collection of urine over a period of hours is inconvenient to the patient, and this method may yield unreliable results. The estimated creatinine clearance is calculated as follows:

$$\text{Estimated Creatinine Clearance (ml/min)} = \frac{\text{Urine Creatinine (µmol/L) x Urine Flow (ml/min)}}{\text{Serum Creatinine (µmol/L)}}$$

The fractional excretion of Na^+ ($FENa^+$) is also used to measure renal function, and is defined as the percentage of the Na^+ filtered by the kidney that is excreted. This is a highly efficient system, as only 0.4% of total Na^+ filtered into the nephron is excreted in the urine (Boron and Boulpaep, 2008). 65% of Na^+ is reabsorbed in the proximal tubule, initially by passive diffusion via the Na^+/H^+ antiporter and Na^+ co-transporters (such as the Na^+/Glucose transporter). 25% of Na^+ is reabsorbed in the thick ascending limb of the loop of Henlé via the Na^+/H antiporter and the $Na^+K^+2Cl^-$ symporter, against its concentration gradient. Finally, the distal convoluted tubule is responsible for 5% of Na^+ reabsorption by NaCl symporters, and the remaining 3% of Na^+ is absorbed by the Na^+ transporting cells in the medullary collecting ducts (Boron and Boulpaep, 2008). $FENa^+$ is, therefore, an indicator of tubular function and is calculated as follows:

$$\text{Fractional Excretion of Sodium (\%)} = \frac{\text{Urine Sodium (mmol/L)} \div \text{Serum Sodium (mmol/L)}}{\text{Urine Creatinine (µmol/L)} \div \text{Serum Creatinine (µmol/L)}}$$

Renal Failure

Renal failure is defined as the loss of renal function, where the kidneys are no longer able to effectively filter the blood of waste products. Acute kidney injury (AKI) and chronic kidney disease (CKD) are both manifestations of renal failure, formerly known as acute renal failure and chronic renal failure, respectively. Both AKI and CKD clinically present with a decrease in GFR and an increase in serum creatinine (SCr) concentration, albeit over different time frames. The causes and development of each disease are very different, and will be discussed subsequently.

Severe AKI and CKD both lead to end stage renal disease (ESRD), which is defined as a GFR of <15ml/min/1.73m^2 (K/DOQI 2002). Patients with ESRD possess suboptimal kidney function due to irreversible, permanent damage to the kidneys, and will require renal replacement therapies (RRT) to survive. Current RRTs include haemodialysis, peritoneal dialysis and renal transplantation.

AKI and CKD may affect people at any time, however incidence increases proportionally with increasing age, with both AKI and CKD notably prevalent in the elderly (Winearls and Glassock, 2011). Currently both the average age of the population and life expectancies in developed countries are increasing, meaning RRTs are far more in demand than they were ten years ago. From 2001 to 2010, the number of patients receiving dialysis increased from 30,000 to 50,000 in the UK alone (Steenkamp et al., 2011). Currently, 90% of total patients on the organ register are waiting for a kidney (this is roughly 6000 people): the waiting time is around 1000 days (UK Renal Association, 2015), and in this time many patients die, even those receiving dialysis.

The exponential increase in patient numbers for RRTs is an ever-increasing burden on the National Health Service, due to the expense, length, and poor success rates of these treatments. This is a major reason why further pre-clinical and clinical studies investigating the mechanisms of these diseases, and the development of new therapeutic strategies, are vital.

Acute Kidney Injury

AKI is defined by the acute kidney injury network (AKIN) as 'an abrupt (within 48 h) reduction in kidney function currently defined as an absolute increase in SCr of more than or equal to 0.3 mg/dl (≥ 26.4 μmol/l), a percentage increase in SCr of more than or equal to 50% (1.5-fold from baseline), or a reduction in urine output (documented oliguria of less than 0.5 ml/kg per h for more than 6 h)' (Mehta et al., 2007).

Approximately 5-7% of hospitalised patients present with AKI, and of this 5-7%, a further 60% will never regain full renal function (Uchino, 2006). On the intensive care unit, AKI is associated with a mortality rate of >50% (Ali et al., 2007), due to the development of ESRD (Uchino, 2006). AKI can occur secondary to clinical conditions such as sepsis (the most common cause of AKI), trauma/haemorrhage and from contrast agents (used in medical imaging e.g. magnetic resonance imaging (MRI)). AKI may also occur following cardiac bypass surgery or during warm ischaemic time before kidney transplantation (Thiele et al., 2015) (Nakamura et al., 2012).

AKI has 3 major aetiologies:

1. Pre-renal azotaemia is the most common cause of AKI, characterised by reduced blood flow to the kidney due to low circulating blood volume, subsequently causing a decrease in GFR (e.g. sepsis, haemorrhage, congestive heart failure). Sufficient renal perfusion is required for the maintenance of a regular GFR. Pre-renal azotaemia can be volume responsive or volume non-responsive, in which the addition of i.v. fluids may or may not restore kidney perfusion (Sharfuddin and Molitoris, 2011).

2. Post-renal azotaemia is caused by urinary obstruction e.g. kidney stones, catheters. Due to compensation of renal function from contralateral kidneys, significant renal failure will only occur if both kidneys are obstructed.

3. Intrinsic azotaemia is caused by intrinsic damage to the kidney, and may affect one or more of the four structures of the kidney:

- Tubules: Acute tubular necrosis (ATN) is a frequent cause of AKI, characterised by the death of epithelial cells that compose the tubules of the kidney. ATN may be caused by ischaemia or nephrotoxicity, causing an acute, usually reversible, loss of renal function (Nath and Norby, 2000). ATN occurs in three main stages, the initial, maintenance and recovery stages, which will be discussed in further detail later in the chapter.

- Glomeruli: AKI may occur from acute glomerulonephritis, an inflammatory condition of the glomerulus, which may present as a primary disease or secondary to a systemic disease, such as systemic lupus erythematosus (Nowling and Gilkeson, 2011).

- Vascular system: Poor perfusion and a reduction in GFR from injury to renal vessels and capillaries may also cause AKI. This type of AKI is seen in severe cases of hypertension (roughly 1% of patients with hypertension) among various other conditions (Khanna and McCullough, 2003).

- Interstitium: Acute interstitial nephritis may also cause AKI, from damage to the interstitial tissue. This is caused by bacterial or viral infections, or more commonly, allergies to certain antibiotics such as penicillin (Perazella and Markowitz, 2010).

All three aetiologies of AKI lead to a reduction in effective perfusion to the kidney (Sharfuddin and Molitoris, 2011). Patients with AKI present with low GFR, a high $FENa^{+}$, and oliguria (reduced urine output) (Atthe et al., 2009). Due to the reduction in GFR, the kidneys become unable to effectively filter blood of waste products, resulting in increased SCr and serum urea concentrations, and a consequent decrease in the urine creatinine concentration.

Previously, AKI was classified by using the RIFLE criteria (Figure 1.2) abbreviated from Risk, Injury, Failure, Loss and End-stage Renal Disease: a method of clinical diagnosis depicting stages of AKI. The RIFLE classification relies on the delayed increase in SCr, at which point irreversible damage to the kidney may have already occurred (Van Biesen et al., 2006). This classification was, however, modified in 2007, and AKI is now classified by the AKIN criteria. This criterion was devised without the 'loss' and 'end-stage' seen in the RIFLE classification, as these two stages are now deemed an outcome of AKI rather than a diagnosis. The AKIN is grouped into three stages, the third stage incorporating patients with RRT (Figure 1.2).

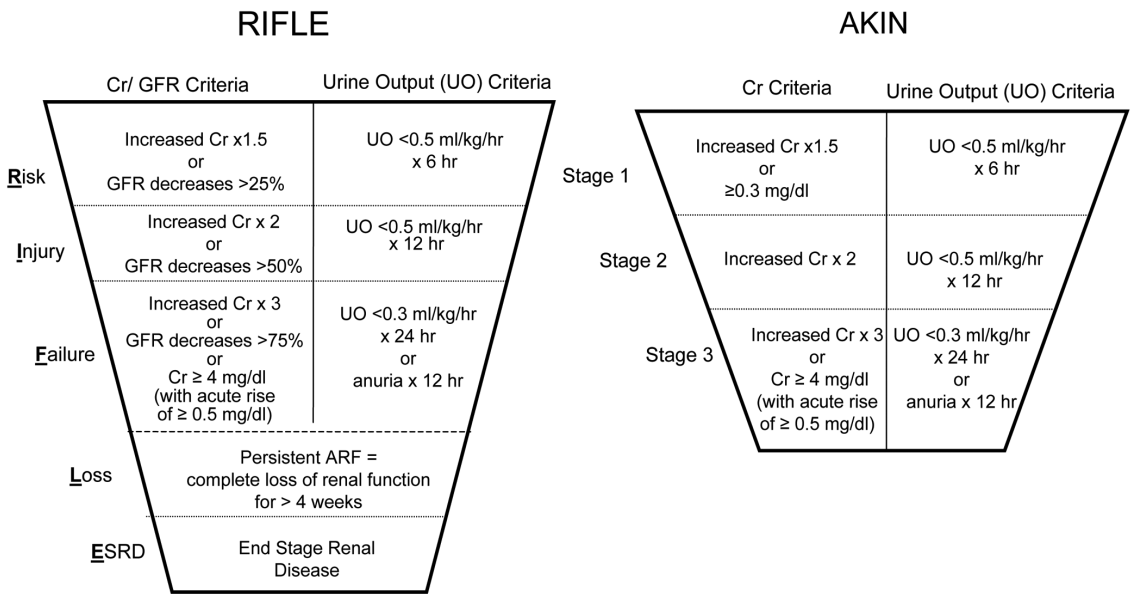

Figure 1.2 The Risk Injury Failure Loss End stage renal disease (RIFLE) and Acute Kidney Injury Network (AKIN) classifications for acute kidney injury (AKI). The RIFLE classification, which is inclusive of creatinine, urine output and glomerular filtration measurements, has now been modified. Cr, Creatinine; GFR, Glomerular Filtration Rate; ARF, Acute Renal Failure; UO, Urine Output. Adapted from Cruz et al. (2009).

Pathophysiology of Ischaemic Acute Kidney Injury

Ischaemia is the most common cause of AKI, caused by a reduction in effective perfusion to the kidney. As previously discussed, renal ischaemia manifests itself in the clinical setting as a primary condition and also secondary to conditions such as sepsis (Keir and Kellum, 2015). Pre-clinically, animal models of renal ischaemia-reperfusion injury (IRI) are used to model AKI, by occluding the renal artery, vein and nerve (the renal pedicle). This is achieved by either bilateral or unilateral occlusion with contralateral nephrectomy (Skrypnyk et al., 2013). Experimental renal IRI commonly uses an ischaemic period between 30 to 60 min, longer periods of ischaemia resulting in more severe injury.

The pathophysiology of ischaemic AKI is both complex and has yet to be fully understood, as it involves multiple pathways affecting many cell types and tissues (Figure 1.3).

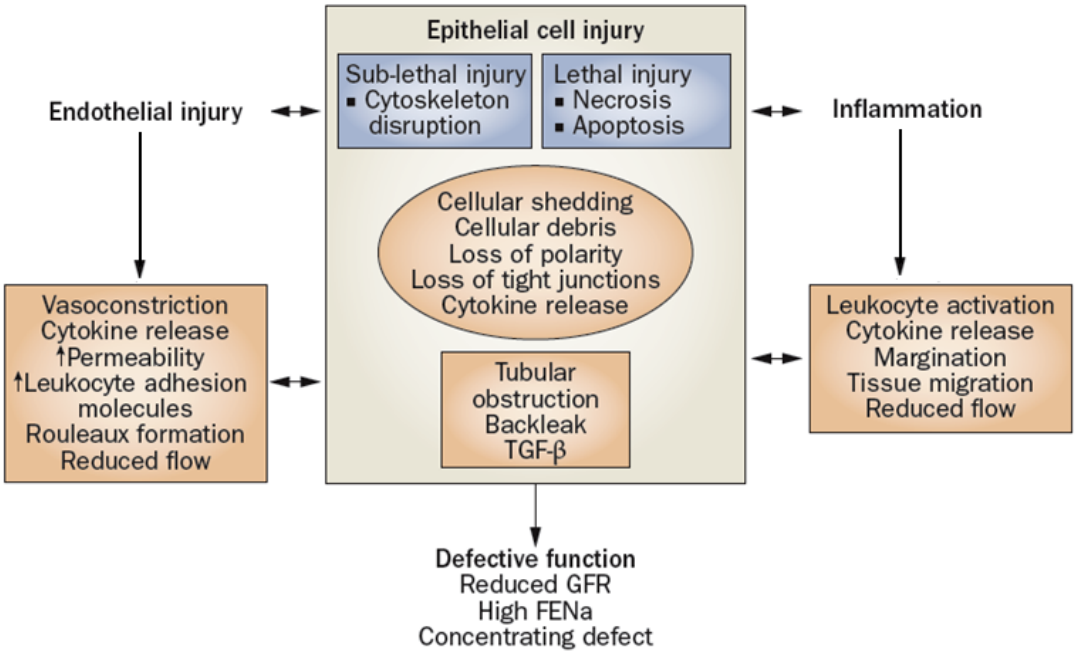

Figure 1.3 The pathophysiology of ischaemic acute kidney injury (AKI). TGF-β1, transforming growth factor-β1; GFR, glomerular filtration rate; $FENa^+$, fractional excretion of sodium. Adapted from Sharfuddin and Molitoris (2011).

The Ischaemic Period

ATP depletion

Ineffective perfusion to the kidney during ischaemia renders renal tubular epithelial cells unable to maintain sufficient adenosine triphosphate (ATP) production to perform basic cell processes (also known as the initiation phase of ATN). The renal tubular epithelium are covered in microvilli forming a 'brush' border on the luminal side of the tubule, increasing the surface area of these cells for specialised transport of water and ions.

Lack of ATP may cause either sub-lethal (reversible) or lethal injury (irreversible) leading to epithelial and endothelial cytoskeletal disruption, or apoptosis and necrosis of cells, respectively (Figure 1.3) (Sharfuddin and Molitoris, 2011). These processes change both structure and function of the renal tubular epithelial cells, with the severity of ischaemic injury dictating the extent of the damage to these cells. Proximal tubule cells are the most sensitive to ischaemia, markedly in the S3 segment, in the outer stripe of the medulla (Bonventre and Weinberg, 2003). Injury to S1 and S2 proximal tubule cells is usually reversible, however injury to the S3 segment may result in cell death by apoptosis or necrosis (Venkatachalam et al., 1978).

Apoptosis and Necrosis

Both apoptosis and necrosis are forms of cell death, or lethal cell injury, and have both been described in AKI (Padanilam, 2003). Apoptosis is described as programmed cell death, characterised by cell shrinkage, nuclear chromatin condensation, and the formation of apoptotic bodies. Apoptosis is an ATP-

dependent process, limiting inflammation and damage to surrounding tissue, as the membrane of the cell stays intact throughout its breakdown, preventing leakage of cellular content (Sanz et al., 2008). Apoptosis may be activated via several pathways.

On the other hand, necrotic cells are characterised by cytoplasmic swelling, irregular chromatin bundling, and eventual bursting of the plasma membrane causing cytoplasmic content to leak into the interstitium, resulting in inflammation and tissue damage (Lieberthal et al., 1998). Both of these processes have been previously described in AKI, with a dose-dependent relationship apparent between ischaemia time and the incidence of apoptosis and necrosis. In a rat IRI model, apoptosis occurs after only 15 min of ischaemia, with increasing incidence of apoptosis and of necrosis after longer ischaemia times (Schumer et al., 1992). This has also been demonstrated *in vitro*, where necrosis is the predominant method of cell death with severe ATP depletion (Wiegele et al., 1998).

Cytoskeletal Alterations

Sub-lethal injury caused by AKI is characterised by the loss of the apical brush border of the proximal tubular cells (Isaac et al., 2007), which occurs approximately 15 min after reperfusion of the kidney (Venkatachalam et al., 1978). ATP depletion causes the disruption of apical F-actin, causing a change in both the structure of the microvilli and the polarity of the cell (Kellerman and Bogusky, 1992). The disruption of apical F-actin causes the formation of blebs, irregular bulges of the plasma membrane, which subsequently break off and are released into the tubular lumen. The loss of cell polarity may also be due to cytoskeletal alterations caused by the loss of expression of transmembrane integrin receptors.

Integrins facilitate cell to cell and cell to extracellular matrix (ECM) interactions, and during AKI, integrins relocate from the basolateral to the apical side of epithelial cells (Goligorsky et al., 1993). This movement causes detachment and clustering of the detached proximal tubular cells, causing tubular obstruction and contributing to the decrease in GFR (Goligorsky et al., 1993). When summated, blebs, brush border remnants and cellular debris all cause blockage of the tubule lumens – leading to a decrease, or halt, in GFR.

Paracellular Permeability

AKI also results in an increase in paracellular permeability due to the loss of tight junction proteins, such as ZO-1/ZO-2 (Tsukamoto and Nigam, 1997), causing back leak of the glomerular filtrate into the interstitium. Epithelial cells lose their attachments to the basement membrane due to the lack of ATP, causing mislocation of the basolateral Na^+/K^+ pumps. The redistribution of these pumps results in directional changes of both Na^+ and water; causing Na^+ to move back into the tubular lumen, therefore causing a high $FENa^+$ (Bonventre and Weinberg, 2003), and consequently a concentrating problem. Thus, the $FENa^+$ is a direct measure of tubular function, and is also used clinically for the differentiation between ATN (acute tubular necrosis) and pre-renal disease.

The impaired reabsorption of Na^+ in the proximal tubule cells contributes to the reduction in GFR via the activation of tubular glomerular feedback mechanisms (Navar and Mitchell, 1990). Tubuloglomerular feedback regulates GFR in normal renal health via the *macula densa*, which detects elevated NaCl concentration in the filtrate, activating purinergic signalling leading to afferent arteriole constriction, and therefore a decrease in GFR to normal levels (Carlstrom et al., 2015).

The Reperfusion Period

The Effects of Continued Hypoxia

On resolution of the ischaemic insult, the reintroduction of blood flow (reperfusion) into the kidney causes a further endothelial and parenchymal cell inflammatory response (known as the extension phase of ATN). Despite the re-introduction of blood flow post-ischaemia, continued hypoxia has been described due to reduced blood flow (Rabb et al., 1997). Under normal conditions, without AKI, the cortex, cortico-medullary junction (CMJ) and the outer medulla have partial pressures of oxygen (pO_2) of 11.9, 4.1 and 7.9 mmHg respectively, as reported by Whitehouse and colleagues (2006) in a rat model (Whitehouse et al., 2006). Even under normoxic (and even more so under hypoxic) conditions, the kidneys possess lower oxygen levels in comparison to other organs (Safran et al., 2006). Both the continued hypoxia following an ischaemic event and inflammation is most pronounced in the CMJ post AKI. The CMJ exhibits a low basal pO_2 under normal circumstances, making this region of the kidney more sensitive to injury caused by poor perfusion.

The Vasculature

Sublethal injury to tubular cells causes activation of the tubuloglomerular feedback mechanism, in turn causing an increase in renal vascular resistance (RVR) (Singh and Okusa, 2011). Vasoconstriction of the intrarenal vessels post AKI occurs to counter the decrease in renal perfusion rendering the kidneys unable to auto-regulate blood flow, persisting up to one week post-injury (Conger and Schrier, 1980). There are several other causes of increased RVR that may occur post AKI, including increased sympathetic nervous activity (Fujii et al., 2003), increased

formation of endothelin-1 (ET-1) (Firth et al., 1988), and primary damage to the renal vasculature. Alongside these, vasoconstriction is also caused by the decreased production and decreased response to vasodilators such as bradykinin, nitric oxide (NO) and acetylcholine (ACh). All of these factors impair vascular homeostasis, which underpins the early decrease in GFR seen in AKI. This is also accompanied by red blood cell 'sludging' (also known as *Roleaux* formation) in the microvasculature, where red blood cells retard and accumulate.

Endothelial Dysfunction and Nitric Oxide Synthase

Constitutively, endothelial cells regulate homeostatic processes such as vascular tone and permeability, however AKI causes dysregulation of the microvasculature promoting prolonged ischaemia, in turn causing further injury (Sutton et al., 2002). Endothelial damage causes a decrease in production of endothelial nitric oxide synthase (eNOS), an enzyme responsible for the production of NO, a cell signalling molecule with powerful vasodilatory properties (Noiri et al., 2001). This decrease in eNOS alongside an increase in ET-1 production further exacerbates vasoconstriction and platelet aggregation in the intrarenal vessels (Arfian et al., 2012).

Neutrophils in Acute Kidney Injury

When damaged, the endothelium produces a plethora of pro-inflammatory and chemotactic cytokines such as tumour necrosis factor-α (TNF-α), monocyte chemotactic protein-1 (MCP-1) interleukin (IL)-8, IL-6, IL-1β and transforming growth factor-β (TGF-β), promoting neutrophil migration into the kidney tissue (Rabb et al., 1997). Neutrophils are the first inflammatory cells to infiltrate and accumulate in the tissue post IRI (Wu et al., 2007). The margination of neutrophils

into the tissue is facilitated by the upregulation of cell surface proteins such as P- and E- selectins on the endothelium, and the strong binding of cluster of differentiation molecule 11B (CD11b) on the neutrophils cell surface to upregulated intercellular adhesion molecule-1 (ICAM-1) on the endothelial cells (Molitoris and Marrs, 1999). This binding slows and eventually ceases the motion of the neutrophils allowing neutrophil diapedesis from the vascular lumen into the tissue towards the injured site. Infiltrating neutrophils exacerbate injury through free radical and eicosanoid production, enhancing the inflammatory response. Results from studies aimed at investigating the potential role of neutrophils in the pathophysiology of AKI have not provided a clear answer: Thornton et al. (1989) demonstrated neutrophil depletion with an antiserum conferred no renal protection compared to control animals subject to AKI (Thornton et al., 1989), whilst Kelly et al. (1996) have shown that mice deficient in ICAM-1, an intercellular adhesion molecule present on the endothelial membrane responsible for facilitating leukocyte-endothelial binding for transmigration of neutrophils into the tissues, were protected against renal IRI (Kelly et al., 1996).

Macrophages in Acute Kidney Injury

Macrophages are derived from monocytes, and produce cytokines such as IL-1, IL-6 and TNF-α when activated. Macrophages also possess phagocytic capabilities. From 1 h post AKI, the number of macrophages in the kidney increases (Li et al., 2008), most noticeably in the outer medulla (Ysebaert et al., 2000). Infiltration into the renal tissue is facilitated by the CX_3CL1 receptor, expressed by injured endothelial cells (Oh et al., 2008), through interactions with CX_3CL1 and CCR2 expressed on the surface of both monocytes and macrophages (Ysebaert et al.,

2000). They are also recruited via selectins on the endothelial cell surface post injury. Once recruited to the renal tissue, macrophages are involved in multiple inflammatory pathways, producing cytokines responsible for many effector functions such as the recruitment of neutrophils into the renal tissue (De Filippo et al., 2013). Ko et al. (2006) have demonstrated that liposomal clodronate depletion of monocytes and macrophages caused a significant reduction in both the structural and functional injury caused by AKI (Ko et al., 2008). Macrophages also play a pivotal role in renal repair (see below).

Reactive Oxygen Species and Superoxide Dismutase

Severe ATP depletion and the cessation of oxidative phosphorylation that occurs during ischaemia, causes epithelial cells to produce reactive oxygen species (ROS) (Weight et al., 1996). ROS include the most abundant superoxide anion (O_2·-), the hydroxyl radical (·OH), and hydrogen peroxide (H_2O_2). O_2·- is created as oxygen molecules accept a single electron from NADPH oxidase or xanthine (Nath and Norby, 2000). O_2·- can consequentially be converted into H_2O_2 via dismutation by superoxide dismutaste (SOD) (Nath and Norby, 2000), and as O_2·- is highly reactive, mammals, plants and bacteria have the ability to produce SOD as an anti-oxidant defense mechanism. Mammals express three forms of SOD, all three of which are present in the kidney: SOD1 (cytoplasmic), SOD2 (mitochondrial) and SOD3 (extracellular) (Fukai and Ushio-Fukai, 2011). Increased SOD expression via recombinant adenovirus containing transgenes for human SOD successfully reduces damage associated with renal IRI such as tubular atrophy and inflammation when compared to control animals (Yin et al., 2001), and SOD1 knockout mice are associated with worse AKI than that of wild-type controls (Yamanobe et al., 2007).

The highly toxic ·OH ion is created from H_2O_2 and O_2·-, catalysed by iron (Fe^{2+}) ions (the Haber-Weiss reaction) or by Fe^{2+}-facilitated decomposition of H_2O_2 (the Fenton reaction) (Zorov et al., 2014). ·OH has the ability to cause oxidative damage to DNA bases, despite its short half-life (Zorov et al., 2014). ROS may also be formed during the impairment of mitochondrial activity via the disruption of the electron transport chain (Gonzalez-Flecha and Boveris, 1995) (Cruthirds et al., 2003) and higher levels of ROS have been measured in the mitochondria of rats subject to renal IRI (Gonzalez-Flecha and Boveris, 1995). Some infiltrating leukocytes demonstrate high levels of nicotinamide adenine dinucleotide phosphate (NADPH) enzyme activity (present on the plasma membrane of the leukocyte) and are therefore also a source of O_2·- anions, contributing to further renal injury (Nath and Norby, 2000).

Constitutively, ROS are involved in normal cell activities; however, at high concentrations (e.g. in AKI), these species damage lipid membranes, proteins and DNA, and cause destabilisation of cell-cell and cell-ECM adhesion via the oxidation of structural proteins and enzymes (Sharfuddin and Molitoris, 2011).

Current Therapies for AKI

AKI is a complex disorder, which is both costly and associated with a high mortality rate. Patients with AKI are usually anaemic, catabolic, and susceptible to sepsis and haemorrhage and have very little appetite. If untreated, serious complications involve cardiac arrest and even death. AKI sufferers require specialist treatment regardless of AKI severity. As of yet, there are no pharmacological therapies shown to safely ameliorate AKI as suggested by the UK Renal Association clinical practice guidelines (UK Renal Association, 2015), however there is an emphasis the prevention of AKI and slowing the progression of existing AKI because of this. Prevention methods include discontinuation of any diuretics, angiotensin converting enzyme (ACE) inhibitors, metformin and non-steroidal anti-inflammatory drugs (NSAIDs) (Bilge et al., 2013). Other measures to slow the progression of AKI include dietary restriction of protein, Na^+ and K^+ and bicarbonate administration to counter acidosis (Turner et al., 2012). There is no current pharmacological cure for AKI, which is instead managed by the above methods. Research into AKI using animal models is required for a better understanding of the pathogenesis of AKI and for testing interventions as potential future treatments.

Chronic Kidney Disease and Renal Fibrosis

CKD currently affects approximately 13-16% of the world's adult population (Meguid El Nahas and Bello, 2005). It occurs secondary to such diseases such as diabetes mellitus, hypertension, and glomerulonephrosis. CKD is defined as a decline in GFR of <60 mL/min/17.3m^2 for a period of three months or more, and unlike AKI, CKD is irreversible. CKD is divided into 5 stages according to severity, depending on the estimated GFR:

Stage	Description	Glomerular filtration rate (ml/min/1.73m^2)
1	Kidney damage with normal or increased GFR	≥ 90
2	Kidney damage with mild decrease in GF	60-89
3	Moderate decreases in GFR	30-59
4	Severe decrease in GFR	15-29
5	End stage renal disease (ESRD)	<15 (or dialysis)

Figure 1.4
The five stages of the chronic kidney disease (CKD) classification. CKD is defined as a GFR of <60 mL/min/17.3m^2 for a period of 3 months or more, and GFR of <15 mL/min/17.3m^2 is classed as end-stage renal disease, where the patient will need some form of renal replacement therapy, such as haemodialysis or transplant. Adapted From Levey et al. (2005).

ESRD is the common end point in both the AKIN and CKD classifications. Patients can live with CKD or AKI without requiring RRTs; however patients that further deteriorate to ESRD experience destruction of the kidney parenchyma and fibrosis of the kidney tissue (Liu, 2006). This pathology renders the kidneys unable to filter the blood efficiently, and from this point patients are unable to live without some

form of RRT. However, patients with CKD exhibit a fivefold increase in the risk of mortality due to cardiovascular disease (Go et al., 2004), and may not reach ESRD.

The progression from CKD to ESRD is characterised by renal fibrosis, an irreversible condition characterised by the excessive accumulation of ECM components and the alterations in the phenotype of both resident and infiltrating cell types (Chevalier et al., 2009). Renal fibrosis is seen in almost all patients with ESRD, and currently there are no successful pharmacological treatments available to reverse fibrosis, or prevent its progression.

Pathophysiology of Renal Fibrosis

Initially, after injury caused by inflammation, wound healing is beneficial to restoring functionality of the kidney. However, there is a fine line between cellular repair and over-production of ECM components (Sharples, 2007). Over-production of the ECM causes renal fibrosis, which manifests itself in 4 stages: the cellular activation and injury phase (priming), the fibrogenic signalling phase (activation), the fibrogenic phase (execution) and the phase of renal destruction (progression). These four stages are not static however, and may occur at the same time (Eddy, 2000). These stages will subsequently be discussed in more detail. It is impossible to highlight the key molecular pathway responsible for renal fibrosis, as the pathophysiology is complex and involves multiple cell types and tissues, all contributing to the activation, production and deposition of the ECM.

Priming

Injury to the renal tissues, such as ischaemia, causes an inflammatory response which 'primes' the conditions of the kidney to fibrosis. Tubular cell damage causes the release of pro-inflammatory cytokines and chemokines such as MCP-1, in an attempt to self-repair (Wang et al., 2007). The release of such molecules creates a chemotactic gradient for immune cell infiltration from the systemic circulation into the interstitial space of the kidney. Such immune cells include monocytes, macrophages, T cells, leukocytes and mast cells (Duffield, 2010). The importance of the role of macrophages in CKD has been recently described (Kinsey, 2014). Infiltrating macrophages accumulate in both the glomerulus and the interstitial tissue, secreting a plethora of mediators influencing the development of renal fibrosis, such as growth factors (notably TGF-β), cytokines, enzymes, lipid mediators, matrix proteins, ROS, and many more upon recruitment and activation (Eddy, 2000). Interventions to deplete macrophages, such as inhibiting/blocking growth factors or chemotaxis have caused a reduction in glomerular inflammation and renal fibrosis (Ko et al., 2008). Macrophages have recently been classified into two subsets, M1 (classically activated) and M2 (alternatively activated). Macrophages recruited to the renal tissue post UUO are predominately M1 macrophages ($F4/80^+$ and $CD301^-$), which are soon polarized to M2 macrophages ($F4/80^+$ and $CD301^+$), which in turn release high levels of TGF-β (Shen et al., 2014a), suppressing inflammation of the kidney whilst promoting renal fibrosis (Anders and Ryu, 2011). Other inflammatory cell types such as dendritic cells, T cells and mast cells are involved in the initial inflammation of the kidney, but their role in the direct promotion of renal fibrosis is debatable. Unresolved renal

inflammation causes further damage to the tissues and a consequent positive feedback loop of chemotaxis and inflammation.

Activation

Alongside inflammatory mediators, resident and infiltrating cell types produce a plethora of growth factors during activation, such as TGF-β; a key mediator of fibrosis. TGF-β is activated by prolonged ischaemia, epithelial injury, angiotensin II and platelet-derived growth factor (PDGF) (Docherty et al., 2002). TGF-β1, the latent form of TGF-β, is produced by all renal resident cells, and is bound to latency-associated peptide (LAP), preventing receptor binding. On removal of LAP by latent TGF-β-binding protein, TGF-β is free to activate a downstream signalling pathway resulting in the activation of matrix-producing cells (Huang et al., 2008). It does so by binding the type II TGF-β receptor, a serine (Ser) threonine kinase, causing phosphorylation of the type I TGF-β receptor. Both type I and type II TGF-β receptors form a hetero-tetrametic complex with TGF-β on the plasma membrane, which phosphorylates downstream receptor-associated Smads 2 and 3. Smad 2 and 3 form a complex with Smad 4, and the resulting Smad complex translocates to the nucleus for gene transcription (Meng et al., 2015) (Figure 1.6). TGF-β has multiple functions in renal fibrosis, including the induction of collagen and fibronectin production, the inhibition of matrix metalloproteinases (therefore preventing ECM breakdown), inducing epithelial-mesenchymal transition (EMT) and endothelial-mesenchymal transition (EndoMT) to the myofibroblast phenotype (Wu et al., 2013), and can increase matrix production through the promotion of mesangial cell proliferation (López-Hernández and López-Novoa, 2012). TGF-β can also function

independently of the Smad pathways, e.g. through p38 and ERK (Derynck and Zhang, 2003).

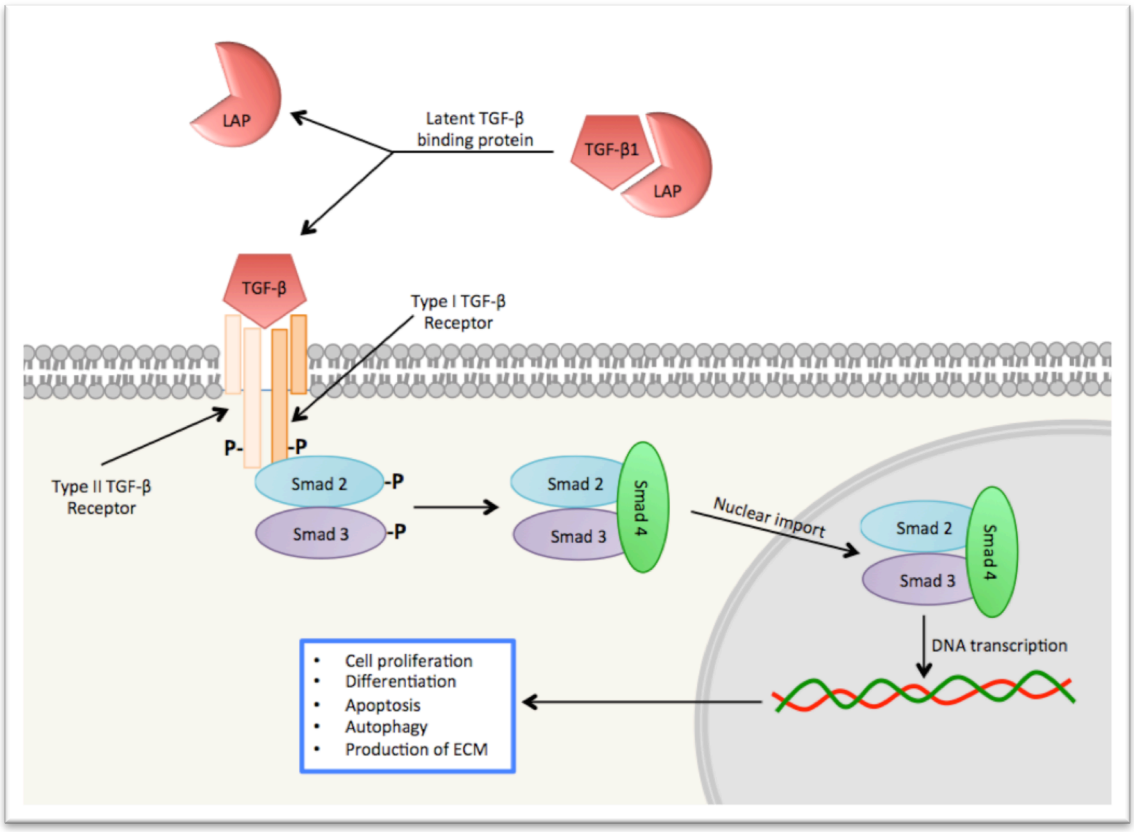

Figure 1.6 The TGF-β pathway. Stimuli such as ischaemia cause dissociation of TGF-β1 from latency-associated peptide (LAP), facilitated by latent TGF-β-binding protein. TGF-β is then free to bind the type II TGF-β receptor causing phosphorylation of type I TGF-β receptor, causing the receptors to form a heterodimer. The TGF-β receptor complex phosphorylates Smad proteins 2 and 3, which in turn bind to Smad 4. The Smad complex then translocates to the nucleus to perform gene transcription of target genes. Adapted from Meng et al. (2015).

The principal matrix-producing cells involved in fibrosis are fibroblasts, located in the interstitial space of the kidney. Physiologically, they maintain the tissue architecture of the kidney, and produce a basal level of ECM to maintain matrix integrity (Kaissling and Le Hir, 2008). Fibrogenic factors such as TGF-β, PDGF, angiotensin II, and fibroblast growth factor (FGF) cause fibroblast activation and promote a change in phenotype from fibroblast to myofibroblast (Liu, 2011), and

new expression of alpha-smooth muscle actin (α-SMA), vimentin and nestin (Sakairi et al., 2007). Myofibroblasts produce a higher volume of ECM components compared to fibroblasts, causing an imbalance in the homeostasis of collagen production. The origin of myofibroblasts is still under debate, however, LeBleu and colleagues estimated that 50% of myofibroblasts originate from proliferating resident renal fibroblasts, 35% from differentiating bone marrow, 10% from EndoMT and 5% from EMT, all contributing to the deposition of fibrotic tissue (LeBleu et al., 2013).

Execution

At this stage of the disease, myofibroblasts continually synthesise collagen I, collagen III and fibronectin (a 440kDa glycoprotein), contributing to the excess of ECM components. The kidney constitutively produces proteases and metalloproteases to degrade matrix components, however in the fibrotic state, protease inhibitors are synthesised preventing degradation of the ECM. Cai et al. (2008) have demonstrated that tissue inhibitor of metalloproteinase-1 (TIMP-1) deficient mice demonstrate more severe renal fibrosis in a model of UUO when compared to wild-type mice (Cai et al., 2008). Further to the inhibition of metalloproteases, the ECM is continually strengthened by cross-linking of proteins by transglutamination (Johnson et al., 1999), causing permanence and irreversibility of the ECM.

Progression

From hereon in, severe irreversible structural damage causes progressive renal insufficiency leading to ESRD. The continuous production of excessive ECM causes expansion of the interstitial space and consequent tubular cell death. 80% of

the kidney volume is composed of tubules, which are vital for the filtration and maintenance of blood composition (Eddy, 2000). The accumulation of matrix causes a gradual obstruction between tubular cells and peritubular capillaries, in turn causing tubular ischaemia and impaired oxygen diffusion vital for tubule function. Excess ECM also causes peritubular rarefaction and tubular hypoxia leading to apoptosis and necrosis of tubular cells (Marcussen, 2000). The gradual loss of renal parenchyma results in ESRD, and clinically, causing the kidneys to shrink due to the contraction of the fibrous scar tissue by myofibroblasts.

Progression of Acute Kidney Injury to Chronic Kidney Disease

Acute Kidney Injury as a Risk Factor for Chronic Kidney Disease

Until recently, survivors of AKI were perceived to regain normal kidney structure and function. However, due to long-term follow-up studies post hospital discharge, this is now known to be untrue. Large population based studies have demonstrated a clear link between AKI and CKD (Hsu, 2012), where the severity of AKI predicts a patients outcome. Patients with severe AKI (especially dialysis-requiring AKI) have a higher probability of developing CKD than those with less severe AKI (Chawla et al., 2011), and an increased risk of cardiovascular mortality and proteinuria (Ishani et al., 2009). Patients experiencing multiple episodes of AKI are also at high risk of developing CKD, with each AKI episode doubling the risk factor for development of stage 4 CKD (Thakar et al., 2011). The stress and damage caused by AKI predisposes patients to CKD; the pathophysiology of which is still poorly characterised pre-clinically. As previously described in this thesis,

AKI causes a series of inflammatory changes in the kidney, not limited to: tubular injury, tubular obstruction, vascular injury, endothelial cell activation and leukocyte recruitment. Following this, the kidneys attempt regenerative processes, where maladaptive and incomplete repair encourage fibrosis development and, therefore, CKD.

The Pathophysiology of the Progression of AKI to CKD

Interstitial Inflammation and the Development of Fibrosis

Inflammation post AKI involves infiltration of immune cells such as monocytes and neutrophils, as described above. The prolonged presence of these cells post AKI may aid the development of fibrosis, as shown by Forbes et al. (2001) who demonstrated macrophage accumulation was attenuated with the administration of an ET-1 antagonist, resulting in a decrease in collagen deposition (Forbes et al., 2001). Other immune cells such as T cells may play a major role in CKD development post AKI (Chandraker et al., 1997), however, the mechanisms by which these cells contribute to the pathophysiology of AKI and their contribution to fibrosis is still unclear.

Endothelial Injury and Vascular Rarefaction

Despite GFR returning to baseline post AKI, structural changes, more specifically in the vasculature, are still apparent. Basile et al. (2001) have described how in a rat model of renal IRI, 60 min of ischaemia followed by a 40 week reperfusion period caused a reduction in peritubular capillary density (around 30-50%) in the CMJ from 4 to 40 weeks after AKI (Basile et al., 2001). This was followed by the development of tubulointerstitial fibrosis at 40 weeks post AKI. In comparison to renal tubular epithelial cells, the endothelium has less affinity for regeneration. Vascular endothelial growth factor (VEGF) is a protein involved in the stimulation of angiogenesis, and is down-regulated post ischaemia (Basile et al., 2008). Lack of VEGF post AKI is a major contributor to vascular dropout seen in these animals (Basile et al., 2008). These data suggest that microvascular rarefaction causes further renal hypoxia, causing increased expression of pro-fibrotic molecules such as TGF-β (Fine et al., 1998), potentially driving AKI to CKD.

The Role of the Cell Cycle in the Development of Chronic Kidney Disease from Acute Kidney Injury

Yang et al. (2010) have recently described the role of cell cycle arrest in the development of renal fibrosis in mouse models of AKI and aristolochic acid induced nephropathy (AAN) (Yang et al., 2010). Arrest in G2/M phase of the cell cycle in proximal tubule cells *in vivo* and *in vitro* showed a strong correlation with the upregulation of profibrotic genes, and the subsequent development of fibrosis (Yang et al., 2010). c-JUN N-terminal kinases (JNK) are activated during G2/M

arrest, promoting upregulation of profibrotic genes and the production of collagen due to increased gene transcription of TGF-β1 and connective tissue growth factor (CTGF) (downstream of TGF-β1). Inhibition of JNK caused a reduction in the level of fibrosis seen in these animals (Yang et al., 2010). Epigenetic modifications may also contribute to CKD development, altering genes such as TNF and CCR2 involved in renal inflammation post AKI. DNA methylations and histone modifications have already been described in both AKI (Zager and Johnson, 2009) and CKD (Wing et al., 2013).

Chronic Kidney Disease as a Risk Factor for Acute Kidney Injury

Conversely, CKD is also a risk factor for AKI. Episodes of AKI can be 'superimposed' on pre-existing CKD, further accelerating the decrease in GFR and progression to ESRD (Okusa et al., 2009). The risk of AKI is proportional to the stage of CKD of the patient (Khosla et al., 2009): more advanced patients experience a higher number of episodes of AKI. It has been proposed that the stress and damage caused by one condition may predispose to the other, resulting in a positive feedback loop of continued deterioration in both structure and function of the kidney (Venkatachalam et al., 2010). The widening of the interstitial space by fibrosis contributes to reduced oxygen diffusion and therefore ischaemia, causing AKI (Palm and Nordquist, 2011).

Current Therapies for Chronic Kidney Disease Development

There is a large unmet need for therapies that both accelerate recovery from AKI and prevent or slow down the progression to CKD. Such therapies, however, can only be administered after diagnosis of AKI, when SCr increases are detected, usually 24 – 72 h post AKI. Multiple potential anti-fibrotic therapies have been studied in clinical trials for the treatment of CKD. Among these include anti-TGF-β antibodies to reduce excessive TGF-β signalling (Trachtman et al., 2011), ET-1 antagonists (Wenzel et al., 2009) and phosphodiesterase inhibitors (Rodriguez-Moran et al., 2006). Unfortunately, many have unpreventable side effects and there is yet to be an intervention that successfully passses all four phases of clinical trials.

Nuclear Factor-κB

Nuclear factor-κB (NF-κB) is a nuclear transcription factor that regulates DNA transcription of many molecules involved in inflammatory pathways (Moynagh, 2005). NF-κB comprises of a group of five proteins; p50 (NF-κB1/p105), p52 (NF-κB2/p100), RelA (p65), RelB and c-Rel (Ghosh et al., 1998), which exist as homo- or hetero-dimers. All NF-κB dimers activate transcription with the exception of the p50/50 and p52/52 homodimers, which inhibit it. NF-κB is activated via two different pathways, the classical and the alternative.

The classical pathway: The classical pathway causes activation of NF-κB through a variety of stimuli. These stimuli include pro-inflammatory cytokines such as IL-1β and TNF-α; receptors such as toll-like receptors (TLRs), antigen receptors and

viruses (Bonizzi and Karin, 2004). On detection by various cell surface receptors, such stimuli cause downstream signalling leading to activation of the IκB kinase (IKK) complex. The IKK family consists of four different protein kinases, IKKα, IKKβ, IKKε and TBK1, all involved in the NF-κB activation pathway. IKKε and TBK1 however, are not involved in direct IκB phosphorylation leading to IκB degradation and will not be further discussed in this thesis. The IKK complex commonly consists of three subunits, IKKα, IKKβ and IKKγ (or NF-κB essential modulator (NEMO)) (Karin and Ben-Neriah, 2000). IKKα and IKKβ share an approximate 50% sequence homology, an N-terminal kinase domain, a dimerization domain and a C-terminal domain that binds IKKγ (or NEMO), a regulatory subunit. Upon activation, IKK causes phosphorylation of IκBα (at Ser residues 32 and 36), through IKKβ in an IKKγ-dependent manner (Schmid and Birbach, 2008). NF-κB is bound to IκBα in the cytoplasm in its inactive state. Upon phosphorylation of IκBα by the IKK subunits, IκBα is then polyubiquitinated (at Lysine residues 21 and 22) and degraded by the 26S proteasome (Karin and Ben-Neriah, 2000). The NF-κB dimers are, therefore, released and subsequently translocate to the nucleus to commence gene transcription of a number of proteins including i) cytokines: IL-6, IL-1β, TNF-α; ii) chemokines: IL-8, MCP-1; iii) enzymes: inducible nitric oxide synthase (iNOS), cyclooxygenase-2 (COX-2); and iv) adhesion molecules: ICAM-1, vascular cell adhesion molecule-1 (VCAM-1), E-selectin (Bonizzi and Karin, 2004). Production of pro-inflammatory cytokines such as IL-8 and TNF-α cause a positive feedback loop resulting in further activation of NF-κB.

The alternative pathway: The alternative NF-κB activation pathway is strictly dependent on IKKα (Senftleben et al., 2001). This pathway is only activated by

cytokines, and the only NF-κB proteins involved in this pathway are p52-RelB dimers. Examples of proteins produced include cytokines such as B-cell activating factor (BAFF), chemokines such as B lymphocyte chemoattractant (BLC) and secondary lymphoid-tissue chemokine (SLC), and lymphoid organogenesis genes (Bonizzi and Karin, 2004). For the purpose of this thesis, the alternative pathway will not be discussed any further.

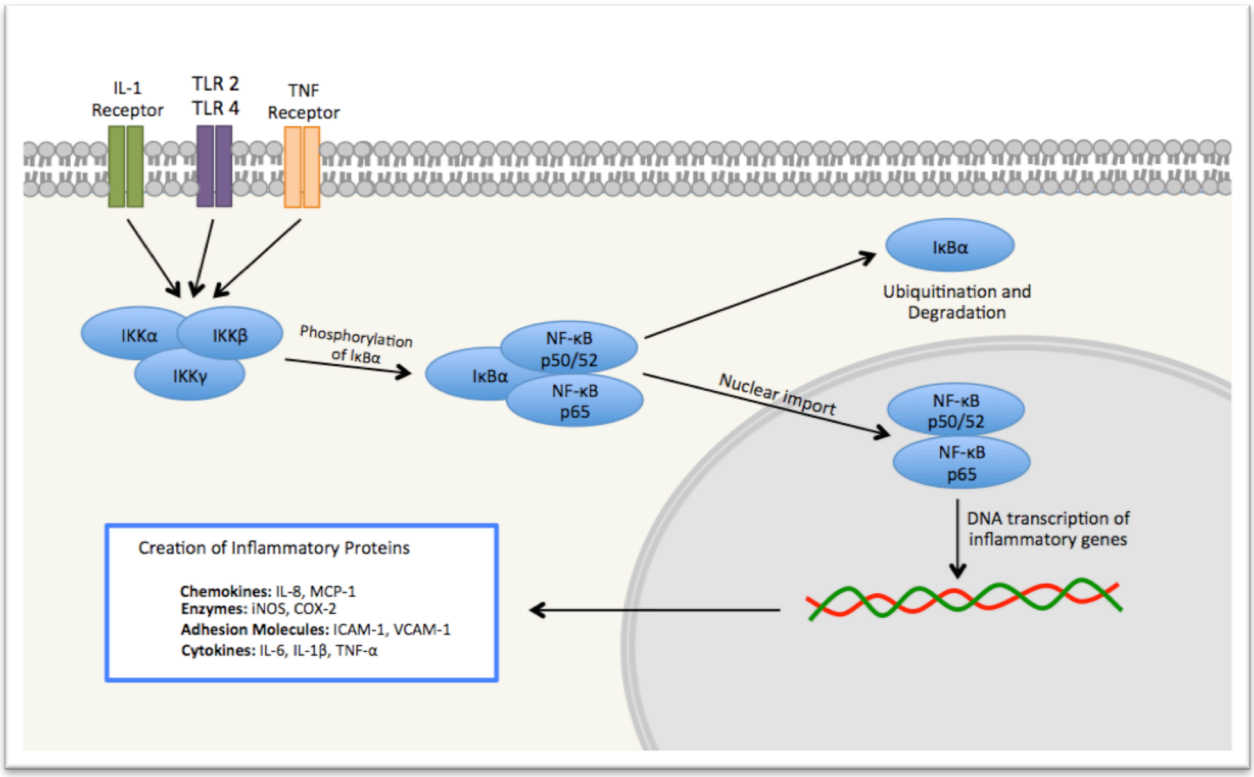

Figure 1.6 The classical NF-κB pathway. Stimuli such as pro-inflammatory cytokines or the activation of toll-like receptors (TLRs) promote a downstream signalling cascade activating inhibitor of IκB kinase (IKK), a 3 subunit kinase comprised of α, β and γ subunits. When activated, IKK phosphorylates Serine residues 32 and 26 on IκBα, causing the dissociation of NF-κB subunits, which translocate to the nucleus for gene transcription of inflammatory proteins. IL-1β, Interleukin-1β ; TNF-α , Tumour Necrosis Factor-α ; TLR, Toll-like Receptor; IKK, Iκ B kinase; mRNA, messenger ribonucleic acid; IL-6, Interleukin-6; IL-8, Interleukin-8; MCP-1, Monocyte Chemoattractant Protein-1; iNOS, inducible nitric oxide synthase; COX-2, Cyclooxygenase-2; ICAM-1, Intracellular Adhesion Molecule-1; VCAM-1, Vascular Cell Adhesion Molecule-1. Adapted from (Bonizzi and Karin, 2004).

NF-κB in Renal Disease

The role of NF-κB in AKI has previously been described. Both its direct and indirect inhibition either prior to, or during, renal IRI has shown to attenuate AKI in animal models (Sanz et al., 2010), demonstrating the importance of this transcription factor and its involvement in AKI. Most notably, the specific inhibition of IKKβ via small interfering RNA (siRNA) before ischaemia reduces injury and/or aids recovery after unilateral renal IRI (Wan et al., 2011a).

Currently, there are no effective anti-fibrotic therapies for preventing progression of CKD to ESRD; patients are limited to medication for symptoms such as anaemia, hypertension and hyperlipidaemia. The role of NF-κB in renal fibrosis has yet to be fully described; however the inhibition of IKKβ in both pulmonary (Inayama et al., 2006) and hepatic (Wei et al., 2011) fibrosis has been proven efficacious, and overexpression of NF-κB in mouse hepatocyte cells causes fibrosis of the liver, an effect which is mediated by macrophages (Shen et al., 2014b). These data indicate the importance of NF-κB in fibrosis, and the potential for new therapies that target the NF-κB pathway.

Aims

Currently, therapeutic interventions reported in the literature are administered before ischaemia (pre-treatment), after ischaemia, before reperfusion (pre-reperfusion treatment), or up to 12 h post reperfusion (post IRI treatment). I have used two different animal models in this thesis:

1. An *in vivo* rat model of renal IRI: Rats were subject to uninephrectomy and unilateral ischaemia (30 min) followed by different lengths of reperfusion (from 24 h to 28 days).

2. An *in vivo* rat model of UUO: Rats were subject to right-hand ureteral ligation with a 14-day recovery period for the development of renal tubulointerstitial fibrosis.

Using these models, the objectives of this thesis are:

- To investigate the acute time course of renal injury and dysfunction in the rat model of renal IRI up to 72 h post reperfusion.
- To investigate potential post reperfusion treatment strategies given during peak SCr values, at which time AKI is diagnosed in the clinical setting. More specifically, the inhibition of NF-κB activity via IKK inhibition, to ameliorate the renal injury and dysfunction associated with AKI.

- To investigate the degree of fibrosis developed in the rat model after 30 min ischaemia when the reperfusion period is extended up to 28 days of reperfusion.
- To investigate whether the early amelioration of renal injury and dysfunction post IRI will successfully reduce or prevent the degree of fibrosis developed after an extended reperfusion period.
- To investigate the inhibition of IKK in a rat model of UUO, after a 14 day recovery period.

Overall, it is hoped that the findings of this study will elucidate the role of IKK in renal IRI, and the subsequent development of fibrosis.

Chapter II

The Delayed Administration of IKK16 Reduces the Severity of Acute Kidney Injury in a Rat Model of Renal Ischaemia-Reperfusion Injury

Introduction

Previous studies have highlighted the benefit of the inhibition of IKK in IRI. In myocardial IRI, IKK inhibition up to 2 h post reperfusion reduces left ventricular infarct size and improves cardiac function when compared to vehicle treated animals (Moss et al., 2007). Further to this, IKK inhibition 1 h prior to cerebral IRI reduces ischaemic brain damage via reducing post ischaemic inflammation (Desai et al., 2010), and both deletion of IKKβ in hepatocytes, and the inhibition of IKKβ (in separate arms of the same study) conferred protection against hepatic IRI; reducing liver necrosis and inflammation when compared to wild-type animals (Luedde et al., 2005). More often than not, AKI in humans is associated with other conditions such as trauma, haemorrhage and septic shock, involving complications such as multiple organ failure. Sordi et al. (2015) have demonstrated that the inhibition of IKK with IKK16, given at resuscitation after haemorrhage, successfully reduced the renal, lung and liver injury associated with haemorrhage after 4 h of reperfusion *in vivo*. Inhibition of IKK also protected HK-2 cells from serum starvation *in vitro* (Sordi et al., 2015). Similarly, administration of IKK16 at 1 h post onset of sepsis (caused by caecum ligation and puncture) attenuated renal dysfunction, cardiac dysfunction and hepatic injury (Coldewey et al., 2013).

There are other interventions that reduce the severity of AKI, which also inhibit the activation of NF-κB. These include inhibitors of glycogen-synthase kinase-3β (GSK-3β) (Nelson and Cantley, 2010), EPO given 4 h post reperfusion (Patel et al., 2012), ARA290, a non-erythropoietic analogue of EPO given 6 h post reperfusion

(Patel et al., 2012), and curcumin administered 12 h prior to IRI (Rogers et al., 2012).

IKK is directly upstream of NF-κB and has an important role in renal IRI, as its inhibition attenuates IRI-dependent changes in biochemical and histological parameters. Previous studies have, however, inhibited IKK pre-ischaemia or during early reperfusion. For instance, Wan et al. (2011a), attenuated renal IRI in rats using small interfering RNA (siRNA) targeting IKKβ, administered via the renal artery 48 h prior to IRI *in vivo* (Wan et al., 2011a). IKKβ siRNA attenuated IRI-dependent increases in SCr and blood urea nitrogen, inhibited IKKβ gene expression, NF-κB binding to DNA, neutrophil gelatinase-associated lipocalin (NGAL) and IL-18 expression (Wan et al., 2011a). The same authors have demonstrated that treatment with siRNA targeting IKKβ to NRK-52E cells 72 h prior to cobalt chloride treatment (which mimics ischaemic AKI) attenuates cobalt chloride-dependent increases in both NGAL and IL-18 protein and mRNA levels, and also reduces the necrosis index in NRK52E cells treated with IKKβ siRNA (Wan et al., 2011b). Although Wan et al. (2011a, b) have shown that the inhibition of IKK is successful in ameliorating IRI in both *in vivo* and *in vitro* models, and therefore have highlighted the importance of the role of IKKβ in renal IRI, the translatability of this potential treatment strategy is limited to clinical situations such as transplantation and coronary artery bypass, where AKI is predictable (Rydén et al., 2014).

Renal ischaemic pre-conditioning has also been shown to inhibit IKKβ, resulting in a reduction in SCr and tubulointerstitial injury score (Chen et al., 2009). These data suggest a detrimental role for the IKK complex in renal IRI.

In this study I have mapped the time course of AKI in a rat model of renal IRI, using both functional (serum urea, SCr, estimated creatinine clearance (eCCL), $FENa^{+}$), structural (histology) and signalling (IKK phosphorylation, IκBα phosphorylation and NF-κB translocation) parameters to determine the best time point at which to treat the animals with a commercially available IKK inhibitor, IKK16, via a more clinically relevant route of administration (i.v.). Following this, I have looked at the effect of the inhibition of IKK on the above parameters (functional, histological and signalling).

Methods and Materials

Animals received standard food and water *ad libitum* and all protocols followed in this study were approved by the local Animal Use and Care Committee in accordance with the derivatives of both the *Home Office Guidance on the Operation of Animals (Scientific Procedures) Act 1986*, published by Her Majesty's Stationary Office (London, UK) and the Guide for the Care and Use of Laboratory Animals of the National Research Council. All results obtained from animals that died during the experiment were excluded from the data analysis and *n* numbers provided in this thesis refer to the 'survivors' of the entire experimental period only.

Renal Ischaemia-Reperfusion Injury

Surgical Procedure and Quantification of Organ Injury/Dysfunction

This study was carried out on 48 male Wistar rats (Charles River Ltd, Margate, UK) weighing between 240 – 290 g and receiving a standard diet and water *ad libitum*. Five animals were excluded from the study due to early mortality, a likely consequence of insufficient reperfusion of the kidney following renal IRI. Animals were anaesthetized using a ketamine (150 mg/kg) (Ketaset, Fort Dodge Animal Health Ltd., Southampton, UK) and xylazine (15 mg/kg) (Rompun, Bayer Plc, Berkshire, UK) mixture i.p. (1.5 ml/kg). The abdominal fur was shaved and the skin cleaned with 70 % alcohol (v/v). The animals were then placed on a homeothermic blanket set at 37°C (Harvard Apparatus Ltd., Kent, UK), and core body temperature was maintained at 35.5 – 36.5°C, monitored by a rectal thermometer. Animals received 0.1 mg/kg s.c. buprenorphine (0.1 ml/kg) (Vetergesic, Rekitt Benckiser Healthcare Ltd., Hull, UK) prior to commencement of surgery. A mid-line laparotomy was then performed. The right renal pedicle (consisting of the renal artery, vein and nerve) was isolated and tied off using sterile 4-0 silk-braided suture (Pearsalls Ltd., Taunton, UK). The right kidney was then surgically removed. The left renal pedicle was isolated and clamped using a non-traumatic microvascular clamp (Fine Science Tools, California) at time 0. After 30 min of unilateral renal ischaemia, the clamp was removed to allow reperfusion. (Sham animals underwent nephrectomy only). For reperfusion, the kidneys were observed for a further 5 min to ensure reflow, following which 8 ml/kg saline at 37^{o}C was injected into the abdomen and all incisions were sutured in two layers (Ethicon Prolene 4-0, Johnson and Johnson, Livingstone, Scotland). Animals were then allowed to recover on the homeothermic blanket and placed into cages upon recovery. Twenty-four hours

prior to the end of the experiment, rats were placed into individual metabolic cages for the collection of urine and the subsequent determination of both eCCL and $FENa^+$. At the end of the experiment, animals were anaethetised with a mixture of ketamine and xylazine (dose as before), and blood was taken by cardiac puncture into non-heparinized syringes and immediately decanted into 1.3 ml serum gel tubes (Sarstedt, Germany). The blood was centrifuged at 9900 *g* for 5 min to separate serum, then snap frozen in liquid nitrogen and stored at -80^{o}C until further analysis. The left kidney was excised following removal of the heart. Half of the left kidney was snap frozen and stored at -80^{o}C, and the other half was stored in 10 % neutral buffered formalin for 48 h, then transferred to 70 % ethanol for storage.

Experimental Design

Acute Time Course

Rats were randomly allocated to the following groups: (i) ***sham + vehicle*** (n=11); (ii) ***24 h reperfusion*** (n=4); (iii) ***48 h reperfusion + vehicle*** (n=8); and (v) ***72 h reperfusion + vehicle*** (n=4).

The Delayed Administration of IKK16, Late Intervention

Rats were randomly allocated to the following groups: (i) ***sham + vehicle*** (n=11); (ii) ***IRI + vehicle*** (n=11); (iii) ***IRI + IKK16 0.1 mg/kg*** (n=5); (v) ***IRI + IKK16 0.3 mg/kg*** (n=7); and ***IRI + IKK16 1.0 mg/kg*** (n=9). Rats were administered vehicle (10% dimethyl sulfoxide (DMSO)) or IKK16 24 h after the onset of reperfusion via the tail vein at a volume of 1 ml/kg. IKK16 was purchased from Tocris Bioscience (R&D systems Europe, Abingdon, UK), and the optimal dose estimated from

previous IC_{50} values (Waelchli et al., 2006). The dose response of IKK16 in renal IRI is displayed in the results section of this chapter.

Measurement of biochemical parameters

All biochemical markers in serum and urine were measured in a blinded fashion by a commercial veterinary testing laboratory (IDEXX Ltd, West Sussex, UK). The following parameters were measured:

1. Serum urea levels (mmol/L) as a measurement of renal function
2. SCr (µmol/L) as an indication of renal function and reduced GFR
3. Urine flow (ml/min) as an indicator of urine production
4. eCCL (ml/min) as an indicator of the GFR, calculated from the urine creatinine, urine flow, and SCr (see chapter I)
5. $FENa^+$ (%) the percentage of Na^+ filtered by the kidneys that is excreted, and therefore an indicator of tubular function. The $FENa^+$ is calculated from urine Na^+ and creatinine and the serum Na^+ and creatinine (see chapter I)

Western Blot Analysis

Western blots were carried out as previously described (Collino et al., 2006). Three to six separate experiments of Western blot analyses were performed for each marker and tissues were done separately for each Western blot experiment. Briefly, previously snap frozen rat kidney samples were homogenized and centrifuged at 4,000 *g* for 5 min at 4°C. Supernatants were removed and centrifuged at 15,000 *g* at 4°C for 40 min to obtain the cytosolic fraction. The pelleted nuclei were re-suspended in extraction buffer. The suspensions were centrifuged at 15,000 *g* for 20 min at 4°C. The resulting supernatants containing nuclear proteins were carefully

removed, and protein content was determined using a bicinchoninic acid (BCA) protein assay following the manufacturer's directions (ThermoFisher Scientific, Massachusetts). Proteins were separated by 8 % Na^+ dodecyl sulphate-polyacrylamide gel electrophoresis (SDS-PAGE) and transferred to a polyvinyldenedifluoride (PVDF) membrane, which was then incubated with a primary antibody; rabbit anti-total IκBα (1:1000 cat#4812 Cell Signalling Technologies, MA); mouse anti-pIκBα $Ser^{32/36}$ (1:1000 cat#9246, Cell Signalling Technologies, MA); rabbit anti-total IKKα/β (1:200, cat#sc-7607, Santa Cruz Biotechnology, TX); rabbit anti-pIKKα/β $Ser^{176/180}$ (1:1000 cat#2697, Cell Signalling Technologies, MA); rabbit anti-NF-κB p65 (1:1000 cat#8242, Cell Signalling Technologies, MA); rabbit-anti phospho eNOS Ser^{1177} (1:200 cat#9570, Cell Signalling Technologies, MA).

Blots were then incubated with a secondary antibody conjugated with horseradish peroxidase (dilution 1:10000) and developed using the enhanced chemiluminescence (ECL) detection system. The immunoreactive bands were visualized by autoradiography. The membranes were stripped and incubated with β-actin monoclonal antibody (1:5000) and subsequently with an anti-mouse antibody (1:10000 cat#7076, Cell Signalling Technologies, MA) to assess gel-loading homogeneity. Densitometric analysis of the bands was performed using Gel Pro®Analyzer 4.5, 2000 software (Media Cybernetics, Silver Spring, MD, USA) and optical density analysis was expressed as fold-increase versus the sham group. In the sham group, the immunoreactive bands of the gel were respectively measured and normalized against the first immunoreactive band (standard sham sample) and the results of all the bands belonging to the same group were expressed

as mean±SEM. This provides SEM for the sham group where a value of 1 is relative to the first immunoreactive band. The membranes were stripped and incubated with β-actin monoclonal antibody and subsequently with an anti-mouse antibody to assess gel-loading homogeneity. Relative band intensity was assessed and normalized against parallel β-actin expression. Each group was then adjusted against corresponding sham data to establish relative protein expression when compared to sham animals.

Histological Evaluation and Scoring

Kidneys were fixed in 10 % neutral buffered formalin for 48 h before being dehydrated with 70 % ethanol. Tissues were embedded in paraffin and sections were cut at 4 μm by a single technician in order to minimize variations in section thickness. The slides were deparaffinised with xylene, stained with haematoxylin and eosin (H&E) and viewed with Nanozoomer Digital Pathology Scanner (Hamamatsu Photonics K.K., Japan). Histological features such as glomerular shrinkage, tubular dilatation, basophilia, necrosis and luminal congestion were noted. Ten random images were taken per slide and quantified for total tissue surface area using ImageJ, as a marker of renal injury.

Materials

Unless otherwise stated, all compounds used in this study were purchased from Sigma-Aldrich Company Ltd. (Poole, Dorset, U.K.).

Statistical Analysis

All values described in the text and figures are expressed as mean±SEM for *n* observations. Each data point represents biochemical measurements obtained from up to 11 separate animals. Statistical analysis was carried out using GraphPad Prism 6.0b (GraphPad Software, San Diego, California, USA). Data without repeated measurements was assessed by one-way ANOVA followed by Bonferroni's multiple-comparison *post hoc* test. A *P* value of less than 0.05 was considered to be significant.

Results

Establishment of the Renal Ischaemia-Reperfusion Model Time Course

Biochemical Markers

In order to understand the progression of AKI in rats, rats were monitored for 72 h following 30 min of unilateral renal ischaemia. Rats were subject to a right-hand nephrectomy and unilateral renal ischaemia at 0 h. Animals were then culled at 0 (sham, no ischaemia), 24, 48 and 72 h post reperfusion. When compared to baseline (sham animals), rats that underwent 30 min of unilateral renal ischaemia developed significant renal (as measured by rises in serum urea (Figure 2.1A) and SCr (Figure 2.1B)) and glomerular (as measured by a fall in eCCL (Figure 2.1C)) dysfunction at 24 h of reperfusion, followed by a progressive recovery of renal and glomerular function without intervention (Figure 2.1).

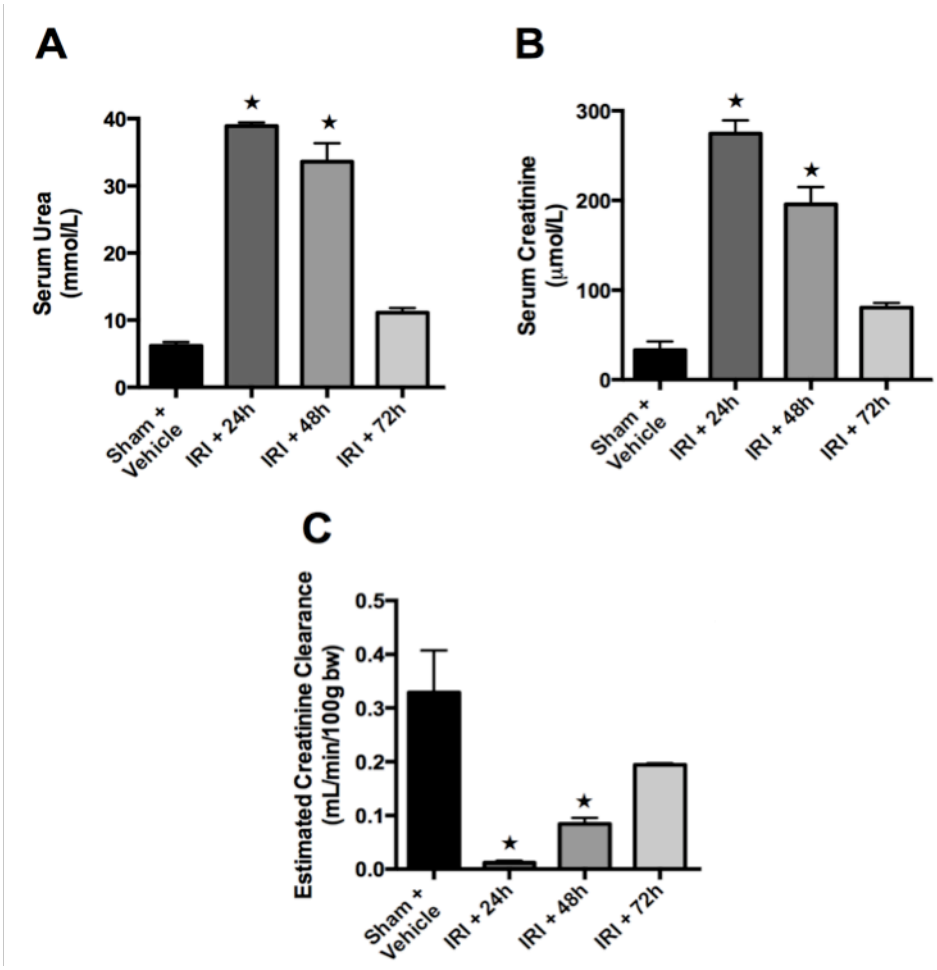

Figure 2.1 The effect of 30 min ischaemia followed by different lengths of reperfusion (24, 48 or 72 h) on renal and glomerular function. IRI; ischaemia-reperfusion injury. Serum urea (A), serum creatinine (B) as indicators of renal function, and the estimated creatinine clearance (C) an estimate of the GFR, as a measure of glomerular function (in different set of animals for each timepoint). The peak of dysfunction in measured time points is 24 h after reperfusion. Sham + vehicle: n=11; 24 h post reperfusion: n=4; 48 h post reperfusion + vehicle: n=8; 72 h post reperfusion + vehicle: n=4. Data are presented as mean ± SEM of n observations, ⋆P<0.05 vs. sham + vehicle.

When compared to baseline (sham animals), rats that underwent 30 min of unilateral renal ischaemia developed significant tubular dysfunction (as measured by a rise in $FENa^+$ (Figure 2.2)) at 24 h of reperfusion, followed by a progressive recovery in tubular function without intervention (Figure 2.2). These findings indicate the development of AKI (Figure 2.1 and 2.2)

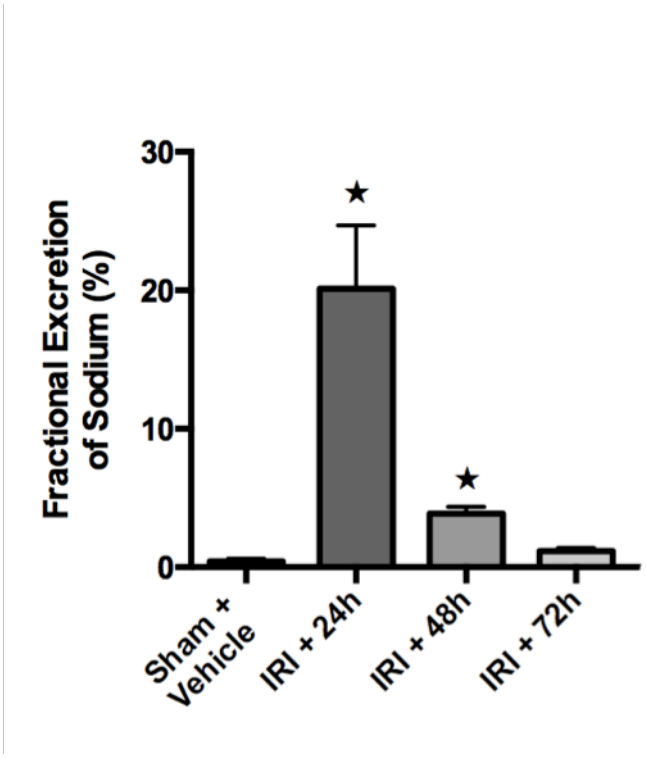

Figure 2.2 The effect of 30 min ischaemia followed by different lengths of reperfusion (24, 48 or 72 h) on tubular function, measured by the fractional excretion of sodium (in different set of animals for each timepoint). The peak of dysfunction in measured time points is 24 h after reperfusion. IRI; ischaemia-reperfusion injury. Sham + vehicle: n=11; 24 h post reperfusion: n=4; 48 h post reperfusion + vehicle: n=8; 72 h post reperfusion + vehicle: n=4. Data are presented as mean ± SEM of n observations, ★P<0.05 vs. sham + vehicle.

Effect of Time on Activation of Intracellular Proteins post Ischaemia-Reperfusion Injury in the Rat Kidney

When compared to baseline (sham animals), kidneys removed (at 48 h of reperfusion) from rats that had been subjected to 30 min of unilateral renal ischaemia exhibited significant phosphorylation of $Ser^{32/36}$ on IκBα (Figure 2.3A), as well as nuclear translocation of the NF-κB subunit p65 (Figure 2.3B). Rats culled at 24 and 72 h post reperfusion demonstrated no significant differences in the phosphorylation of $Ser^{32/36}$ on IkBα or the p65 nucleus/cytosol ratio when compared to sham-operated rats (Figure 2.3).

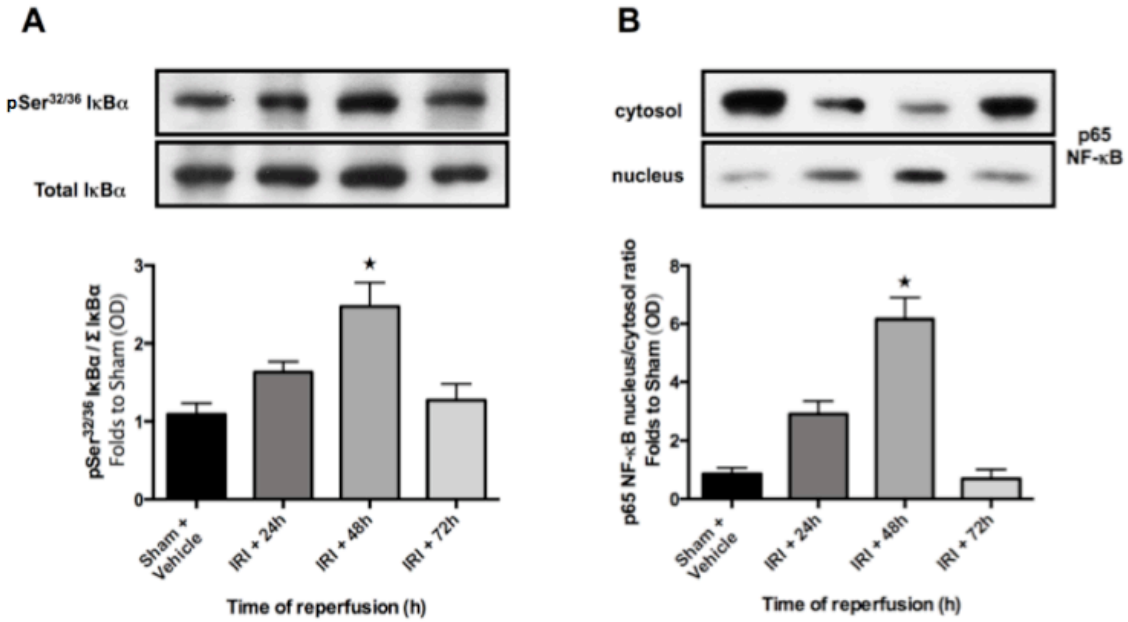

Figure 2.3 The effect of 30 min ischaemia followed by different lengths of reperfusion (24, 48 or 72 h) on the activation of IκBα and NF-κB. Activation of IκBα (A) was measured as phosphorylation of $Ser^{32/36}$ on IκBα during the course of reperfusion. The activation of IκBα results in the activation of IKK and the subsequent nuclear translocation of the p65 subunit of NF-κB (B). Sham + vehicle: n=4; 24 h post reperfusion: n=4; 48 h post reperfusion: n=4; 72 h post reperfusion: n=4. IRI; ischaemia-reperfusion injury. Densitometric analysis of the bands is expressed as relative optical density (OD) of IκBα phosphorylation at $Ser^{32/36}$, corrected for the corresponding total IκBα content and normalised using the sham operated band. NF-κB nuclear translocation was evaluated by measuring NF-κB p65 subunit expression in both cytosolic and nuclear fractions, and expressing the results as nucleus/cytosol ratio. Each immunoblot is from a single experiment. Data are presented as mean ± SEM of n observations, ★P<0.05 vs. sham + vehicle. Western blots performed by Massimo Collino & Fausto Chiazza.

I then measured the phosphorylation of IKK to study its activation. When compared to baseline (sham animals), kidneys removed (at 48 h of reperfusion) from rats that had been subjected to 30 min of unilateral renal ischaemia exhibited significant phosphorylation of $Ser^{176/180}$ on IKKα/β and, hence, activation of the IKK complex (Figure 2.4). Rats culled at 72 h post reperfusion demonstrated no significant differences in the phosphorylation of $Ser^{176/180}$ on IKKα/β when compared to sham-operated rats (Figure 2.4).

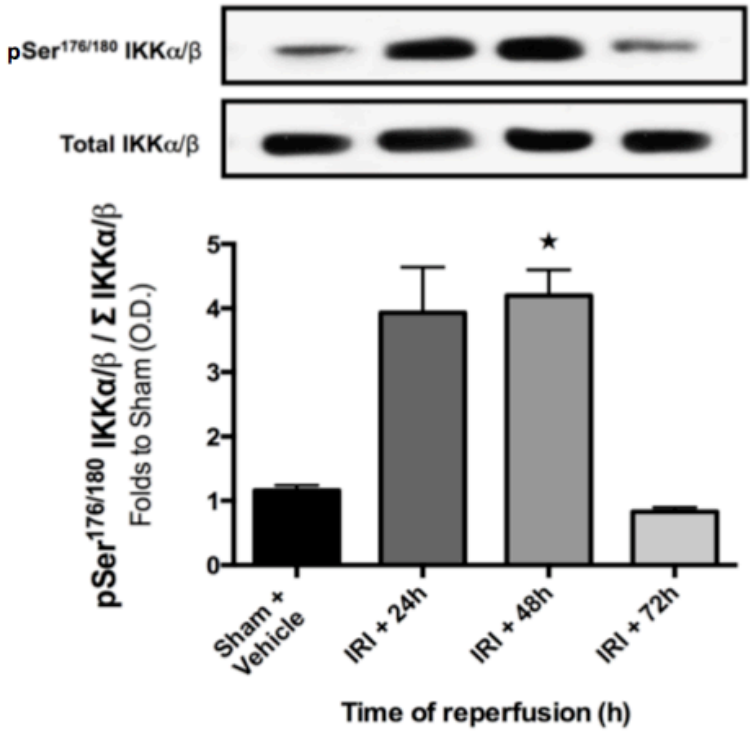

Figure 2.4 The effect of 30 min ischaemia followed by different lengths of reperfusion (24, 48 or 72 h) on the activation of IKK. Activation of IKK was measured as phosphorylation of $Ser^{176/180}$ on IKKα/β during the course of reperfusion. Sham + vehicle: n=4; 24 h post reperfusion: n=4; 48 h post reperfusion: n=4; 72 h post reperfusion: n=4. IRI; ischaemia-reperfusion injury. Densitometric analysis of the bands is expressed as relative optical density (OD) of IKKα/β phosphorylation at $Ser^{176/180}$, corrected for the corresponding total IKKα/β content and normalised using the sham operated band. Each immunoblot is from a single experiment. Data are presented as mean ± SEM of n observations, ★$P<0.05$ vs. sham + vehicle. Western blots performed by Massimo Collino & Fausto Chiazza.

When compared to baseline measurements (sham animals), kidneys removed from rats subjected to 30 min unilateral renal ischaemia culled at 48 h post reperfusion exhibited a significant increase in the phosphorylation of Ser^{1177} on eNOS when compared to baseline (Figure 2.5).

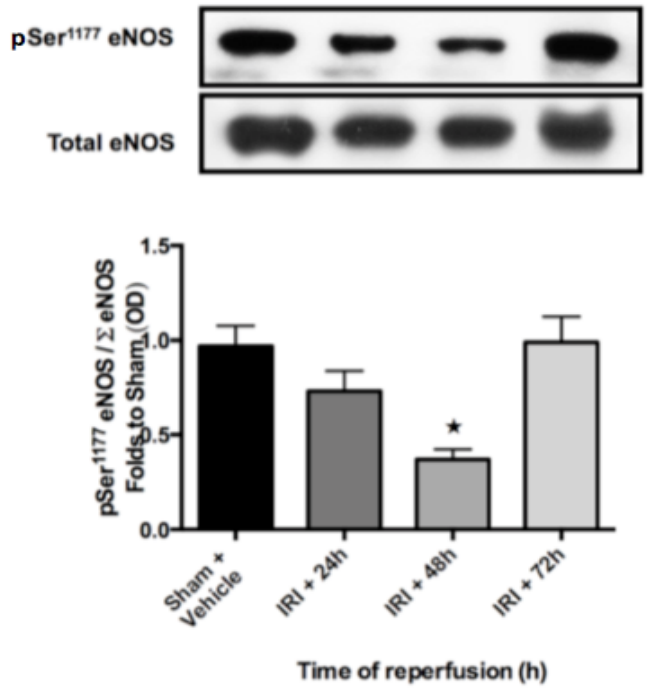

Figure 2.5 The effect of 30 min ischaemia followed by different lengths of reperfusion (24, 48 or 72 h) on the activation of eNOS, measured by the phosphorylation of Ser^{1177} during the course of reperfusion. Sham + vehicle: n=4; 24 h post reperfusion: n=4; 48 h post reperfusion: n=4; 72 h post reperfusion: n=4. IRI; ischaemia-reperfusion injury. Densitometric analysis of the bands is expressed as relative optical density (OD) of eNOS phosphorylation at Ser^{1177}, corrected for the corresponding total eNOS content and normalised using the sham operated band. Each immunoblot is from a single experiment. Data are presented as mean ± SEM of n observations, ★$P<0.05$ vs. sham + vehicle. Western blots performed by Massimo Collino & Fausto Chiazza.

Rationale for delayed treatment with an IKK inhibitor, IKK16

Using these data, I decided to treat the animals at 24 h post reperfusion because:

i) Renal dysfunction was greatest at 24 h post reperfusion (Figure 2.6A), as measured by SCr, most commonly used for the clinical diagnosis of AKI.

ii) This timepoint (24 h) is prior to the activation of NF-κB (which peaks at 48 h) (Figure 2.6B).

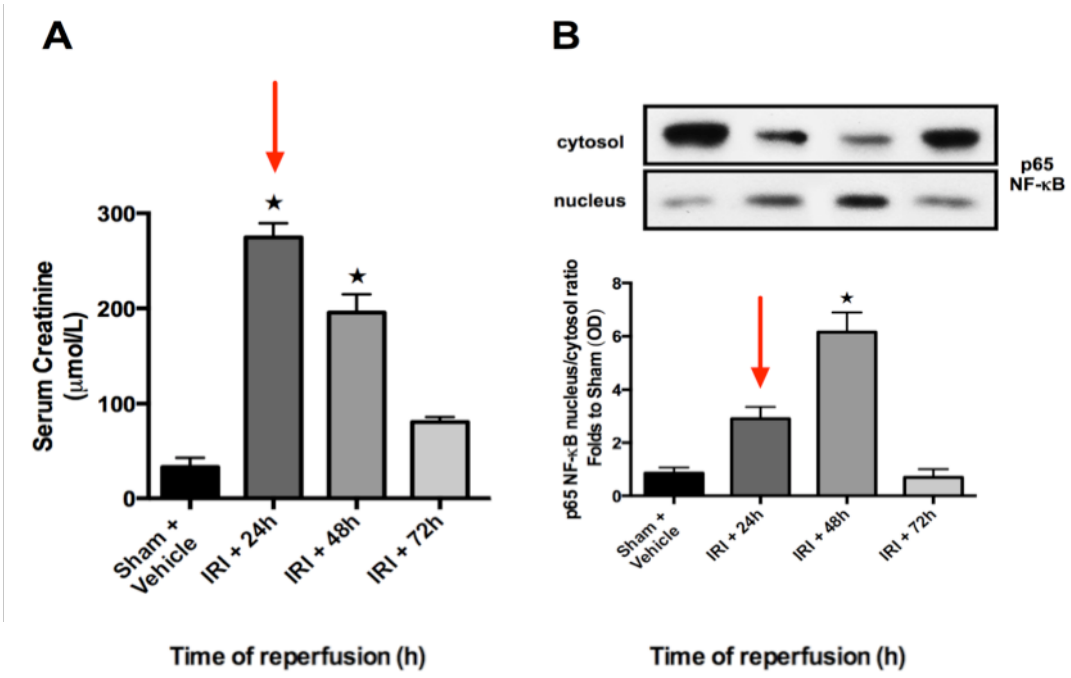

Figure 2.6 The effect of 30 min ischaemia followed by different lengths of reperfusion (24, 48 or 72 h) on serum creatinine (A) a marker of renal function, and on the activation of NF-κB (B) as measured by the p65 nucleus/cytosol ratio. IRI; ischaemia-reperfusion injury. Sham + vehicle: n=4; 24 h post reperfusion: n=4; 48 h post reperfusion: n=8 (Figure A) n= 4 (Figure B); 72 h post reperfusion: n=4. Densitometric analysis of the bands is expressed as relative optical density (OD) of NF-κB p65 subunit expression in both cytosolic and nuclear fractions, and expressing the results as nucleus/cytosol ratio. Each immunoblot is from a single experiment. (B). Data are presented as mean ± SEM of n observations, ★P<0.05 vs. sham + vehicle.

The Effect of Late Inhibition of IKK on Renal, Glomerular and Tubular Function

Having discovered that peak renal dysfunction of the kidney occurs at 24 h of reperfusion and the activation of IKK occurs at 48 h of reperfusion following 30 min of unilateral renal ischaemia, IKK16 was administered 24 h after the onset of reperfusion (which lasted for a total of 48 h). Compared to rats subjected to renal IRI only, treatment of rats with IKK16 (1.0 mg/kg) at 24 h into reperfusion resulted in a significant and substantial attenuation of renal and glomerular and tubular dysfunction at 48 h post reperfusion, while lower doses of IKK16 (0.1 and 0.3 mg/kg) had no significant effect (Figure 2.7).

Group	Serum Urea mmol/L	Serum Creatinine µmol/L	Estimated Creatinine Clearance ml/min/100g bw	Fractional Excretion of Sodium %
Sham + Vehicle	5.50 ± 0.26 *	41.91 ± 1.71 *	0.40 ± 0.03 *	0.9 ± 0.13 *
IRI + Vehicle	34.22 ± 2.53	198.58 ± 21.63	0.09 ± 0.01	4.13 ± 0.57
IRI + IKK16 0.1 mg/kg	31.93 ± 13.28	172.02 ± 60.66	0.08 ± 0.03	4.77 ± 0.82
IRI + IKK16 0.3 mg/kg	27.37 ± 3.11	183.14 ± 28.82	0.10 ± 0.03	4.81 ± 1.38
IRI + IKK16 1.0 mg/kg	16.41 ±1.32 *	80.99 ± 6.47 *	0.25 ± 0.03*	1.42 ± 0.15 *

Figure 2.7 A dose response of the late administration of IKK16 (at 24 h into reperfusion) in a rat model of 30 min of renal ischaemia followed by 48 h of reperfusion on markers of renal, glomerular and tubular function. Serum urea, serum creatinine were measured as indicators of renal function and estimated creatinine clearance were measured as an indicator of glomerular dysfunction, and fractional excretion of sodium as indicator of tubular dysfunction at 48 h of reperfusion. IRI; ischaemia-reperfusion injury. Sham + Vehicle: n=11, 10 % DMSO (1 ml/kg i.v.) 24 h into reperfusion; IRI + Vehicle: n=8, 10 % DMSO (1 ml/kg i.v.) 24 h into reperfusion; IRI + IKK16 0.1 mg/kg: n=5, 0.1 mg/kg IKK16 (1 ml/kg i.v.) 24 h into reperfusion; IRI + IKK16 0.3 mg/kg: n=7, 0.3 mg/kg IKK16 (1 ml/kg i.v.) 24 h into reperfusion; IRI + IKK16 1.0 mg/kg: n=9, 1.0 mg/kg IKK16 (1.0 ml/kg i.v.) 24 h into reperfusion. Data are presented as mean ± SEM of n observations, ★P<0.05 vs. IRI + vehicle.

The delayed administration of 1.0 mg/kg IKK16 24 h post reperfusion significantly attenuated IRI-dependent increases in serum urea (Figure 2.8A) and SCr (Figure 2.8B), and IRI-dependent decreases in the eCCL when compared to control animals administered vehicle, culled at 48 h post reperfusion (Figure 2.8C).

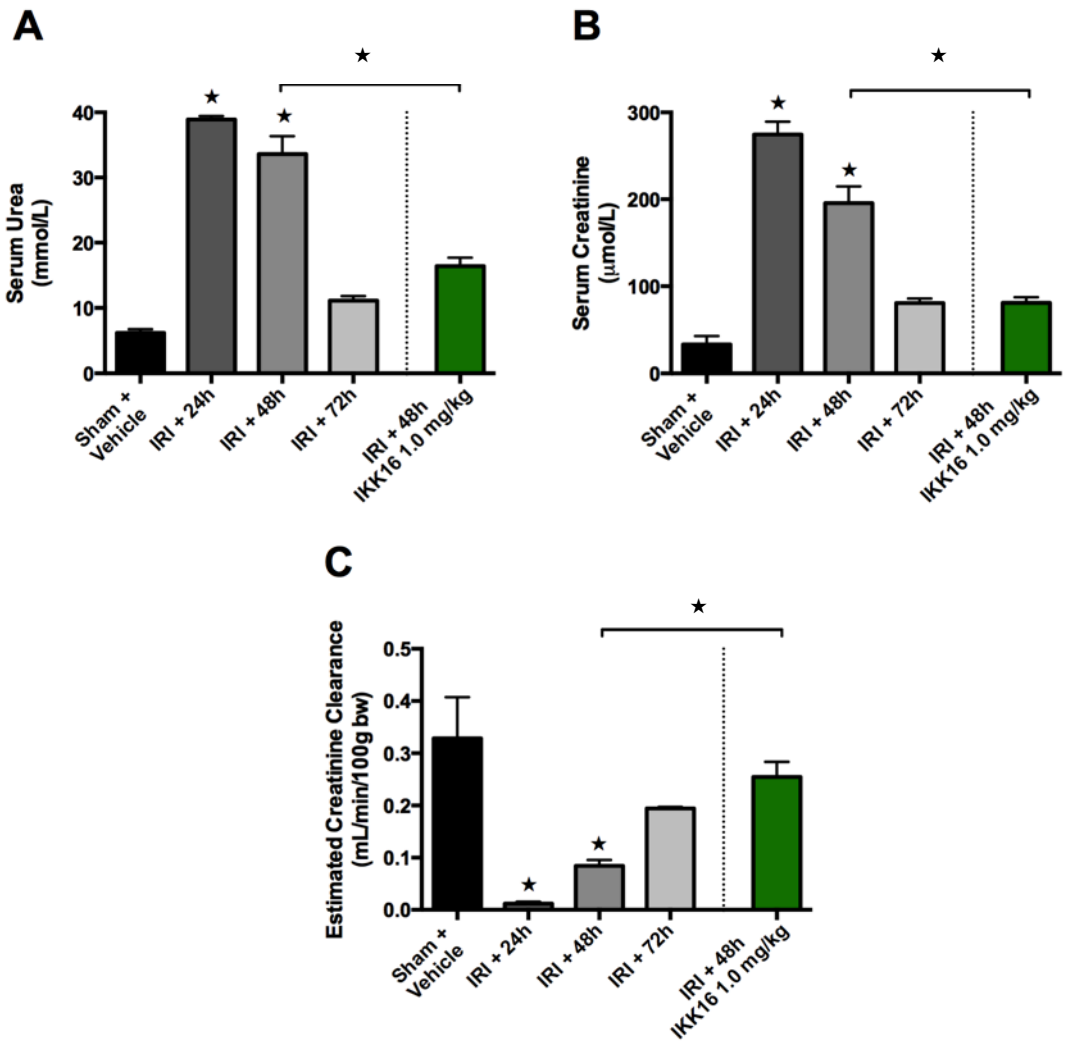

Figure 2.8 The effect of late administration of IKK16 (at 24 h into reperfusion) in a rat model of 30 min of renal ischaemia followed by 48 h of reperfusion on markers of renal and glomerular function, and its comparison to the effect of 30 minutes ischaemia followed by different lengths of reperfusion (0, 24, 48 and 72 h). IRI; ischaemia-reperfusion injury. Serum urea (A), and serum creatinine were measured as indicators of renal function (B) and estimated creatinine clearance (C) was measured as an indicator of glomerular function. Sham + vehicle: n=11; IRI + 24 h: n=4; IRI + 48 h + vehicle: n=8; IRI + 72 h + vehicle: n=4; IRI + 48 h + IKK16 1.0 mg/kg: n=9. Data are presented as mean ± SEM of n observations, ★P<0.05 vs. sham + vehicle.

The delayed administration of 1.0 mg/kg IKK16 24 h post reperfusion significantly attenuated IRI-dependent increases in the $FENa^+$, a measure of tubular function (Figure 2.9).

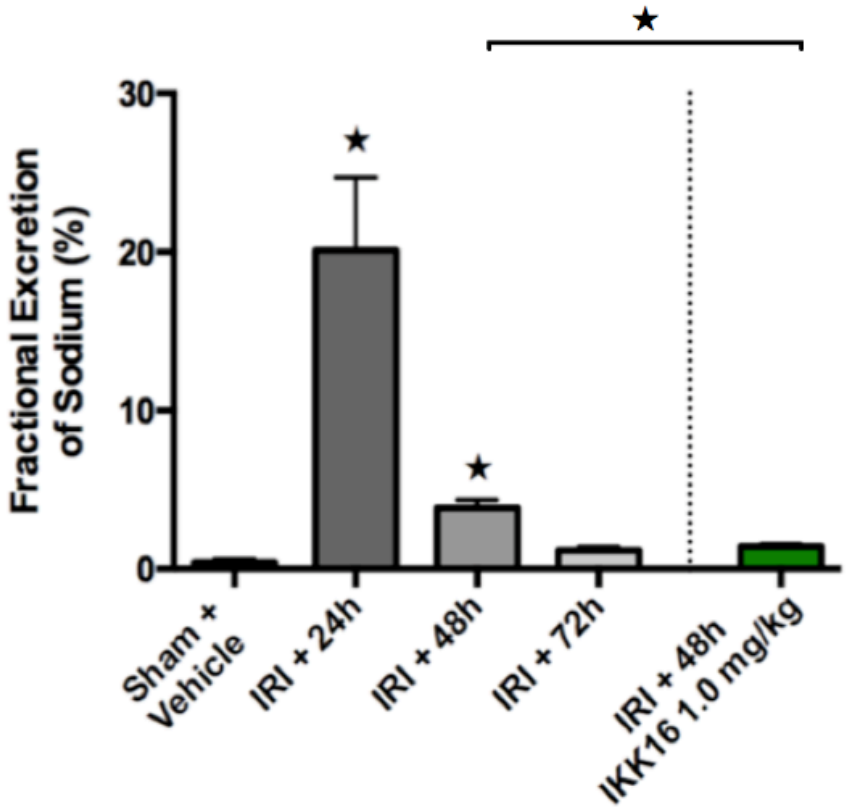

Figure 2.9 Effects of late administration of IKK16 (at 24 h into reperfusion) in a rat model of 30 min of renal ischaemia followed by 48 h of reperfusion on the fractional excretion of sodium, a measure of tubular function, and its comparison to the effect of 30 minutes ischaemia followed by different lengths of reperfusion (0, 24, 48 and 72 h). IRI; ischaemia-reperfusion injury. Sham + Vehicle: n=11; IRI + 24 h: n=4; IRI + 48 h: n=8; IRI + 72 h: n=4; IRI + 48 h + IKK16 1.0 mg/kg: n=9. Data are presented as mean ± SEM of n observations, ⋆P<0.05 vs. sham + vehicle.

When compared with sham-vehicle rats, kidney homogenates prepared from rats that underwent 30 min of unilateral renal ischaemia and 48 h of reperfusion exhibited a significant increase in the phosphorylation of IκBα on $Ser^{32/36}$ (Figure 2.10A) and nuclear translocation of the p65 NF-κB subunit (Figure 2.10B). Interestingly, administration of 1.0 mg/kg IKK16 24 h after the onset of reperfusion significantly attenuated the increase in the phosphorylation of IκBα on $Ser^{32/36}$ (Figure 2.10A) and the subsequent nuclear translocation of the p65 NF-κB subunit (Figure 2.10B) caused by unilateral IRI.

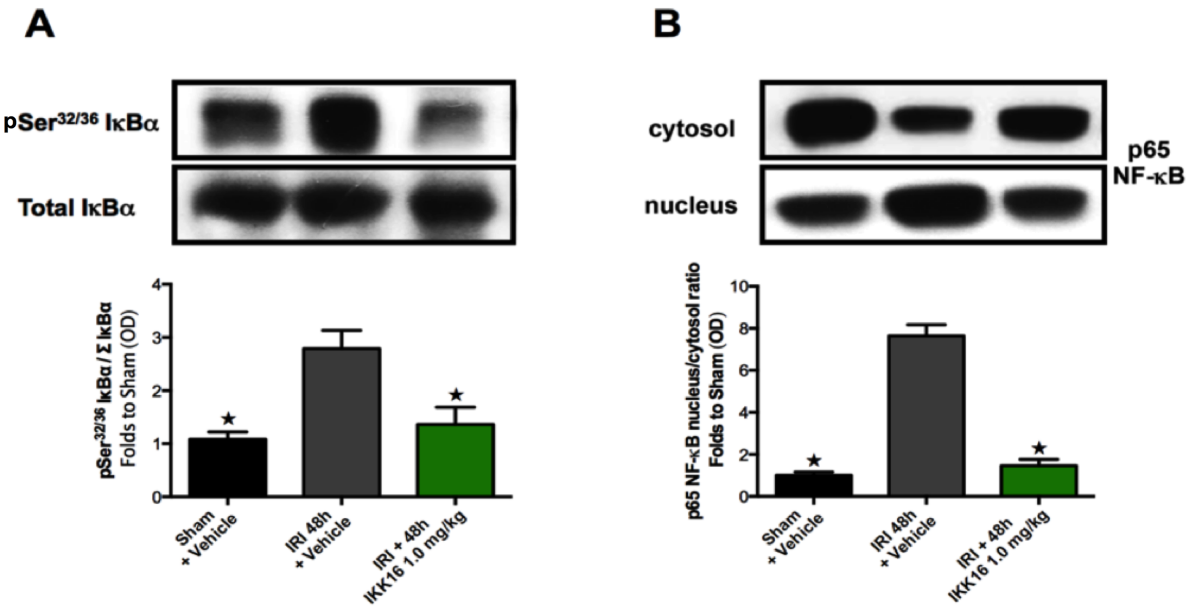

Figure 2.10 The effect of late administration of 1.0 mg/kg IKK16 (24 h into reperfusion) on ischaemia-reperfusion injury on the activation of IκBα and NF-κB nuclear translocation at 48 h of reperfusion. Activation of IκBα (A) was measured as the phosphorylation of $Ser^{32/36}$ on IκBα. The activation of IκBα results in nuclear translocation of the p65 subunit of NF-κB (B). Sham + vehicle: n=4; IRI + 48 h: n=4; IRI + 48 h + IKK16 1.0mg/kg: n=4. IRI; ischaemia-reperfusion injury. Densitometric analysis of the bands is expressed as relative optical density (OD) of IκBα phosphorylation at $Ser^{32/36}$, corrected for the corresponding total IκBα content and normalised using the sham operated band, and NF-κB nuclear translocation was evaluated by measuring NF-κB p65 subunit expression in both cytosolic and nuclear fractions, and expressing the results as nucleus/cytosol ratio. Each immunoblot is from a single experiment. Data are presented as mean ± SEM of n observations, ⋆P<0.05 vs. sham + vehicle. Western blots performed by Massimo Collino & Fausto Chiazza.

To show that the inhibition of IKK by IKK16 was successful, the phosphorylation of IKK at $Ser^{176/180}$ was measured to confirm its activation. When compared with sham-vehicle rats, kidney homogenates prepared from rats that underwent 30 min of unilateral renal ischaemia and 48 h of reperfusion exhibited a significant increase in the phosphorylation of IKKα/β at $Ser^{176/180}$ (Figure 2.11). The administration of 1.0 mg/kg IKK16 24 h after the onset of reperfusion significantly attenuated the increase in the phosphorylation of IKKα/β on $Ser^{176/180}$ caused by unilateral IRI (Figure 2.11).

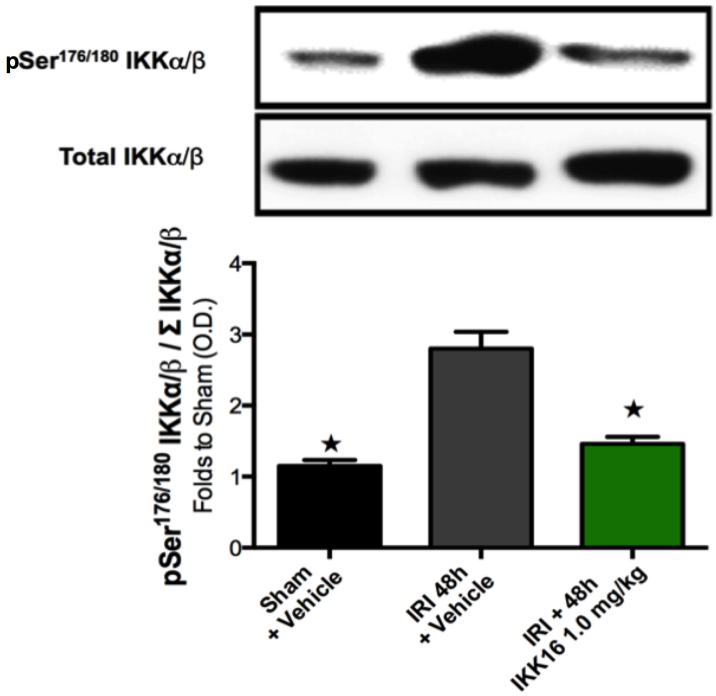

Figure 2.11 The effect of late administration of 1.0 mg/kg IKK16 (24 h into reperfusion) on ischaemia-reperfusion injury on the activation of IKKα/β at 48 h of reperfusion. Activation of IKKα/β was measured as the phosphorylation of $Ser^{176/180}$ on IKKα/β. The activation of IKKα/β results in nuclear translocation of the p65 subunit of NF-κB. Sham + vehicle: n=4; IRI + 48 h: n=4; IRI + 48 h + IKK16 1.0mg/kg: n=4. IRI; ischaemia-reperfusion injury. Densitometric analysis of the bands is expressed as relative optical density (OD) of IKKα/β phosphorylation at $Ser^{176/180}$, corrected for the corresponding total IKKα/β content and normalised using the sham operated band. Each immunoblot is from a single experiment. Data are presented as mean ± SEM of n observations, ★$P<0.05$ vs. sham + vehicle. Western blots performed by Massimo Collino & Fausto Chiazza.

The Effect of Late Inhibition of IKK on the Phosphorylation of eNOS in the Rat Kidney

Rats subject to 30 min of unilateral renal ischaemia demonstrated a significant reduction in the phosphorylation of Ser^{1177} on eNOS when compared to sham-vehicle rats (Figure 2.12). The administration of 1.0 mg/kg IKK16 24 h after the onset of reperfusion also successfully attenuated the IRI-dependent decrease in the phosphorylation of Ser^{1177} on eNOS (Figure 2.12).

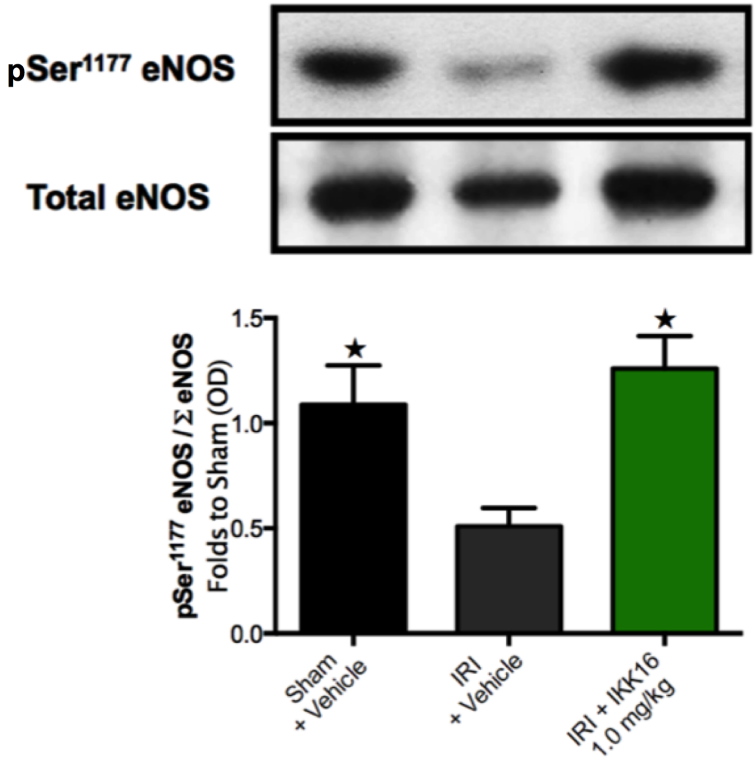

Figure 2.12 The effect of late administration of 1.0 mg/kg IKK16 (24 h into reperfusion) on ischaemia-reperfusion injury on the activation of endothelial nitric oxide synthase (eNOS) at 48 h of reperfusion. The activation of eNOS was measured as phosphorylation of Ser^{1177}. Sham + vehicle: n=4; IRI + 48 h: n=4; IRI + 48 h + IKK16 1.0mg/kg: n=4. IRI; ischaemia-reperfusion injury. Densitometric analysis of the bands is expressed as relative optical density (OD) of eNOS phosphorylation at Ser^{1177}, corrected for the corresponding total eNOS content and normalised using the sham operated band. Each immunoblot is from a single experiment. Data are presented as mean ± SEM of n observations, ★P<0.05 vs. IRI 48 h + vehicle. Western blots performed by Massimo Collino & Fausto Chiazza.

Effect of Time on Renal Injury post Ischaemia-Reperfusion and the Effect of Late Inhibition of IKK on Tubular Dilatation

When compared to baseline (sham animals), rats that underwent 30 min of unilateral renal ischaemia developed histological signs of significant renal injury at 48 h of reperfusion, such as glomerular shrinkage, tubular dilatation, basophilia, necrosis and luminal congestion (Figure 2.13).

When compared with sham-operated rat kidneys (Figure 2.13A), kidneys from rats that underwent 30 min of unilateral renal ischaemia and 48 h of reperfusion (Figure 2.13C), and 72 h of reperfusion (Figure 2.13D) exhibited a significant degree of renal injury (tubular dilatation), which was significantly reduced by administration of IKK16 (1.0 mg/kg; at 24 h after the onset of reperfusion; Figure 2.13 E, F).

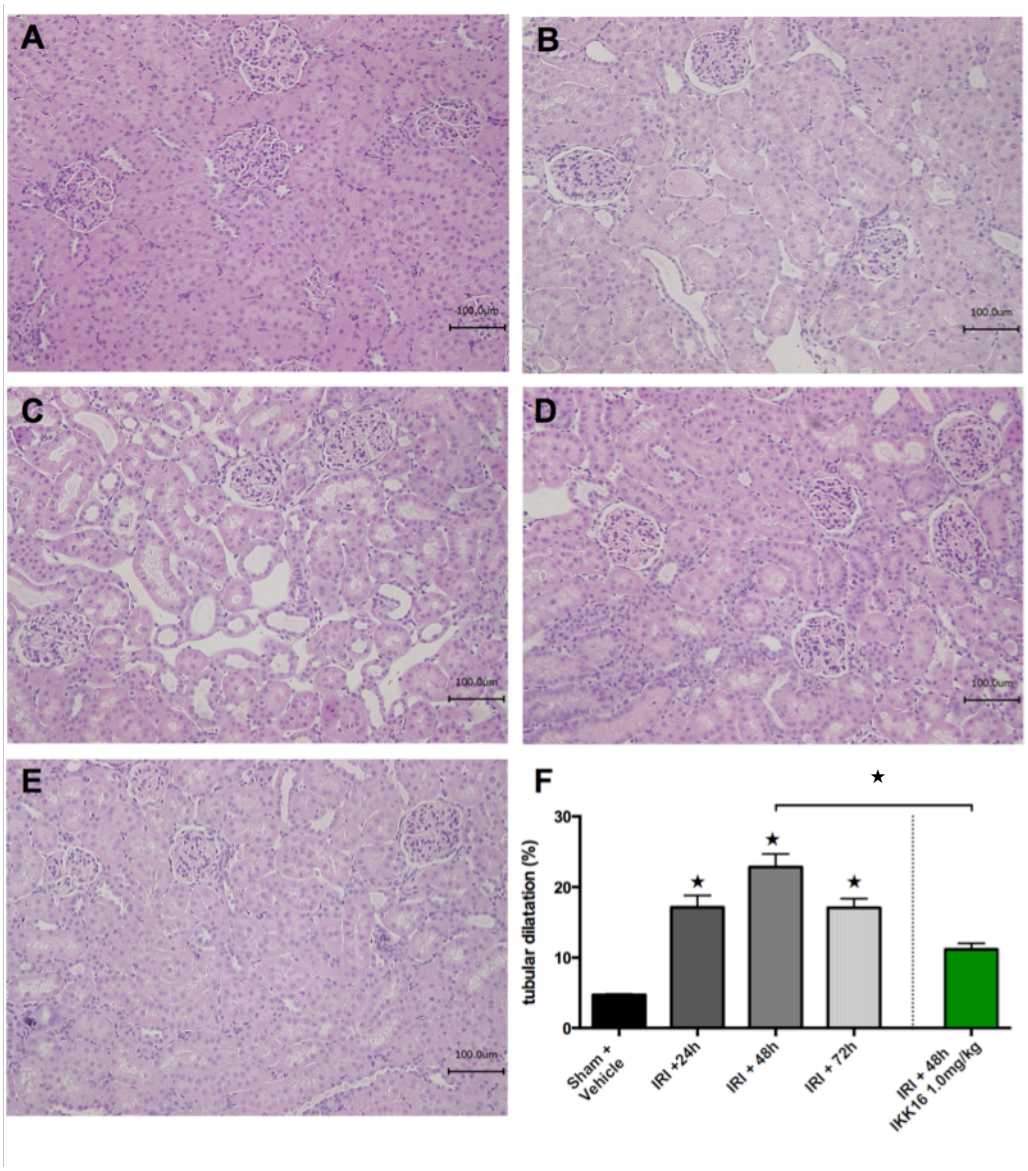

Figure 2.13 The effect of late administration of IKK16 (24 h into reperfusion) on ischaemia-reperfusion injury on histological injury subsequent to 30 min ischaemia and 48 h reperfusion. IRI; ischaemia-reperfusion injury. Representative histological H&E images of rat renal tissue were taken from sham + vehicle (A), after 24 h of reperfusion, IRI + 24 h (B) after 48 h of reperfusion, IRI + vehicle (C), after 72 h of reperfusion, IRI + 72 h (D) and after 48 h of reperfusion with treatment of IKK16 (1.0 mg/kg i.v.) 24 h into reperfusion (E). IRI: ischaemia-reperfusion injury. Ten randomly selected fields from three individual kidneys (n=3) per group were selected and analysed (total fields per group = 30) for the determination of percentage background white space using ImageJ software and represented as percentage tissue surface area per field (F). Data are presented as mean ± SEM of n observations, ⋆P<0.05 vs. sham + vehicle

Discussion

In this chapter, I have characterised the time course of AKI in a rat model of renal IRI. Thirty min of ischaemia caused a significant renal (as demonstrated by serum urea and SCr), glomerular (as demonstrated by the eCCL) and tubular (as demonstrated by the $FENa^+$) dysfunction after 24 h of reperfusion, with subsequent reversal towards baseline after this period. AKI is a reversible condition; in this chapter I have demonstrated an acute injury phase, with function returning to near baseline after 72 h of reperfusion. The AKIN guidelines state that the definition for AKI is 'an abrupt (within 48 h) reduction in kidney function currently defined as an absolute increase in SCr of more than or equal to 0.3 mg/dl (≥26.4μmol/l), a percentage increase in SCr of more than or equal to 50% (1.5-fold from baseline), or a reduction in urine output (documented oliguria of less than 0.5ml kg/h for more than 6 h)' (Mehta et al., 2007). The IRI time course here demonstrates a similar increase in SCr at 48 h post reperfusion as described in the AKIN guidelines (sham + vehicle 41.91±1.71 to 198.58±21.63). The urine output was not measured in the first 24 h after IRI in these animals due to home office regulations.

In addition to studying the renal function of these animals, I measured the activation of IκB and IKK and the NF-κB nucleus to cytosol ratio. NF-κB is activated in inflammatory states such as AKI (Sanz et al., 2010) by a wide range of stimuli e.g. TLR activation (TLR2 and TLR4 in renal IRI) (Mudaliar et al., 2013), TNF-α (Donnahoo et al., 2000) and angiotensin II (Ono et al., 2015). In this chapter, I have demonstrated a significant increase in the p65 NF-κB nucleus/cytosol ratio (indicating nuclear translocation of p65), the phosphorylation

of IKKα/β at $Ser^{176/180}$ and the phosphorylation of IκBα at $Ser^{32/26}$ in the renal tissue at 48 h post reperfusion. The phosphorylation of IKKα/β at $Ser^{176/180}$ indicates IKK activation, which in turn causes phosphorylation of $Ser^{32/36}$ on IκBα. IκBα then dissociates from NF-κB, resulting in NF-κB translocation to the nucleus and DNA transcription of inflammatory genes. Similarly, Patel et al. (2012) have demonstrated an increase in the p65 NF-κB nucleus/cytosol ratio at 48 h in a bilateral rat model of IRI (Patel et al., 2012). At 72 h post reperfusion, the phosphorylation of IKKα/β at $Ser^{176/180}$, the phosphorylation of IκBα at $Ser^{32/26}$ and the p65 nucleus/cytosol ratio return to sham-like levels, indicating an acute inflammatory period.

Furthermore, at 48 h post reperfusion, the phosphorylation of eNOS at Ser^{1177} was significantly reduced when compared to sham animals. The degree of IRI is directly proportional to the activity of eNOS: more severe IRI is associated with a lower eNOS expression (Shoskes et al., 1997), and the generation of superoxide radicals (Noiri et al., 2001). Reduced eNOS expression in this case may be explained by eNOS 'coupling' and 'uncoupling'. eNOS is a homodimer consisting of an oxygenase and a reductase domain (Raman et al., 1998). Upon activation, eNOS dissociates from caveolin-1 (to which it is constitutively bound) (Gratton et al., 2000). Electron flow is generated by the oxidation of NADPH to $NADP^+$, and the electrons continue through flavin adenine dinucleotide (FAD) and flavin mononucleotide (FMN) in the reductase domain. The cofactor tetrahydrobiopterin (BH4) is critical in this reaction, facilitating the interaction between the reductase and oxygenase domains (Raman et al., 1998), passing the electron flow from FMN in the reductase domain into the haem complex of the oxygenase domain. Here, NO

is produced from molecular oxygen, via the oxidation of L-arginine to L-citrulline. The role of BH4 in this pathway is described as being 'coupled' to eNOS (Schmidt and Alp, 2007) (Figure 2.12). In pathological conditions, including ischaemia, the level of BH4 is limiting or absent (Channon, 2004). This causes the electron transfer from the flavins to L-arginine oxidation to become 'uncoupled', producing superoxide from molecular oxygen (Schmidt and Alp, 2007) (Figure 2.12). BH4 therefore is critical for the normal function of eNOS, which when 'uncoupled' causes oxidative stress to tissues. The activation of eNOS is measured at multiple sites, the most studied include Ser^{1177}, the activation site, which is only possible to measure when eNOS is coupled, and Thr^{495}, the inhibitory site (Chen et al., 1999).

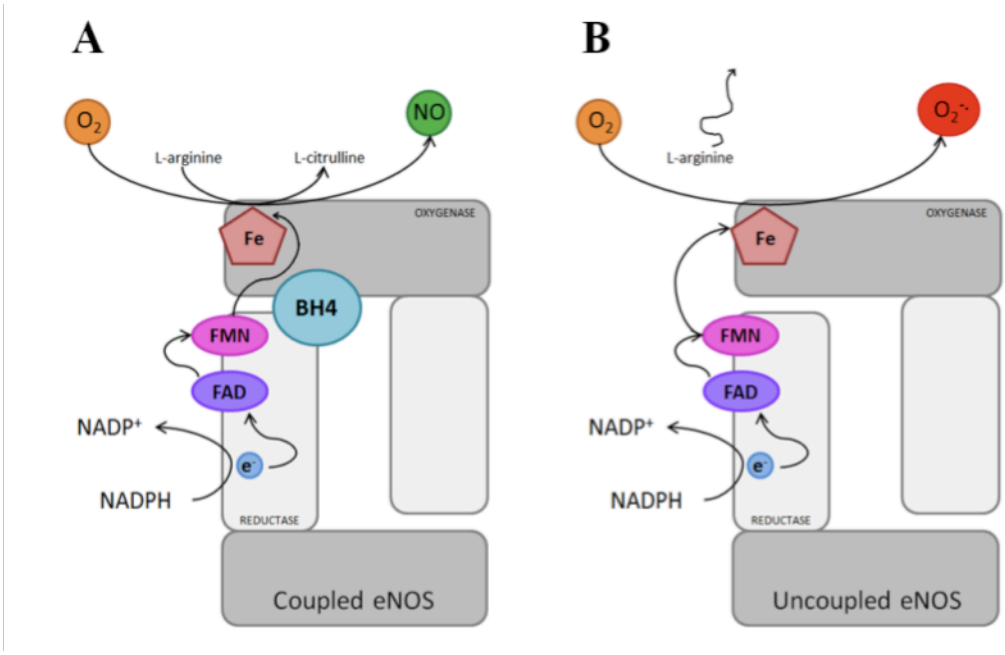

Figure 2.12 The mechanism of eNOS A) coupling and B) uncoupling. When eNOS is coupled, oxidation of NADPH to NAPD+ generates electron flow, through flavins FAD and FMN in the reductase domain of the enzyme. Electron flow to the oxygenase domain is facilitated by tetrahydrobiopterin (BH4) where the catalysation of L-arginine is oxidated to L-citrulline occurs (A). BH4 is limited or absent when eNOS is 'uncoupled', causing electron transfer to from the flavins to L-arginine to become uncoupled. eNOS now produces superoxide radicals, causing oxidative stress in tissue (B). NADPH, nicotinamide adenine dinucleotide phosphate; NADP, the oxidised form of NADPH; FAD, flavin adenine dinucleotide; FMN flavin mononucleotide; BH4, tetrahydrobiopterin; Fe, the ferrous- dioxygen complex; O2, molecular oxygen; NO, nitric oxide; O2-.superoxide. Adapted from (Channon, 2004).

Previous studies have similarly demonstrated a decrease in eNOS expression post IRI at both 24 h (Zhang et al., 2014) and 48 h (da Costa et al., 2015) when compared to sham-operated animals. I therefore propose that eNOS is uncoupled at 48 h post reperfusion in this model of renal IRI.

As there are no proven medical therapies to improve short-term prognosis of AKI (Heung and Chawla, 2012), i.e. to aid recovery or tissue repair, I have sought to identify a novel drug target to attenuate the course of AKI during its development (not as a pre-treatment and not on reperfusion, but after initiation of disease). In this study, I have identified the development of AKI using SCr and eCCL to be at 24 h after the onset of reperfusion (peak dysfunction). Patients with AKI present with high SCr, which is usually diagnosed between 24 and 72 h after the insult (Bagshaw et al., 2010). Using the time course data generated so far, I decided to treat the animals at 24 h post reperfusion as this was i) the peak of renal dysfunction measured in these animals, (increases in serum urea, SCr and the $FENa^{+}$, and a decrease in the eCCL) and ii) prior to NF-κB activation (as shown by the p65 nucleus/cytosol ratio).

With this information, I selected an IKK inhibitor, IKK16, screened from a Novartis compound archive for 'hits' with a typical kinase motif and the dose range for this study determined based on previously calculated IC_{50} values (Waelchli et al., 2006). Animals were administered 0.1, 0.3 or 1.0 mg/kg IKK16 i.v. at 24 h post reperfusion. Lower doses of IKK16 (0.1 and 0.3 mg/kg) had no significant effects of any of the biochemical parameters measured, however the administration of 1.0 mg/kg IKK16 at 24 h after the onset of reperfusion significantly attenuated markers of renal and glomerular dysfunction (as measured by SCr, urea and eCCL) and

tubular dysfunction (as measured by $FENa^+$). For the purpose of this thesis, the dose of 1.0 mg/kg IKK16 was used for all further experiments.

The activation of IκBα and the translocation of the NF-κB p65 subunit from the nucleus to the cytosol were abolished following the inhibition of IKK with IKK16 at 24 h of reperfusion. Further to this, the phosphorylation of IKKα/β was attenuated by the administration of IKK16. These results indicate that 1.0 mg/kg IKK16 was sufficient to inhibit IKK, preventing IκBα phosphorylation, IKK activation and subsequent NF-κB dissociation and translocation to the nucleus for the transcription of inflammatory genes. In both clinical and pre-clinical renal IRI, NF-κB activation plays a major role in the inflammatory response, regulating the cell biology of neutrophils, macrophages, lymphocytes and dendritic cells (Sanz et al., 2010). Previous studies have inhibited NF-κB via decoy DNA oligodeoxynucleotides, attenuating renal IRI injury, MCP-1, ICAM-1, (and therefore monocyte/macrophage infiltration), iNOS and ET-1 expression compared to control animals, highlighting the impact NF-κB has on the inflammatory response post IRI (Cao et al., 2004). The inhibition of IKKβ with siRNA 48 h prior to renal IRI *in vivo*, caused a significant reduction in macrophage infiltration, NF-κB DNA binding activity, NGAL and IL-18 expression (Wan et al., 2011a). I anticipate that if measured, there would be a similar attenuation in inflammatory markers in my model after the inhibition of IKK, due to the successful inhibition of IKK, the prevention of NF-κB nuclear translocation and therefore the reduction in inflammatory gene transcription.

Interestingly, the inhibition of IKK with a single dose of IKK16 administered 24 h post reperfusion restored the IRI-dependent decrease in the level of eNOS in the kidney tissue. eNOS is upstream of IKK, however, Chen et al. (2002) have demonstrated that heat shock protein 90 (hsp90), a molecular chaperone protein important in eNOS regulation, binds IKKα and IKKβ at their kinase domains (Chen et al., 2002). Hsp90 interacts with eNOS and Akt (involved in cell survival) functioning as a 'scaffold', facilitating Ser^{1177} phosphorylation when eNOS is activated (Fontana et al., 2002). Mohan et al. (2009) have previously inhibited IKKβ expression by wedelolactone (an IKKβ inhibitor) or by siRNA in endothelial cells subject to high glucose conditions. The inhibition of IKKβ resulted in an increased eNOS-Hsp-90 interaction and a subsequent increase in NO production, demonstrating eNOS re-coupling (Mohan et al., 2009). Aside from the high glucose conditions, the resultant uncoupling of eNOS and the production of superoxide radicals (Lin et al., 2005) mirrors the pathogenesis of IRI. These experiments have only been performed in malignant or transformed cell lines however, and have yet to be confirmed *in vivo.*

The restoration of phosphorylated eNOS to sham-like levels in IKK16 treated animals is beneficial, as NO production causes local vasodilatation, inhibition of platelet aggregation and is involved in the regulation of angiogenesis (Luque Contreras et al., 2006). Compounds which restore eNOS coupling and NO production are beneficial in the treatment of renal IRI. I speculate that IKK16 administration inhibits IKK, resulting in an increase in eNOS-Hsp90 interaction. An increase in eNOS-Hsp90 interaction causes Ser^{1177} phosphorylation and the consequent 're-coupling' of eNOS (and therefore an increase in the production of

NO). The mechanism of this is still unclear as the relationship of IKK and eNOS has yet to be described further.

In addition to functional data, kidney sections were stained with H&E to analyse structural changes before and after renal IRI. Using Image J software I quantified tubular dilatation in each image. In this chapter, I demonstrate a significant increase in tubular dilatation at 24, 48 and 72 h post IRI, a hallmark of AKI pathology. The inhibition of IKK at 24 h post reperfusion significantly reduced tubular dilatation. It was previously thought that the kidney had the ability to recover completely both functionally and structurally after acute injury (Sharples, 2007), however this was dispelled recently as tubules may exhibit growth arrest, failure to redifferentiate and atrophy post AKI, which may aid a prolonged inflammatory state, the production of fibrosis and the development of CKD (Venkatachalam et al., 2015). The delayed administration of IKK may, therefore, accelerate the rate of structural recovery and potentially retard the development of fibrosis. This will be discussed in greater detail in the next chapter.

In this chapter, I have studied the time course of AKI, presenting the activation of NF-κB over a 72 h reperfusion period following 30 min of IRI. Using this time course I decided to treat the animals 24 h post reperfusion at the peak of renal dysfunction (maximal SCr) and before the activation of NF-κB. The inhibition of IKK successfully attenuated renal dysfunction and structural alterations seen in AKI, likely caused by a reduction in the transcription of inflammatory genes resulting in a reduction in excessive inflammation. Moreover, I have shown in this chapter that renal IRI causes a significant decrease in eNOS phosphorylation at

Ser^{1177} (eNOS 'uncoupling') at 48 h post reperfusion, which was restored and possibly 'recoupled' by the delayed inhibition of IKK at 24 h post reperfusion. The most interesting and novel finding presented in this chapter is that renal IRI may be successfully treated at 24 h post reperfusion, during peak SCr, at which time AKI is diagnosed.

Chapter III

The Delayed Administration of IKK16 Reduces Renal Fibrosis After an Extended Reperfusion Period in a Rat Model of Renal Ischaemia-Reperfusion Injury

Introduction

It is now widely recognised that AKI is a major risk factor for CKD even in those patients who regain full renal function post AKI (Hsu, 2012). For patients who recover from AKI, there is a 25% increase in the risk of CKD, and this is associated with a mortality rate of up to 50% after 10 years (Bucaloiu et al., 2012). AKI to CKD progression has been demonstrated in both the clinical (Hsu, 2012), and the pre-clinical setting (experimental animal models) (Basile et al., 2001) (Clements et al., 2013). Progression from AKI to CKD is associated with a series of inflammatory changes in the kidney including tubular injury, tubular obstruction, vascular injury, endothelial cell activation and leukocyte recruitment (Isaac et al., 2007) (Arfian et al., 2012). Following AKI, prolonged inflammation, and maladaptive or incomplete regenerative processes encourage the development of fibrosis and CKD (Lee and Kalluri, 2010), which may or may not result in ESRD.

Common animal models used to study CKD include the 5/6 nephrectomy model (5/6 of the kidney mass is removed resulting in a reduction in GFR and the development of fibrosis), and the UUO model (ureteral ligation causes back leak of urine and increased pressure in the kidney resulting in a widespread tubulointerstitial fibrosis, which is not dissimilar to human disease) (Chevalier et al., 2009). However, in light of new clinical data describing the progression of AKI to CKD following the development of renal fibrosis, a new approach to studying its pathophysiology has emerged. Now, extension of the reperfusion period of the renal IRI model for a number of weeks gives a more accurate representation of the clinical situation. The renal IRI may be bilateral, unilateral, or unilateral with contralateral nephrectomy. Previously, the acute phase of AKI was studied in great

detail and experiments terminated soon after injury, with the assumption that the complete functional recovery is associated with complete structural recovery (Sharples, 2007). However, it is now known that even one episode of ischaemia may lead to the production of fibrotic tissue (Azuma et al. 1997). Models of AKI with an extended reperfusion period have been used to target multiple proteins and receptors, such as αKlotho (a cytoprotective protein) (Shi et al., 2015), IL-34 (upregulated after IRI, worsening subsequent fibrosis) (Baek et al., 2015) and antagonism of the mineralcorticoid receptor (Barrera-Chimal et al., 2013), to name a few. The role of IKK has not yet been studied in progression of AKI to CKD; however, non-specific GSK-3 inhibitors have been studied in a similar model (Singh et al., 2015). GSK-3 is a kinase that converges many signalling pathways, and has the ability to phosphorylate more than 40 proteins (Jope and Johnson, 2004). GSK-3 inhibitors inhibit NF-kB, however, as GSK-3 is involved in the Wnt pathway and insulin signalling, it is impossible to say with certainty that the effects of these inhibitors is through NF-kB inhibition alone (Ansaldi et al., 2011). Singh et al. (2015) used a mouse model of bilateral IRI with either pre- (GSK-3 inhibitor TDZD 1 hr prior to surgery and once per day thereafter for 12 days) or post (GSK-3 inhibitor TDZD 48 h after surgery and once per day thereafter for 12 days) ischaemia, concluding that GSK-3 could promote fibrosis of the kidney through the activation of TGF-β signalling pathways (Singh et al., 2015). TDZD has previously been shown to decrease the activity of NF-kB in a rat model of myocardial IRI (Gao et al., 2009).

I decided to target IKK as it is directly upstream of NF-kB, and may play a role in the development of fibrosis. NF-kB has previously been shown to be activated in CKD; in rats, adenine diet-induced CKD exhibited a prolonged activation of NF-kB

and a significant development of fibrosis when compared to rats given a normal chow diet (Vaziri et al., 2014).

The role of IKK in renal fibrosis has yet to be described. However, early IKK inhibition has proven to be an effective therapeutic target in other fibrotic diseases. The early inhibition of IKK, i.e. before and during the development of injury, in a mouse model of non-alcoholic fatty liver disease successfully attenuated the formation of myofibroblasts (Wei et al., 2011). In addition, the constitutive activation of IKKβ in cardiomyocytes in an inducible transgenic mouse model resulted in heart failure with concomitant collagen deposition (Maier et al., 2012) suggesting IKK to be an important inducer of fibrosis following inflammation. Furthermore, the inhibition of IKK suppresses airway remodelling in a mouse model of chronic asthma, via the attenuation of collagen formation, myofibroblast formation and total TGF-β1 production and activation (Ogawa et al., 2011).

In this chapter, I sought out to determine the effect of IKK inhibition on an extended reperfusion period following renal IRI, to see whether early reduction in renal dysfunction and injury after the delayed administration (at 24 h) of an IKK inhibitor, IKK16 (as seen in Chapter II), would prevent subsequent development of fibrosis (and consequent CKD). I used Sirius red staining as a marker of collagen deposition, and analysed whole cross sections of rat kidneys to study the effect that IKK inhibition has on the development of renal fibrosis.

Methods and Materials

Animal experiments were carried out as previously described in Chapter II, however the reperfusion period was extended up to 28 days. This study was carried out on 45 male Wistar rats. Three animals were excluded from the study due to early mortality, a likely consequence of insufficient reperfusion of the kidney following renal IRI. Mortality occurred in the first three days post-IRI. Surviving animals gained significant weight and displayed no signs of illness from days 4-28.

Experimental Design

Renal Ischaemia-Reperfusion injury, with extended reperfusion period

Rats were randomly allocated into the following groups: (i) **Sham + vehicle**: n=8 (i) **1 day post reperfusion**: n=4; (iii) **2 days post reperfusion**: n=4; (iv) **7 days post reperfusion**: n=4; (v) **14 days post reperfusion**: n=4; (vi) **28 days post reperfusion**: n=7; (vii) **1.0 mg/kg IKK16 24 h post reperfusion + 7 day reperfusion**: n=7; (viii) **1.0 mg/kg IKK16 24 h post reperfusion + 28 day reperfusion**: n=7. Rats were administered vehicle (10% DMSO) or IKK16 24 h after the onset of reperfusion via the tail vein at a volume of 1 ml/kg. IKK16 was purchased from Tocris Bioscience (R&D systems Europe, Abingdon, UK), and used at the previous efficacious dose of 1.0 mg/kg as determined in chapter II.

Measurement of biochemical parameters

All biochemical markers in serum and urine were measured in a blinded fashion by a commercial veterinary testing laboratory (IDEXX Ltd, West Sussex, UK). Parameters measured were described as in Chapter II.

Picrosirius Red Staining

Sections were deparraffinized and rehydrated through graded alcohols to distilled water. Sections were treated with phosphomolybdic acid (Polysciences, Warrington, PA), rinsed in distilled water and stained with picrosirius red (Polysciences, Warrington, PA) for 60 min at room temperature. Sections were then immediately immersed in hydrochloric acid for 2 min (Polysciences, Warrington, PA) before being dehydrated through graded alcohols and cleared. Images of whole cross sections were taken with a Nanozoomer Digital Pathology Scanner (Hamamatsu Photonics K.K., Japan), and quantification of Sirius red performed using ImageJ analysis software. Sirius Red staining was used to measure collagen deposition.

Immunohistochemistry

Sections cut at 4 μm were de-waxed, and deparaffinized to phosphate-buffered saline (PBS). Antigen retrieval was performed by microwaving (700W) sections in citrate buffer (pH 6.0) for 15 min. Once cooled, sections were incubated with 0.03% H_2O_2 for 20 min to inactivate endogenous peroxidases (Dako EnVision+ System-HRP-DAB, K4010), and subsequently treated with 10% normal goat serum (Dako, UK) to reduce non-specific absorption. Sections were subsequently incubated at 37^{o}C for 1 h with the following primary antibodies: anti-α-SMA antibody (1:400, cat#ab5694, Abcam, UK) or anti-CD68 antibody ED1 (1:400;

cat#MCA341R, AbD Serotec, UK), washed with PBS and then incubated at room temperature for 30 min with labelled polymer-HRP antibody (Dako EnVision+ System-HRP-DAB). Sections were developed in DAB chromagen solution, and the reaction stopped by immersion of sections in water. Counterstaining was performed with Harris haematoxylin before sections were dehydrated and mounted in DPX mounting medium. Images of whole sections (for α-SMA analysis) and ten images per section (for $CD68^+$ analysis) were acquired with a Nanozoomer Digital Pathology Scanner (Hamamatsu Photonics K.K., Japan), in a double-blinded manner. Quantification of staining was then performed using ImageJ analysis software.

Western Blots

Western blots were performed in the same fashion as described in chapter II. Membranes were incubated with primary antibody; rabbit anti-TGF-β (1:1000, cat#ab66043); rabbit anti-fibronectin (1:1000, cat#ab2413, Abcam, UK); rabbit anti-pSmad2 $Ser^{465/467}$/Smad3 $Ser^{423/425}$ (1:1000, cat#D27F4, Cell Signalling Technologies, MA); rabbit anti-Smad2/3 (1:1000, cat#D7G7, Cell Signalling Technologies, MA); rabbit anti-vimentin (1:1000, cat#D21H3, Cell Signalling Technologies, MA). The blots were then incubated with the appropriate secondary antibody conjugated with horseradish peroxidase (dilution 1:10000) and developed using the ECL detection system. The immunoreactive bands were visualized by autoradiography. The membranes were stripped and incubated with rabbit glyceraldehyde-3-phosphate dehydrogenase (GADPH) antibody (1:1000, cat#D16H11, Cell Signalling Technologies, MA) instead of β-actin due to the involvement of β-actin the in cytoskeleton.

Materials

Unless otherwise stated, all compounds used in this study were purchased from Sigma-Aldrich Company Ltd. (Poole, Dorset, U.K.).

Statistical Analysis

All values described in the text and figures are expressed as mean±SEM for *n* observations. Each data point represents biochemical measurements obtained from up to 11 separate animals. Statistical analysis was carried out using GraphPad Prism 6.0b (GraphPad Software, San Diego, California, USA). Data without repeated measurements was assessed by one-way ANOVA followed by Bonferroni's multiple-comparison *post hoc* test. Linear regressions were calculated by the least squares method and their significance were estimated by a Fisher *F* test. A *P* value of less than 0.05 was considered to be significant.

Results

The Effect of 28 days Reperfusion on Renal Functional Biomarkers Following Renal Ischaemia-Reperfusion Injury

After an extended reperfusion period of 28 days, animals subject to 30 min of unilateral renal ischaemia and administered either vehicle or IKK16 24 h post reperfusion demonstrated no significant differences in serum urea or SCr when compared to sham animals (Figure 3.1A and 3.1B)

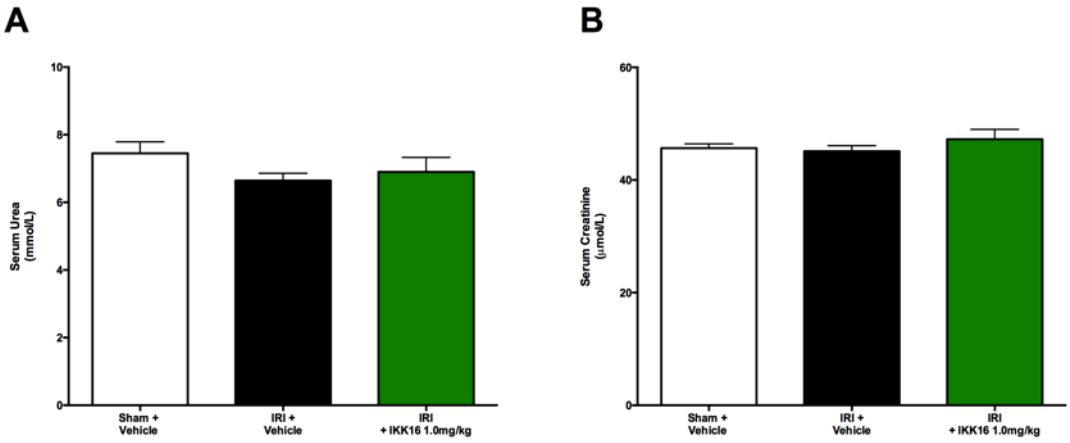

Figure 3.1 The effect of an extended reperfusion period (28 days) after 30 min renal ischaemia on markers of renal function. (A) Serum urea and (B) serum creatinine were measured as indicators of renal function. Sham + vehicle: n=4; IRI + vehicle: n=8; IRI + IKK16 1.0 mg/kg: n=7. Data are presented as mean ± SEM of *n* observations.

The Effect of 28 days Reperfusion on Kidney Weight Following Renal Ischaemia-Reperfusion Injury

Compared to sham animals, animals subject to 30 min of ischaemia and 28 days of reperfusion administered either vehicle control or IKK16 24 h post reperfusion demonstrate significant increases in the kidney weight as % of body weight. There was no significant difference between vehicle control or IKK16 treated groups (Figure 3.2).

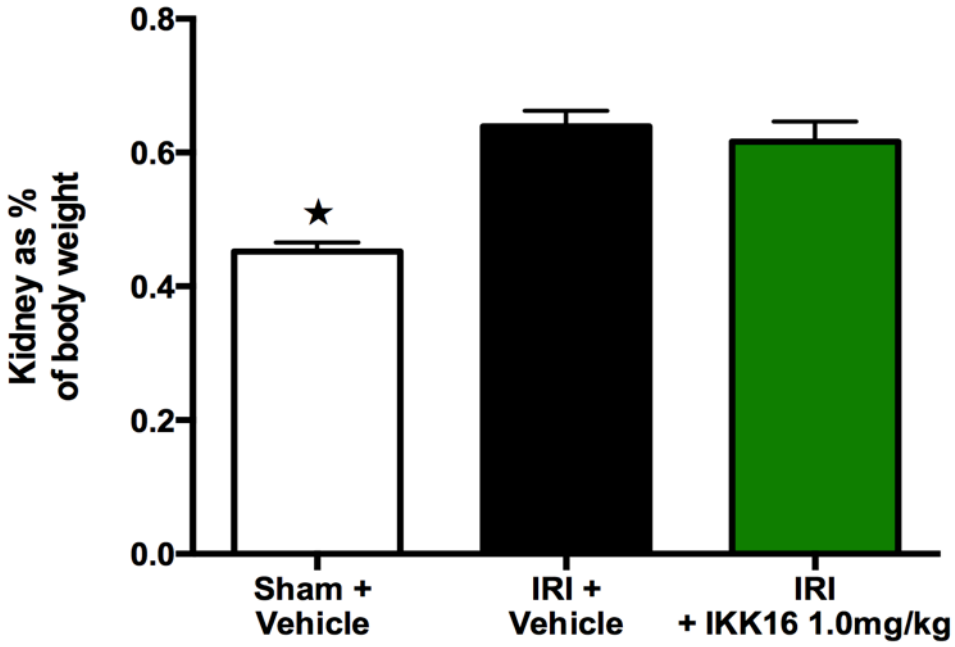

Figure 3.2 The effect of an extended reperfusion period (28 days) after 30 min renal ischaemia on kidney weight as a percentage of total body weight. Sham + vehicle: n=4; IRI + vehicle: n=8; IRI + IKK16 1.0 mg/kg: n=7. Data are presented as mean ± SEM of *n* observations. ★P<0.05 vs. IRI + vehicle.

Effect of Late Inhibition of IKK on Sirius Red staining in the Rat Kidney after 28 days Reperfusion

Despite no change in renal functional parameters after renal IRI at 28 days post IRI (Figure 3.2), when compared with sham-operated rats, kidneys from rats that underwent 30 min of unilateral renal ischaemia and 28 days of reperfusion exhibited a significant increase in Sirius red staining, indicating the development of fibrosis (Figure 3.3). Administration of IKK16 (1.0 mg/kg) 24 h after the onset of reperfusion significantly attenuated the increase in Sirius red staining for collagen I and III, and therefore fibrosis, when compared to vehicle treated animals (Figure 3.3).

Representative cross sections of the kidneys from the time course, stained for Sirius red are displayed in Figure 3.4, and representative images at x20 magnification in Figure 3.5.

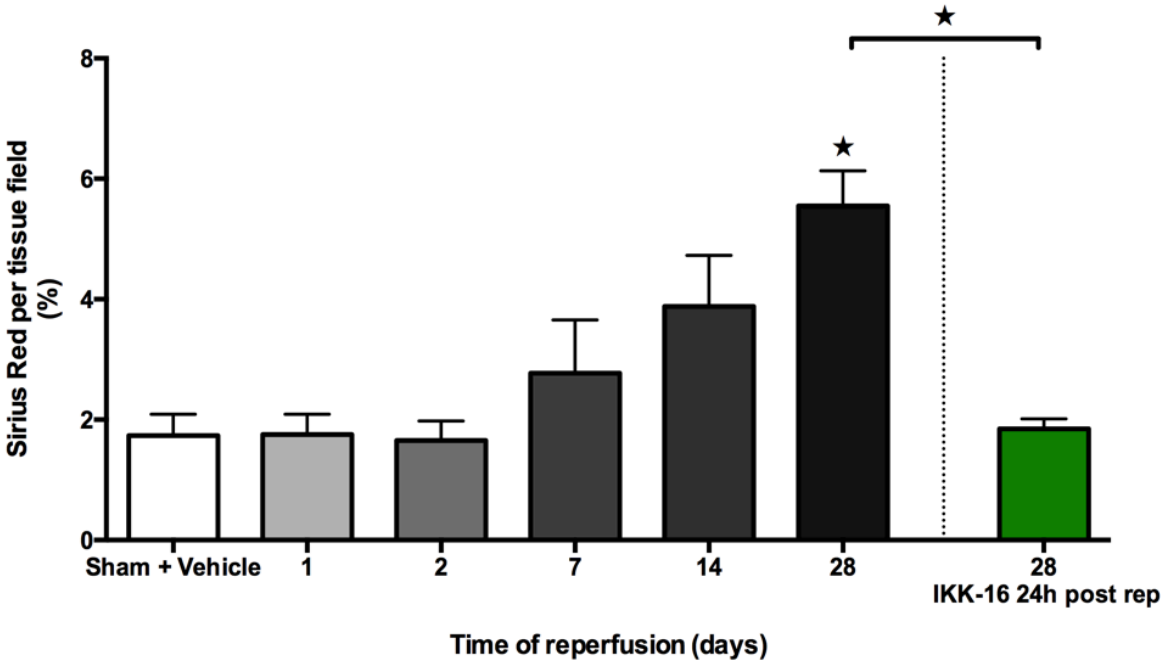

Figure 3.3 The time course of development of fibrosis (as measured by Sirius red for Collagen I and III) after unilateral renal ischaemia (30 min) and reperfusion (up to 28 days), and the effect of the late administration of IKK16 at 24 h post reperfusion. Sham + vehicle: n=4; 1 day post reperfusion: n=4; 2 days post reperfusion: n=4; 7 days post reperfusion: n=4; 14 days post reperfusion: n=4; 28 days post reperfusion: n=8; 1.0 mg/kg IKK16 24 h post reperfusion + 28 day reperfusion: n=7. Due to the concentration of the fibrosis in the corticomedullary junction, whole tissue cross sections (as seen in Figure 3.4) were analysed and the % staining for Sirius red per tissue field calculated by ImageJ software. Data are presented as mean ± SEM of n observations, ⋆P<0.05 vs. sham + vehicle, unless otherwise stated.

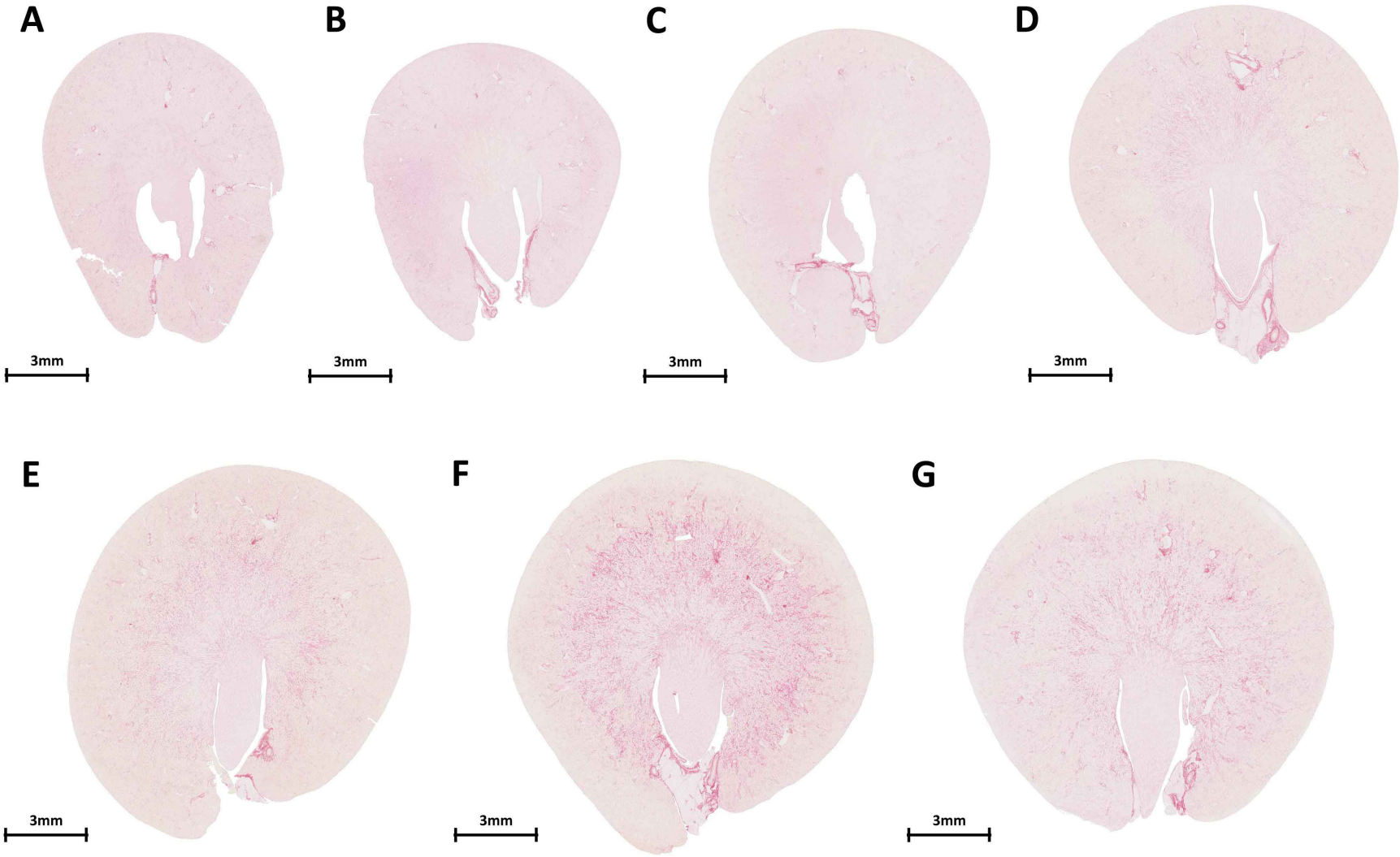

Figure 3.4 The time course of development of fibrosis (as measured by Sirius red for Collagen I and III) after unilateral renal ischaemia (30 min) and reperfusion (up to 28 days), and the effect of the late administration of IKK16 (24 h post reperfusion. Images depict representative cross sections of kidneys, quantative data can be found in Figure 3.3. (A) Sham + vehicle (B) 1 day post reperfusion (C) 2 days post reperfusion (D) 7 days post reperfusion (E) 14 days post reperfusion (F) 28 days post reperfusion (G) 1.0 mg/kg IKK16 24 h post reperfusion + 28 days reperfusion. Due to the concentration of the fibrosis in the corticomedullary junction, whole tissue cross sections were analysed and the % staining for Sirius red per tissue field calculated by ImageJ software. These values were then normalised to surface area percentage.

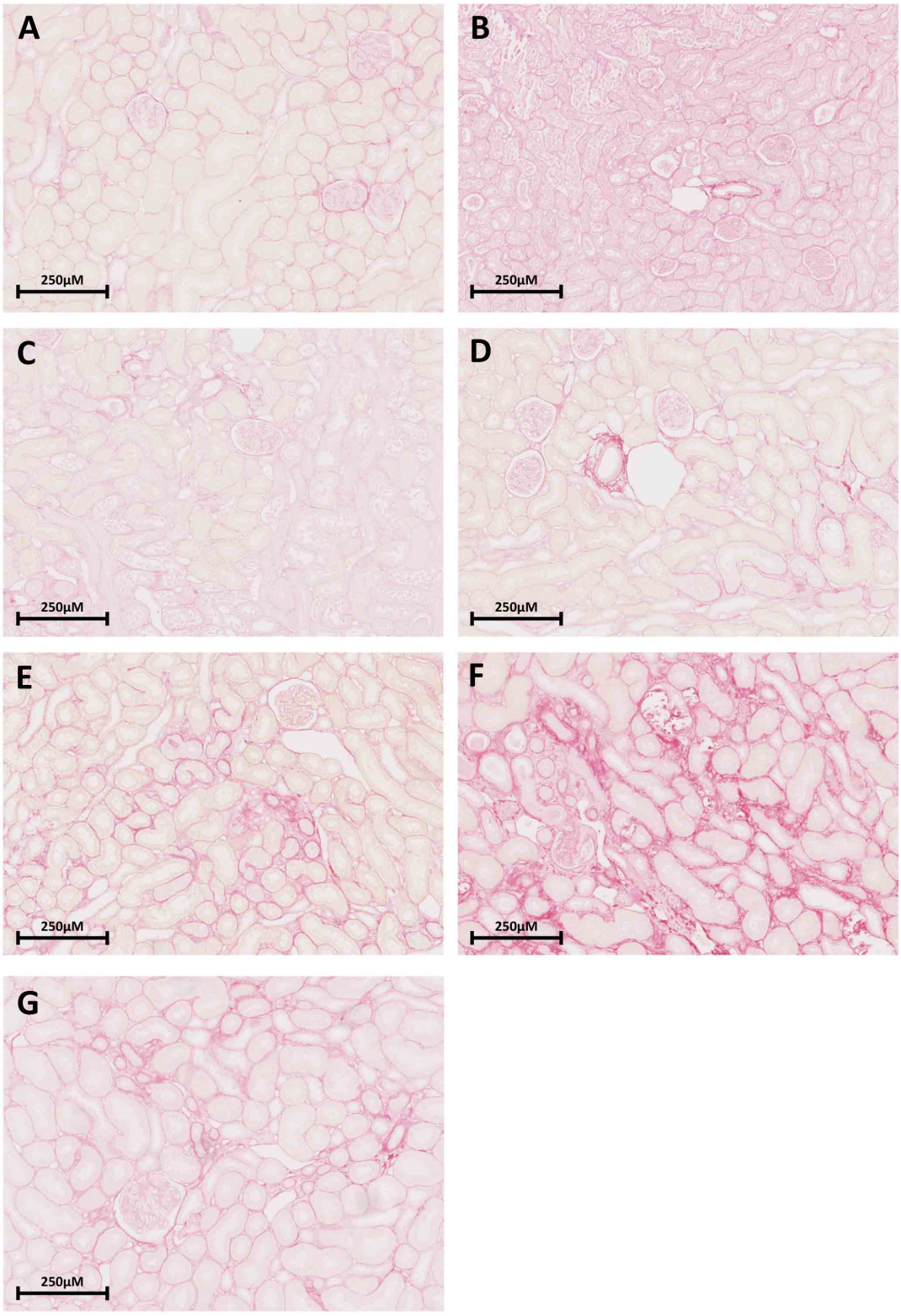

Figure 3.5 The time course of development of fibrosis (as measured by Sirius red for Collagen I and III) after unilateral renal ischaemia (30 min) and reperfusion (up to 28 days), and the effect of the late administration of IKK16 (24 h post reperfusion. Images depict representative images of Sirius red stained kidneys at x20 magnification, quantitative data can be found in Figure 3.3. (A) Sham + vehicle (B) 1 day post reperfusion (C) 2 days post reperfusion (D) 7 days post reperfusion (E) 14 days post reperfusion (F) 28 days post reperfusion (G) 1.0 mg/kg IKK16 24 h post reperfusion + 28 days reperfusion.

Interestingly, regression analysis revealed a significant linear relationship between SCr time course evolution (AUC) and Sirius red staining (Figure 3.5C). More specifically, Sirius red staining after 28 days was significantly related to SCr levels or eCCL at day 2 (Figure 3.5A, 3.5B).

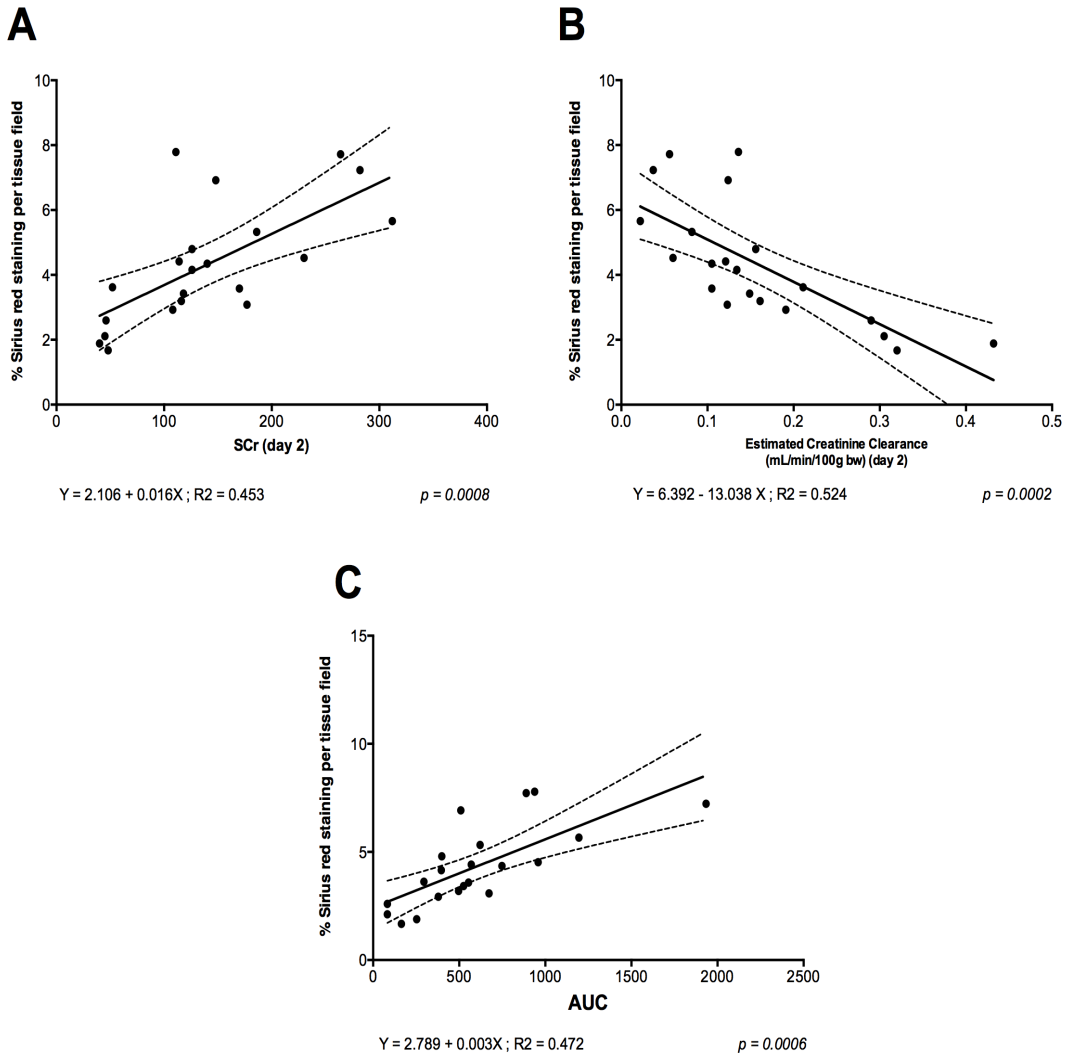

Figure 3.6 Correlation data to show (A) serum creatinine at day 2 vs. Sirius red percentage per tissue field (indicative of fibrosis) at day 28 (B) the estimated creatinine clearance at day 2 v.s. Sirius red percentage per tissue field at day 28 and (C) the area under the curve (AUC) (from day 0 to day 28) vs. Sirius red percentage per tissue field at day 28. All animal data generated in this study (sham + vehicle, IRI + vehicle and IRI + 1.0 mg/kg IKK16 24 h post reperfusion) is included in these graphs. Linear regressions were calculated by the least squares method and their significance were estimated by a Fisher *F* test. P<0.05 was considered to be significant.

Effect of Late Inhibition of IKK on Myofibroblast Activation in the Rat Kidney after 28 days Reperfusion

I then stained sections from the entire time course for α-SMA to determine myofibroblast activation. When compared with sham-operated rats, kidneys from rats that underwent 30 min of unilateral renal ischaemia and 7 days of reperfusion exhibited a significant increase in α-SMA staining, and therefore myofibroblast activation (Figure 3.7). Administration of IKK16 (1.0 mg/kg) 24 h after the onset of reperfusion significantly attenuated the increase in α-SMA staining at 7 days post reperfusion (Figure 3.7). Interestingly, vehicle treated rats culled at 7 days post reperfusion were the only group in the entire time course (from sham to 28 days), displaying significant increases in myofibroblast formation when compared to sham-operated rats. Representative cross sections of kidneys from the time course stained for α-SMA are displayed in Figure 3.8, and representative images at x20 magnification in Figure 3.9.

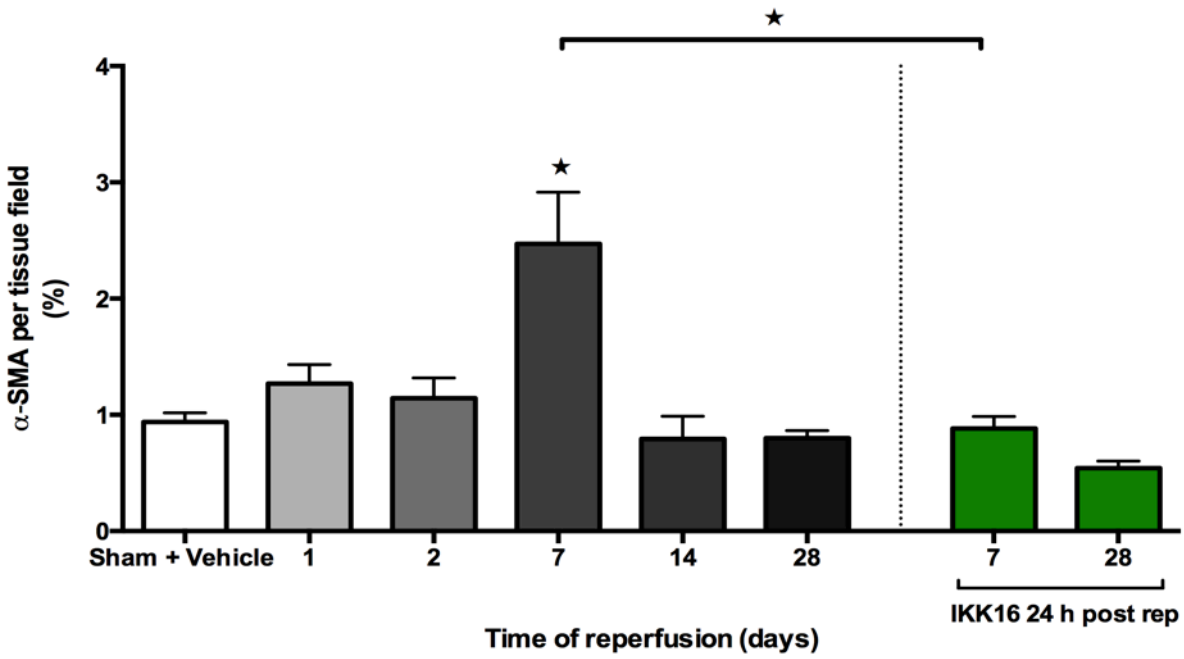

Figure 3.7 The effect of the late administration of IKK16 (24 h post reperfusion) on α-SMA staining for α-SMA-positive myofibroblasts after unilateral renal ischaemia (30 min) and reperfusion (up to 28 days). Sham + vehicle: n=8, 1 day post reperfusion: n=4; 2 days post reperfusion: n=4; 7 days post reperfusion: n=4; 14 days post reperfusion: n=4; 28 days post reperfusion: n=7; 1.0 mg/kg IKK16 24 h post reperfusion + 7 day reperfusion: n=7; 1.0 mg/kg IKK16 24 h post reperfusion + 28 day reperfusion: n=7. Due to the concentration of α-SMA in the corticomedullary junction, whole tissue cross sections (as seen in Figure 3.8) were analysed and the % staining for α-SMA per tissue field calculated by ImageJ software. Data are presented as mean ± SEM of n observations, ⋆P<0.05 vs. sham + vehicle, unless otherwise stated.

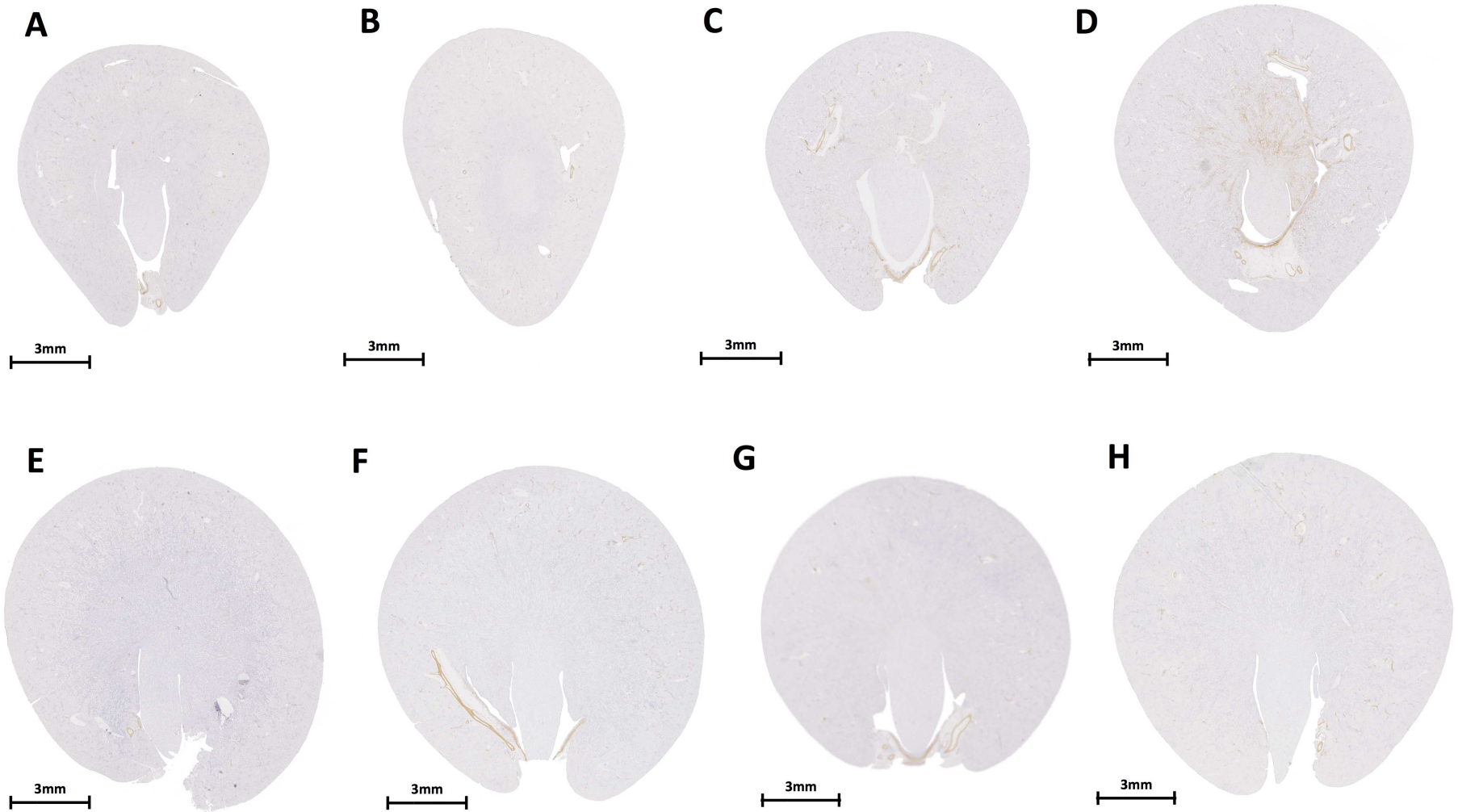

Figure 3.8 The effect of the late administration of IKK16 (24 h post reperfusion) on α-SMA staining for α-SMA-positive myofibroblasts after unilateral renal ischaemia (30 min) and reperfusion (up to 28 days). Images depict representative cross sections of kidneys; quantative data can be found in Figure 3.7. (A) Sham + vehicle (B) 1 day post reperfusion (C) 2 days post reperfusion (D) 7 days post reperfusion: (E) 14 days post reperfusion (F) 28 days post reperfusion (G) 1.0 mg/kg IKK16 24 h post reperfusion + 7 days reperfusion (H) 1.0 mg/kg IKK16 24 h post reperfusion + 28 days reperfusion. Due to the concentration of the fibrosis in the corticomedullary junction, whole tissue cross sections were analysed and the % staining for α-SMA per tissue field calculated by ImageJ software. These values were then normalised to surface area percentage.

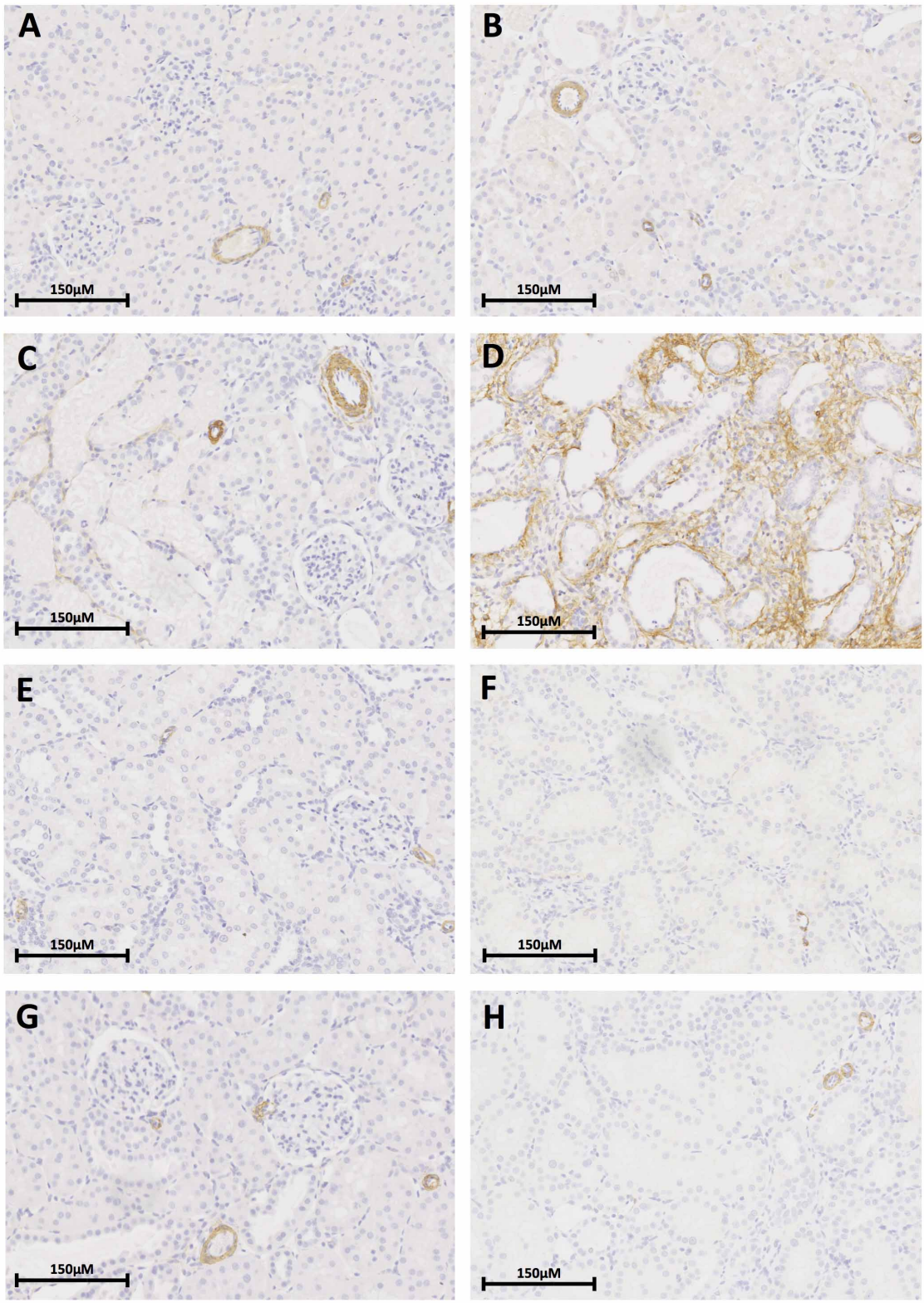

Figure 3.9 The effect of the late administration of IKK16 (24 h post reperfusion) on α-SMA staining for α-SMA-positive myofibroblasts after unilateral renal ischaemia (30 min) and reperfusion (up to 28 days). Images depict representative images of α-SMA stained kidneys at x20 magnification. Quantative data can be found in Figure 3.7. (A) Sham + vehicle (B) 1 day post reperfusion (C) 2 days post reperfusion (D) 7 days post reperfusion (E) 14 days post reperfusion (F) 28 days post reperfusion (G) 1.0 mg/kg IKK16 24 h post reperfusion + 7 days reperfusion (H) 1.0 mg/kg IKK16 24 h post reperfusion + 28 days reperfusion.

Effect of Late Inhibition of IKK on CD68$^+$ staining in the Rat Kidney after 28 days Reperfusion

It is known that macrophages are a major producer of TGF-β in fibrosis (Kim et al., 2015). Thus, I stained the entire time course for CD68$^+$, a glycoprotein found in cytoplasmic granules of cells of the macrophage lineage. When compared with sham-operated rats, kidneys from rats that underwent 30 min of unilateral renal ischaemia and 7 days of reperfusion exhibited a significant increase in CD68$^+$ staining, and therefore macrophage infiltration (Figure 3.10). Administration of IKK16 (1.0 mg/kg) 24 h after the onset of reperfusion significantly attenuated the increase in CD68$^+$ staining at 7 days post reperfusion (Figure 3.10). Interestingly, vehicle treated rats culled at 7 days post reperfusion were the only group in the time course (from sham to 28 days), which displayed significant increases CD68$^+$ when compared to sham-operated rats. Representative images at x40 magnification are displayed in Figure 3.11.

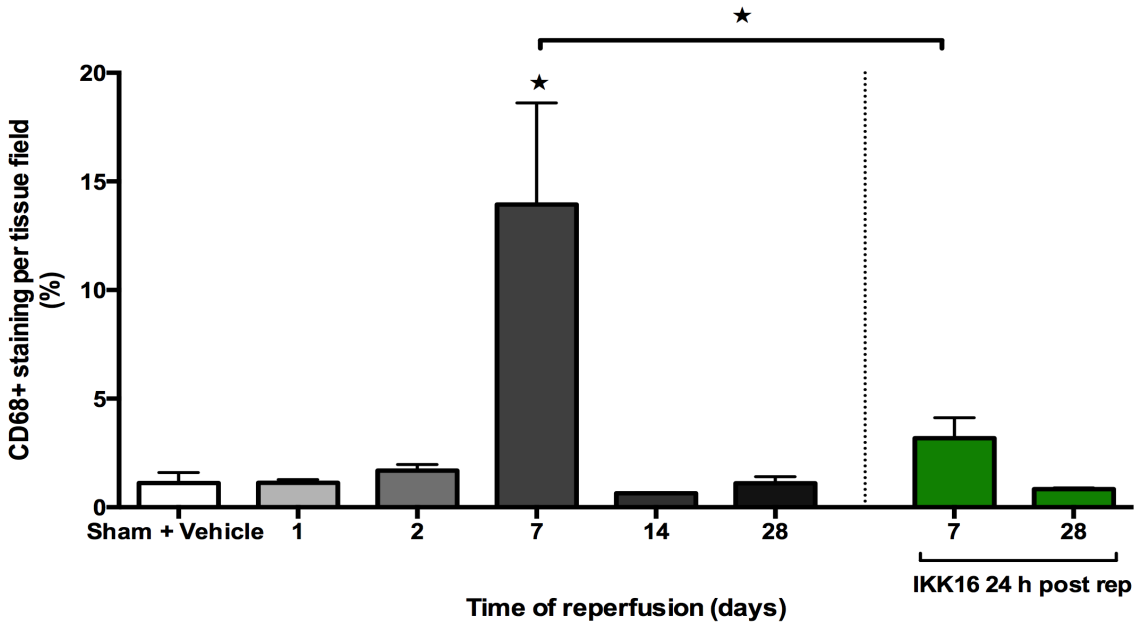

Figure 3.10 The effect of the late administration of IKK16 (24 h post reperfusion) on $CD68^+$ staining, indicative of macrophages, after unilateral renal ischaemia (30 min) and reperfusion (up to 28 days). Ten randomly selected fields (at x40 magnification) from each kidney were selected and analysed for the determination of percentage stained rat kidney tissue using ImageJ software. Sham + vehicle: n=8 (80 total fields), 1 day post reperfusion: n=4 (40 total fields); 2 days post reperfusion: n=4 (40 total fields); 7 days post reperfusion: n=6 (60 total fields); 14 days post reperfusion: n=4 (40 total fields); 28 days post reperfusion: n=7 (70 total fields); 1.0 mg/kg IKK16 24 h post reperfusion + 7 day reperfusion: n=7 (70 total fields); 1.0 mg/kg IKK16 24 h post reperfusion + 28 day reperfusion: n=7 (70 total fields). Data are presented as mean ± SEM of n observations, ⋆P<0.05 vs. sham + vehicle, unless otherwise stated.

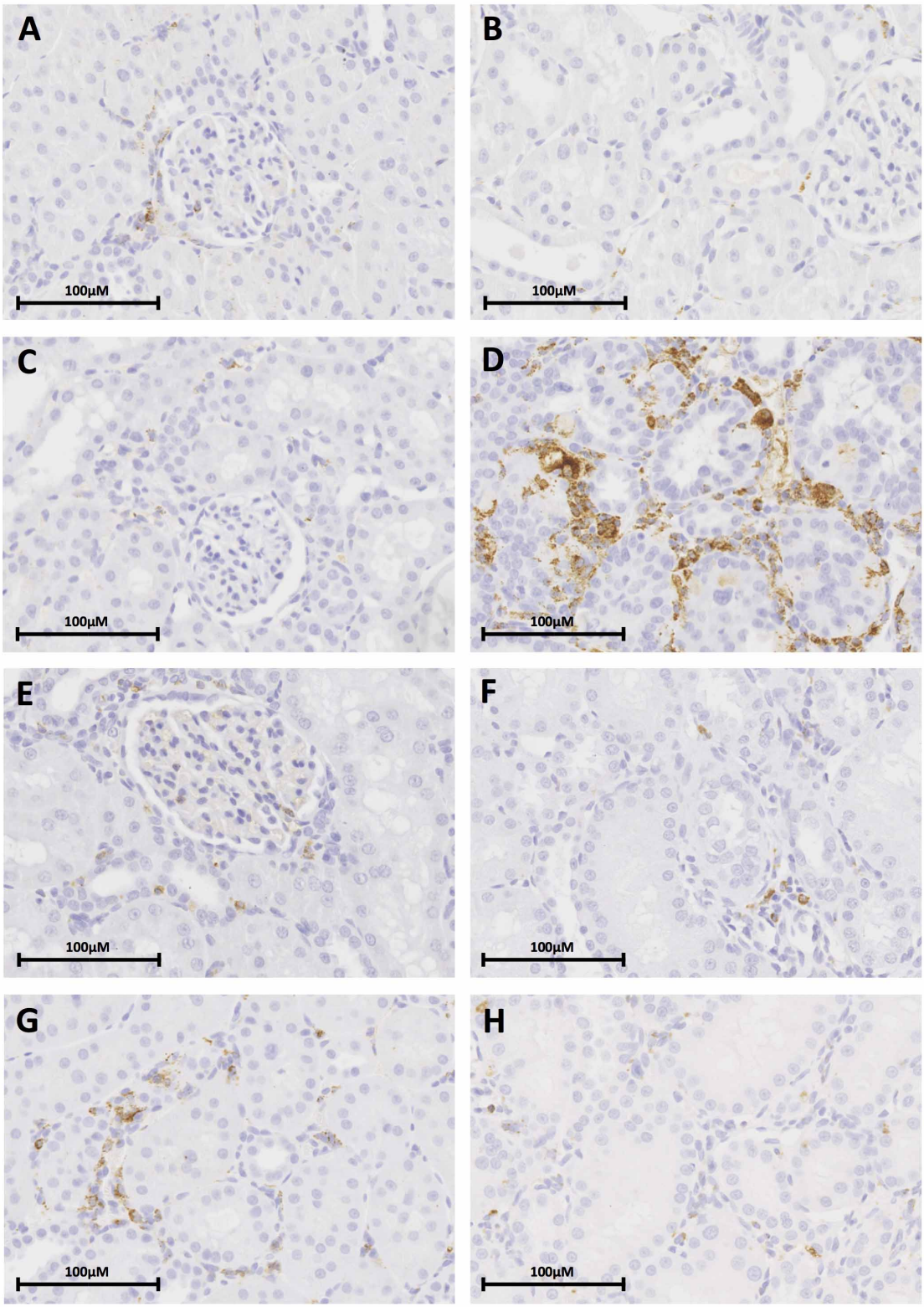

Figure 3.11 The effect of the late administration of IKK16 (24 h post reperfusion) on $CD68^+$ staining, indicative of macrophages, after unilateral renal ischaemia (30 min) and reperfusion (up to 28 days). Images depict representative images of $CD68^+$ stained kidneys at x40 magnification. Quantative data can be found in Figure 3.10. (A) Sham + vehicle (B) 1 day post reperfusion (C) 2 days post reperfusion (D) 7 days post reperfusion (E) 14 days post reperfusion (F) 28 days post reperfusion (G) 1.0 mg/kg IKK16 24 h post reperfusion + 7 days reperfusion (F) 1.0 mg/kg IKK16 24 h post reperfusion + 28 days reperfusion.

Effect of Late Inhibition of IKK on Pro-fibrotic markers in the Rat Kidney at 7 days Post Reperfusion

When compared with sham-operated rats, kidneys from rats that underwent 30 min of unilateral renal ischaemia and 7 days of reperfusion exhibited a significant increase in TGF-β (Figure 3.12), and Smad2/3 phosphorylation (Figure 3.13). TGF-β causes downstream Smad2/3 phosphorylation after type I/II TGF-β receptor binding. Administration of IKK16 (1.0 mg/kg) 24 h after the onset of reperfusion significantly attenuated the increase in TGF-β (Figure 3.12) and the phosphorylation of Smad2/3 (Figure 3.13).

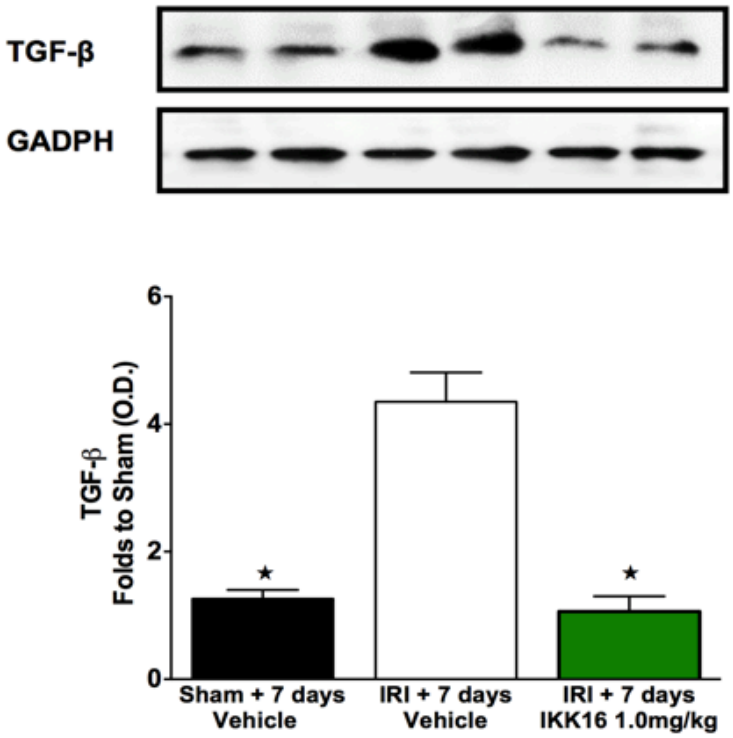

Figure 3.12 The effect of the late administration of IKK16 (24 h post reperfusion) on the expression of TGF-β at 7 days post reperfusion. Sham 7 days + Vehicle: n=4; IRI + 7 days Vehicle: n=5: IRI + 7 days, IKK16 1.0 mg/kg: n=5. Densitometric analysis of the bands is expressed as relative optical density (OD) of TGF-β, normalised using the sham operated band. Each immunoblot is from a single experiment. Data are presented as mean ± SEM of n observations, #P<0.05 vs. Sham, ⋆P<0.05.

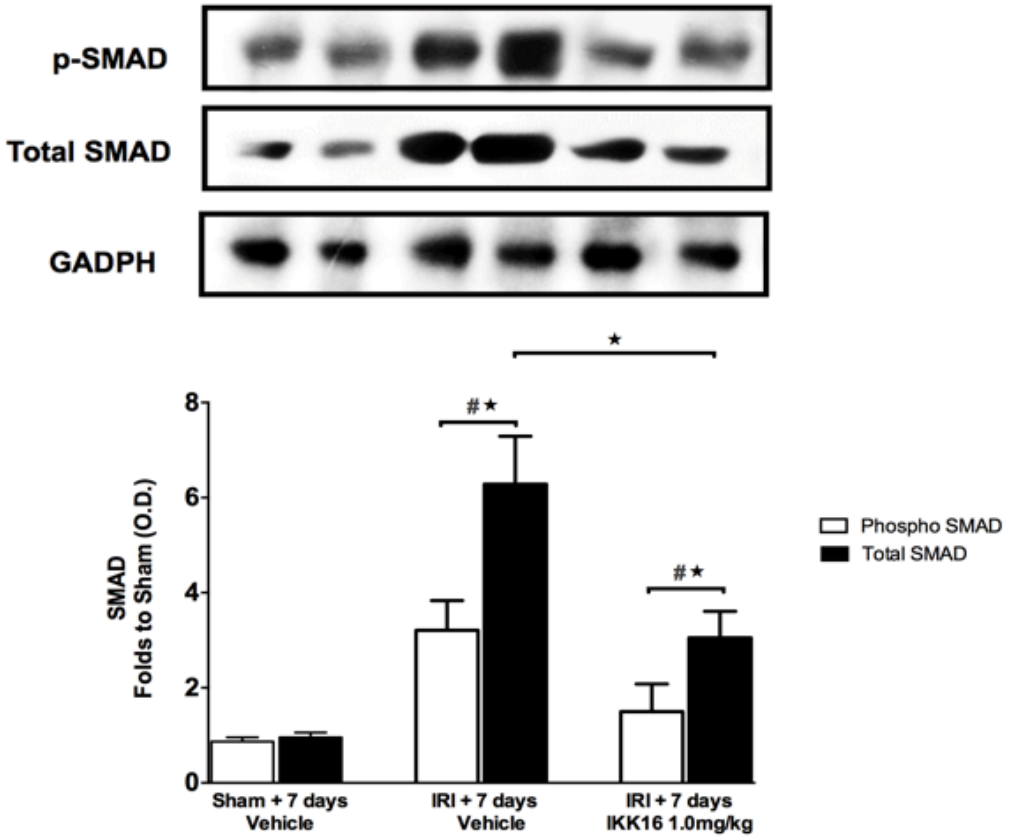

Figure 3.13 The effect of the late administration of IKK16 (24 h post reperfusion) on the expression of both phosphorylated and total Smad2/3 at 7 days post reperfusion. Sham + 7 days, Vehicle: n=4; IRI + 7 days, Vehicle: n=5: IRI + 7 days, IKK16 1.0 mg/kg: n=5. Densitometric analysis of the bands is expressed as relative optical density (OD) of phosphorylated Smad 2/3, corrected for the corresponding total Smad 2/3 content and normalised using the sham operated band. Each immunoblot is from a single experiment. Data are presented as mean ± SEM of n observations, #P<0.05 vs. Sham, ★P<0.05.

Effect of Late Inhibition of IKK on Pro-Fibrotic Markers in the Rat Kidney at 28 days Post Reperfusion

When compared with sham-operated rats, kidneys from rats that underwent 30 min of unilateral renal ischaemia and 28 days of reperfusion exhibited a significant increase in TGF-β (Figure 3.14). Administration of IKK16 (1.0 mg/kg) 24 h after the onset of reperfusion significantly attenuated the increase in TGF-β when compared to vehicle treated control (Figure 3.14).

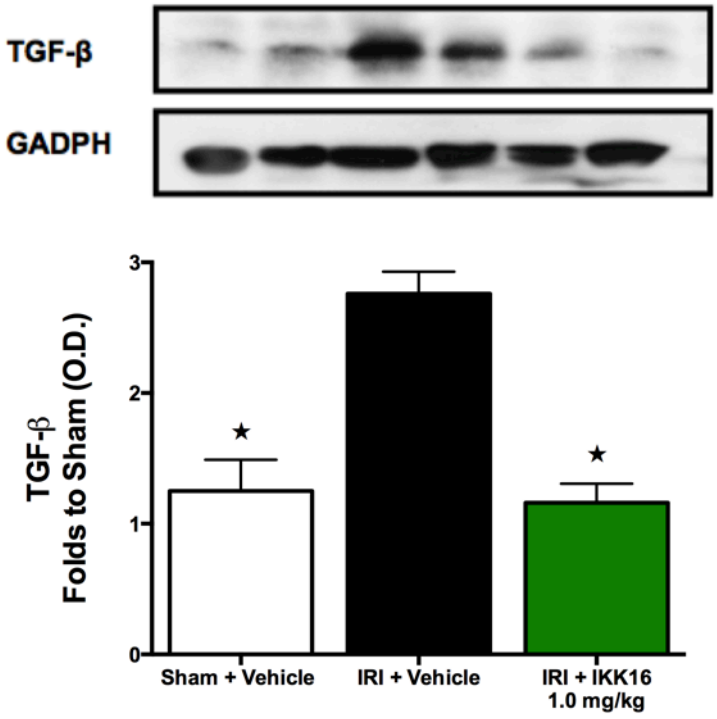

Figure 3.14 The effect of the late administration of IKK16 (24 h post reperfusion) on the expression of TGF-β. Sham 28 days + Vehicle: n=4; IRI + 28 days Vehicle: n=5: IRI + 28 days, IKK16 1.0 mg/kg: n=5. Densitometric analysis of the bands is expressed as relative optical density (OD) of TGF-β, normalised using the sham operated band. Each immunoblot is from a single experiment. Data are presented as mean ± SEM of n observations, ★P<0.05 vs. IRI + vehicle.

Effect of Late Inhibition of IKK on Extracellular Matrix Proteins in the Rat Kidney at 28 days post reperfusion

When compared with sham-operated rats, kidneys from rats that underwent 30 min of unilateral renal ischaemia and 28 days of reperfusion exhibited an increase in vimentin (expressed by myofibroblasts) (Figure 3.15). Administration of IKK16 (1.0 mg/kg) 24 h after the onset of reperfusion significantly attenuated the increase in vimentin (Figure 3.15) caused by unilateral IRI after a 28-day reperfusion period.

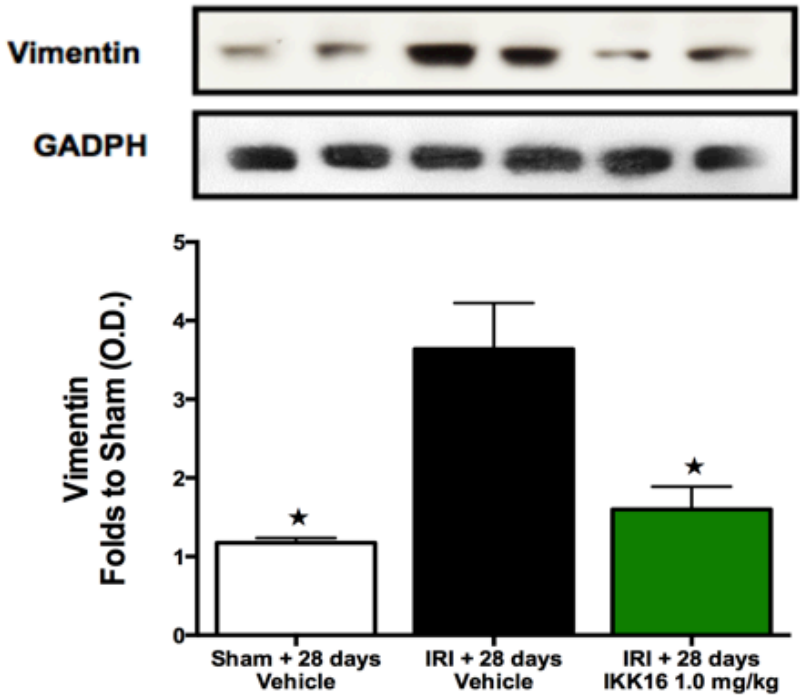

Figure 3.15 The effect of the late administration of IKK16 (24 h post reperfusion) on the expression of vimentin at 28 days post reperfusion. Vimentin expressed late after injury as an indicator of defective repair and abnormal epithelium, and is also a marker of myofibroblast formation. Sham 28 days + Vehicle: n=4; IRI + 28 days Vehicle: n=5: IRI + 28 days, IKK16 1.0 mg/kg: n=5. Densitometric analysis of the bands is expressed as relative optical density (OD) of total vimentin, normalised using the sham operated band. Each immunoblot is from a single experiment. Data are presented as mean ± SEM of n observations, ⋆P<0.05 vs. IRI + vehicle.

When compared with sham-operated rats, kidneys from rats that underwent 30 min of unilateral renal ischaemia and 28 days of reperfusion exhibited an increase in fibronectin (an extracellular matrix component) (Figure 3.16). Administration of IKK16 (1.0 mg/kg) 24 h after the onset of reperfusion significantly attenuated the increase in fibronectin (Figure 3.16) caused by unilateral IRI after a 28-day reperfusion period.

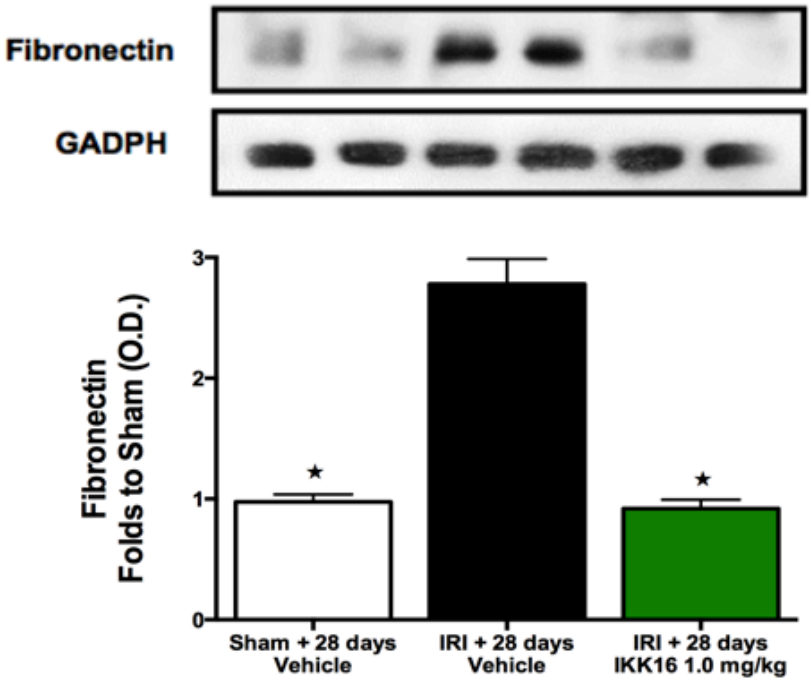

Figure 3.16 The effect of the late administration of IKK16 (24 h post reperfusion) on the expression of fibronectin at 28 days post reperfusion. Fibronectin is a component of the extracellular matrix, and is over produced in fibrotic states. Sham + 28 days, Vehicle: n=4; IRI + 28 days, Vehicle: n=5: IRI + 28 days, IKK16 1.0 mg/kg: n=5. Densitometric analysis of the bands is expressed as relative optical density (OD) of total fibronectin, normalised using the sham operated band. Each immunoblot is from a single experiment. Data are presented as mean ± SEM of n observations, ⋆P<0.05 vs. IRI + vehicle.

Discussion

Epidemiological and outcome analysis studies have recently discovered the role of AKI in the progression to CKD to ESRD, with tubulointerstitial fibrosis being the predominant pathology promoting progression to CKD (Venkatachalam et al., 2010). The more severe and prolonged the initial ischaemic insult, the higher the probability of developing CKD later in life (Chawla et al., 2011). Therefore, the quick amelioration of the IRI-dependent changes in biochemical markers following AKI by new therapies may reduce the probability of developing CKD. The timing of therapy initiation in patients with AKI is currently under debate, with the consensus being to deliver early RRTs to these patients to maintain fluid balance and solute clearance until recovery of renal function (Shiao et al., 2009). However, in practice RRTs are started after complete renal shutdown (Macedo and Mehta, 2010). As there are no proven medical therapies to improve short-term prognosis of AKI (Heung and Chawla, 2012), i.e. to aid recovery or tissue-repair, I have sought to identify a novel drug target to attenuate the course of AKI during its development (not as a pretreatment and not on reperfusion, but after initiation of disease). Therefore, the diagnosis of AKI with eGFR or novel biomarkers (e.g. NGAL) plays an important role for the determination of when to start treatment.

By extending the reperfusion period to 28 days, I have shown that animals subject to only 30 min of renal ischaemia develop fibrosis. This is not a model of CKD: the animals culled between 7 and 28 days post reperfusion have a renal function comparable to sham treated animals. However, this may represent the start of the fibrotic process, detrimental to kidney function, which may ultimately lead to CKD and even ESRD.

Previous pre-clinical studies have similarly demonstrated an increase in renal tubulointerstitial fibrosis at 28 days post renal IRI, described as: ‘mild (fibrosis), but there remain significant increases in parameters of fibrosis after IRI’ (Gobe et al., 2014), similar to that I have shown in this chapter. Here, I have demonstrated that the inhibition of IKK, at 24 h post reperfusion, reduces Sirius red staining for collagen I and III and therefore fibrosis, following a 28-day reperfusion period. The fibrosis measured was mild, but significantly elevated in vehicle treated animals, however, severe enough to demonstrate a reduction in fibrosis after the inhibition of IKK.

I found a significant increase in the kidney weight of both vehicle control and IKK16 treated animals, when compared to sham animals. Similar studies demonstrate increased kidney weight in relation to total body weight after male Wistar rats are subject to IRI for 45 min/42 days (Gonçalves et al., 2014). An increase in the kidney weight in animals subject to IRI was explained by Gonçalves et al. (2014) as an increase in the fractional interstitial area (Gonçalves et al., 2014). There was no significant difference between vehicle treated and IKK16 treated groups.

I have also shown a significant correlation between both SCr and the eCCL on day 2 post IRI vs. fibrosis score at 28 days. Previous clinical studies have demonstrated that AKI is a major risk factor for CKD, highlighting the relationship between elevated SCr and the risk of CKD development (Coca et al., 2012). SCr is still the major clinical biomarker for AKI diagnosis, and its magnitude after events such as cardiac surgery has been associated with increased risk of CKD development, progression and ESRD (Ishani et al., 2011). This is, however, in reality, more

complicated; a recent clinical meta-analysis performed by Coca et al. (2015) studied the relationship between acute rises in SCr levels and CKD incidence and mortality months later (Coca et al., 2015). This study found no correlation between acute rises in SCr and outcome. Underlying clinical conditions (e.g. heart failure), age, any interventions given, and curt follow-up periods make translatability of this pre-clinical correlation to a meaningful clinical correlation difficult. However, the meta-analysis by Coca et al. (2015) did not measure SCr values of patients over a longer period of time (Coca et al., 2015) – something I have done in this study. Using these data, I found that the AUC of SCr over the 28 day period following renal IRI predicted the severity of fibrosis; which may be a more reliable prediction of outcome due to the measurement of SCr over a longer period post AKI. Longer follow-up studies with regular measurement of SCr should be executed to investigate whether the AUC of SCr is predictive of outcome (fibrosis/CKD) in the clinical setting.

In this chapter, I have demonstrated that even when SCr values are 'normal' at day 28, there is a significant development of fibrosis when compared to sham-operated animals, and that the development of fibrosis is very much underway before any sign of renal functional decline. Barrera-Chimal et al. (2012) used a similar rat model of IRI, (bilateral ischaemia, 45 min) with a reperfusion period of 270 days (Barrera-Chimal et al., 2013). During the reperfusion period the animals developed a progressive renal dysfunction characterized by a reduction in eCCL, a reduction in renal blood flow and an increase in proteinuria when compared to sham-operated rats (Barrera-Chimal et al., 2013). I speculate there would be a similar decline in renal function in vehicle-treated control rats in my model if the reperfusion period

was extended to 270 days, furthermore, it would be useful to study whether the early amelioration of IRI by the inhibition of IKK would still have benefit (i.e. reduced fibrosis/improved renal function) at this time point.

Interestingly, at 7 days post reperfusion after 30 min of renal IRI, there is a significant increase in immunohistochemical staining for both α-SMA and $CD68^+$, markers for myofibroblast formation and macrophages, respectively. This is prior to the development of the formation of fibrosis, and is most likely involved in the production of fibrosis seen at 28 days. Both of these parameters returned to near baseline at 14 days. Similar data by Ysebaert et al. (2000) have shown an increase in macrophage accumulation after renal IRI from 24 h, which is most prominent at 5 days post reperfusion, and a complete abolishment of macrophages in the renal tissue at day 10 (Ysebaert et al., 2000). Macrophages have recently been classified into two subsets, M1 ($F4/80^+$ and $CD301^-$, and M2 ($F4/80^+$ and $CD301^+$); after renal IRI iNOS-positive pro-inflammatory M1 macrophages polarize to arginase-1 and mannose receptor positive non-inflammatory macrophages (M2) (Lee et al., 2011). This switch of phenotype has been described to accompany the change from tubular injury to tubular repair (Lee et al., 2011). The phenotype of macrophages has also been studied in the development of fibrosis following renal IRI, with M2 macrophages most abundantly present at 7 days post reperfusion (Lee et al., 2011). M2 macrophages are useful in tissue repair (Wang et al., 2007), however they are most likely pro-fibrotic in the AKI to CKD progression, synthesizing TGF-β, causing downstream signalling through Smad proteins 2/3 regulating transcription of genes coding for collagens. There is still much debate whether M2 macrophages are beneficial in tissue repair or detrimental because of their role in the

development of fibrosis (Braga et al., 2015), however, Myung-Gyu Kim et al. (2015) have demonstrated that M2 macrophages were the most predominant phenotype 7 – 14 days post unilateral IRI but returned to sham-levels at 28 days post unilateral IRI in a mouse model (Kim et al., 2015). Similarly, both studies show a peak of macrophage infiltration at 7 days and a reduction in macrophages to baseline levels at 28 days. Furthermore, the depletion of macrophages by liposome clodronate attenuated IRI-dependent increases in type IV collagen and levels of TGF-β, and the re-introduction of M2 macrophages caused an increase in TGF-β expression by 2.5 fold when compared to M1 macrophage re-introduction (Kim et al., 2015). Similarly, Gharib et al. (2014) found that reduced M2 polarisation conferred protection from bleomycin-induced pulmonary fibrosis in a mouse model (Gharib et al., 2014). It has previously been demonstrated that macrophage numbers closely correlate with glomerular scarring and interstitial fibrosis, demonstrated in the biopsy samples of 215 CKD patients (Eardley et al., 2006). I speculate that the macrophages at 7 days post reperfusion (reported in this chapter) are M2 macrophages, that may well be in part responsible for both the increase in TGF-β seen at 7 days post reperfusion and the increase in fibrosis at 28 days in vehicle treated groups. The inhibition of IKK caused a significant reduction in $CD68^+$ staining, and therefore macrophages, at 7 days post reperfusion. Izmailova et al. (2006) have previously demonstrated that the inhibition of IKKβ in a murine model of arthritis caused a significant reduction in $CD68^+$ macrophages (Izmailova et al., 2007). The inhibition of NF-κB in bone-marrow derived macrophages via a recombinant adenovirus (Ad-IκB) causes a re-orientation of macrophages to an anti-inflammatory state, causing a reduction in glomerular inflammation *in vivo*

(Wilson et al., 2005). The exact mechanism of the reduction in macrophages post IKK inhibition should be further investigated, as this is still not well understood.

In this rat model of renal IRI I have demonstrated increases in both TGF-β and the phosphorylation of Smad2/3 at 7 days post reperfusion. TGF-β directly induces fibrosis through Smad3, binding directly to promoter regions to trigger collagen production (Meng et al., 2015). TGF-β also induces fibronectin production (Mack and Yanagita, 2015), which is significantly increased in this study at 28 days post reperfusion in vehicle-treated animals. Furthermore, TGF-β itself promotes the transition of various cell types to the myofibroblast phenotype via pericyte-myofibroblast transition (Wu et al., 2013), EndoMT (Piera-Velazquez et al., 2011), EMT (Lan, 2003) and activation of bone-marrow derived sources (LeBleu et al., 2013), and can directly activate resident renal cells, promoting α-SMA expression and fibrosis (Barnes and Glass, 2011). α-SMA is expressed by myofibroblasts, major players in the production and deposition of collagen, seen increased here at 7 days in vehicle treated animals. The inhibition of IKK not only reduced both the expression of α-SMA and the infiltration of $CD68^+$ macrophages, but also reduced TGF-β and the phosphorylation of Smad2/3. The p65 subunit of NF-κB has previously been associated with fibrosis in lung fibroblasts (Sun et al., 2015), and the inhibition of IKKβ significantly reduced pulmonary fibrosis in a bleomycin mouse model (Inayama et al., 2006). Mia and Bank (2015) have demonstrated that IKK inhibition attenuates myofibroblast formation and collagen I production induced by TGF-β1, in dermal fibroblasts in vitro (Mia and Bank, 2015), which may explain the reduction of TGF-β in IKK treated animals at 7 days, seen in this chapter.

Proximal tubule cells do not constitutively express vimentin, however, AKI causes de-differentiation and proliferation of surviving proximal tubule cells, causing an increase in vimentin expression later after the insult (Polichnowski et al., 2014). Vimentin expressed late after injury is indicative of defective repair and abnormal epithelium (Gröne et al., 1987). Vimentin does not only play a role in mechanical stabilisation: it is also expressed in cells of mesenchymal origin and therefore is commonly used as a marker of EMT (Dave and Bayless, 2014). Renal IRI causes a significant increase in vimentin expression in the kidney in vehicle treated animals when compared to sham animals, shown here in this chapter. The inhibition of IKK at just 24 h post reperfusion caused a significant reduction in vimentin expression at 28 days. From previous evidence, this suggests that IKK inhibition in this rat model of renal IRI with the development of fibrosis, causes a reduction in EMT and a reduction in defective repair and abnormal epithelium (Gröne et al., 1987) (Dave and Bayless, 2014).

In this study, I have characterized a rat model of unilateral IRI and contralateral nephrectomy, with a subsequent development of fibrosis. I have demonstrated that the episode of AKI was acute and all functional parameters measured had resolved by day 7 onwards. However, during this period, despite the renal function of all groups being comparable to sham animals, there was a significant activation of macrophages and myofibroblasts, key players the in production of fibrotic tissue and the development of fibrosis. The fibrosis measured at 28 days may allude to the beginnings of CKD that these animals could develop had the reperfusion period been extended. The administration of IKK16, an IKK inhibitor, as a single bolus at

24 h post reperfusion significantly attenuated macrophages in the kidney and myofibroblast activation at 7 days post reperfusion, which in turn, most likely prevented the increase in collagen I and III and therefore fibrosis seen at 28 days in the IKK16 treated animals. Further to this, SCr measured at day 2 after IRI was predictive of fibrotic score at day 28, and the AUC of SCr measured from day 0 to 28 was also predictive of fibrotic score at day 28. The early amelioration of IRI is therefore important in the prevention of fibrosis and the subsequent progression to CKD.

Chapter IV

The Delayed Administration of IKK16 Reduces Renal Fibrosis in a Rat Model of Unilateral Ureteral Obstruction

Introduction

Currently, the most commonly used *in vivo* model for renal interstitial fibrosis is UUO. When compared to other animal models of renal fibrosis, UUO is a relatively short, cheap and easily reproducible model, mimicking many features of CKD seen in humans (Eddy et al., 2012). These include: (i) release of proinflammatory cytokines and chemokines causing inflammatory mononuclear cell infiltration and inflammation, (ii) the production of profibrotic molecules, such as TGF-β (Boor et al., 2010) (iii) fibroblast to myofibroblast transition and the consequent expression of α-SMA, vimentin and nestin (Grande and López-Novoa, 2009) (iv) EMT (another source of myofibroblast generation) (Kalluri and Neilson, 2003) (v) increased production of ECM components by myofibroblasts (vi) and expansion of the interstitial space due to continuous over production of ECM components resulting in tubular hypoxia leading to apoptosis and necrosis of tubular cells (Cachat et al., 2003). This pathology is achieved via obstruction of the ureter by permanent ligation, causing back leak of urine into the kidney. The resulting hydrostatic pressure destroys the kidney architecture, causing apoptosis and necrosis of tubular cells (Dendooven et al., 2011). This triggers an inflammatory response followed by the development of fibrosis.

As previously discussed in Chapter III, inhibition of NF-κB in animal models of fibrosis has proven to be beneficial. Previous studies have demonstrated an increase in NF-κB expression up to 7 days post UUO (Kuwabara et al., 2006), and the inhibition of NF-κB with curcumin (200 mg/kg/day or 800 mg/kg/day p.o. 7 days before UUO and daily thereafter) or the NF-κB inhibitor pyrrolidine dithiocarbamate (PDTC) (200 mg/kg/day p.o 1 h before surgery and daily thereafter) inhibited NF-κB activation, interstitial macrophage infiltration and

fibrosis at 7 days post UUO (Kuwabara et al., 2006). Curcumin from the spice turmeric, is known to inhibit NF-κB activation (Singh and Aggarwal, 1995), but has also been shown to inhibit c-Jun *N*-terminal kinase-c-Jun/AP-1 (Chen and Tan, 1998) and block TGF-β signalling in rat renal fibroblasts (Gaedeke et al., 2004). Previous studies have highlighted the role of TGF-β in renal fibrosis: anti-TGF-β antibodies prevent renal tubular fibrosis and apoptosis in NRK-52E cells (Miyajima et al., 2000) and targeted disruption of Smad3 (directly downstream of TGF-β) causes a significant reduction in renal fibrosis, monocyte influx and EMT post UUO (Sato et al., 2003). Therefore, the amelioration of fibrosis by curcumin, may be partly achieved via inhibition of TGF-β signalling, rather than NF-κB inhibition alone.

A similar study by Tashiro et al. (2003) used PSI, a proteosome inhibitor, blocking NF-κB translocation through stabilization of the endogenous NF-κB inhibitor, IκB (Tashiro et al., 2003). The administration of 3 mg/kg PSI b.i.d. s.c. attenuated UUO-dependent increases in NF-κB DNA binding activity and UUO-dependent increases in cortical IκB expression, and a reduction in fibrosis (Tashiro et al., 2003). EPO, administered q.a.d., has also proven to be successful in reducing fibrosis after 14 days of UUO, via the reduction of NF-κB expression (Acikgoz et al., 2014). Despite these studies showing the inhibition of NF-κB to be beneficial in obstructive nephropathy, the role of IKK, (which is directly upstream of NF-κB) or indeed its inhibition, has yet to be studied. In this chapter, I have studied the inhibition of IKK in a rat model of UUO, focusing on some of the main hallmarks of fibrosis (collagen, myofibroblast formation, TGF-β, fibronectin), to understand whether IKK plays a role in the development of fibrosis.

Methods and Materials

Animals received standard food and water *ad libitum* and all protocols followed in this study were approved by the local Animal Use and Care Committee in accordance with the derivatives of both the *Home Office Guidance on the Operation of Animals (Scientific Procedures) Act 1986*, published by Her Majesty's Stationary Office (London, UK) and the Guide for the Care and Use of Laboratory Animals of the National Research Council. One animal was excluded from the study due to mortality during the surgical procedure.

Unilateral Ureteral Obstruction

Surgical Procedure and quantification of organ injury

This study was carried out on 23 male Wistar rats (Charles River Ltd, Margate, UK) weighing between 240 – 290 g and receiving a standard diet and water *ad libitum*. Animals were anaesthetized using a ketamine (150 mg/kg) (Ketaset, Fort Dodge Animal Health Ltd., Southampton, UK) and xylazine (15 mg/kg) (Rompun, Bayer Plc, Berkshire, UK) mixture i.p. (1.5 ml/kg). The abdominal fur was shaved and the skin cleaned with 70 % alcohol (v/v). The animals were then placed on a homeothermic blanket set at 37^{o}C (Harvard Apparatus Ltd., Kent, UK). Animals received 0.1 mg/kg s.c. buprenorphine (0.1 ml/kg) (Vetergesic, Reckitt Benckiser Healthcare Ltd., Hull, UK) prior to commencement of surgery. A mid-line laparotomy was then performed. The right renal ureter was isolated and tied off 0.5 cm from the renal pelvis using sterile 5-0 silk-braided suture (Pearsalls Ltd., Taunton, UK) following which 8 ml/kg saline at 37^{o}C was injected into the abdomen and all incisions were sutured in two layers (Ethicon Prolene 5-0, Johnson

and Johnson, Livingstone, Scotland). Animals were then allowed to recover on the homeothermic blanket and placed into cages upon recovery. At the end of the experiment, both kidneys were removed following removal of the heart, with half stored in 10 % neutral buffered formalin and half snap frozen in liquid nitrogen. The non-ligated ureteral kidney served as sham.

Experimental Design (Late Intervention)

Rats were randomly allocated into the following groups: (i) ***UUO (7 days)*** (n=6); (ii) ***UUO (14 days) + vehicle*** (n=8); and (iii) ***UUO (14 days) + IKK16 1.0 mg/kg*** (n=9). Rats were administered vehicle (10% DMSO) or IKK16 through days 7-13 post ureteral obstruction s.c. at a volume of 1.0 ml/kg. Contralateral kidneys of all groups served as 'sham' kidneys.

Picrosirius Red Staining

Picrosirius red staining was carried out as detailed in Chapter III.

Immunohistochemistry

Immunohistochemical staining for α-SMA and $CD68^{+}$ was carried out as detailed in Chapter III.

Western Blots

Western blots were performed in the same fashion as described in chapter II. Membranes were incubated with primary antibody; rabbit anti-total IκBα (1:1000 cat#4812 Cell Signalling Technologies, MA); mouse anti-pIκBα $Ser^{32/36}$ (1:1000 cat#9246, Cell Signalling Technologies, MA); rabbit anti-total IKKα/β (1:200, cat#sc-7607, Santa Cruz Biotechnology, TX); rabbit anti-pIKKα/β $Ser^{176/180}$

(1:1000 cat#2697, Cell Signalling Technologies, MA); rabbit anti-NF-κB p65 (1:1000 cat#8242, Cell Signalling Technologies, MA); rabbit anti-TGF-β (1:1000, cat#ab66043); rabbit anti-pSmad2 $Ser^{465/467}$/Smad3 $Ser^{423/425}$ (1:1000, cat#D27F4, Cell Signalling Technologies, MA); rabbit anti-Smad2/3 (1:1000, cat#D7G7, Cell Signalling Technologies, MA); rabbit anti-vimentin (1:1000, cat#D21H3, Cell Signalling Technologies, MA); rabbit anti-fibronectin (1:1000, cat#ab2413, Abcam, UK). The blots were then incubated with the appropriate secondary antibody conjugated with horseradish peroxidase (dilution 1:10000) and developed using the ECL detection system. The immunoreactive bands were visualized by autoradiography. The membranes were stripped and incubated with rabbit GADPH antibody (1:1000, cat#D16H11, Cell Signalling Technologies, MA) instead of β-actin due to the involvement of β-actin the in cytoskeleton.

Materials

Unless otherwise stated, all compounds used in this study were purchased from Sigma-Aldrich Company Ltd. (Poole, Dorset, U.K.).

Statistical Analysis

All values described in the text and figures are expressed as mean±SEM for *n* observations. Each data point represents biochemical measurements obtained from up to 11 separate animals. Statistical analysis was carried out using GraphPad Prism 6.0b (GraphPad Software, San Diego, California, USA). Data without repeated measurements was assessed by one-way ANOVA followed by Bonferroni's multiple-comparison *post hoc* test. A *P* value of less than 0.05 was considered to be significant.

Results

The Time Course of Renal Function up to 14 days Post Unilateral Ureteral Obstruction

The renal function of animals subject to UUO was measured before, and up to 14 days post UUO. There was no significant change in the renal function of these animals at 7 or 14 days post UUO, when compared to baseline values taken 3 days prior to UUO surgery (Figure 4.1).

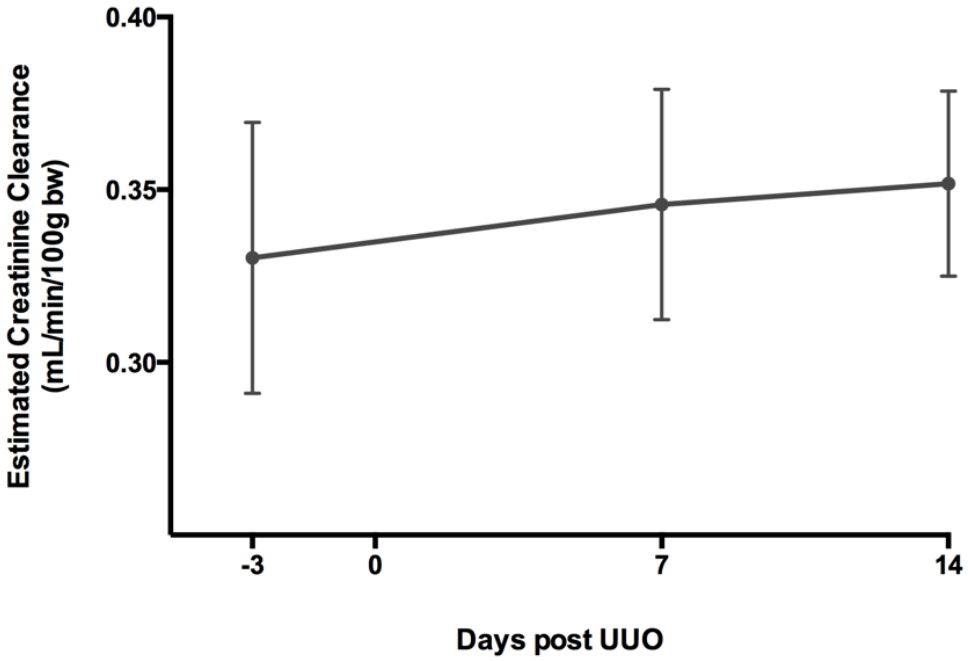

Figure 4.1 The time course of the estimated creatinine clearance (mL/min/100g body weight) over a 14 day period post UUO. Each point represents n=4. Data are presented as mean ± SEM of n observations.

Effect of Late Inhibition of IKK on Sirius Red Staining in the Rat Kidney after Unilateral Ureteral Obstruction

When compared to contralateral kidneys, kidneys subject to 14 days of UUO (+ vehicle) demonstrate significant increases in the % Sirius red per tissue field, indicating the development of fibrosis (Figure 4.2). There was no significant increase in fibrosis at 7 days post UUO when compared to contralateral kidneys, indicating the development of fibrosis from days 7-13. For this reason, I decided to treat the animals from days 7 – 13. Administration of IKK16 (1.0 mg/kg) on days 7 – 13 post UUO significantly attenuated the increase in Sirius red staining for collagen I and III, and therefore fibrosis, when compared to vehicle treated animals after 14 days of UUO (Figure 4.2). Representative images of Sirius red sections are displayed in Figure 4.3.

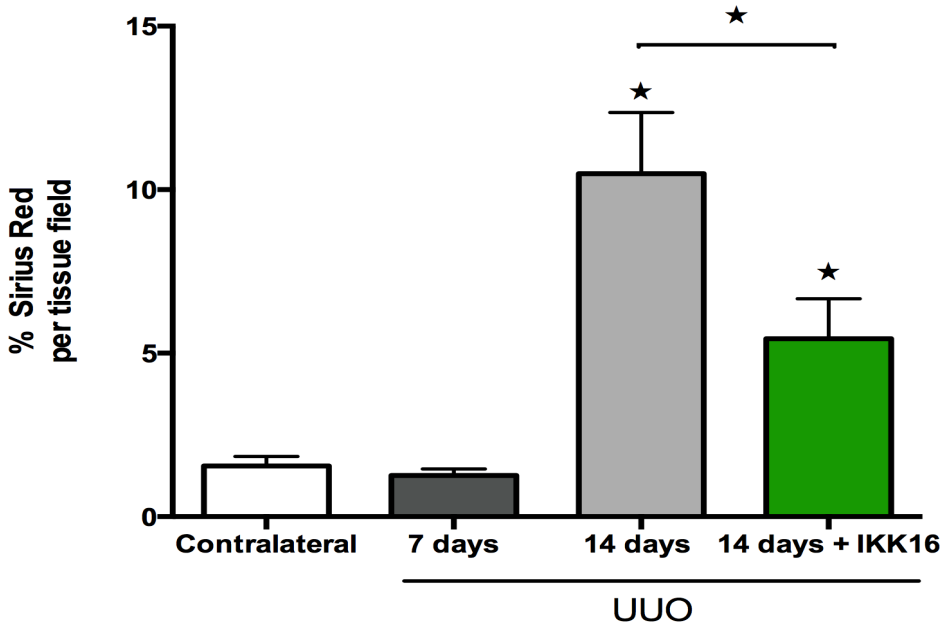

Figure 4.2 The time course of development of fibrosis (as measured by Sirius red for Collagen I and III) after unilateral ureteral obstruction (UUO) at 7 and 14 days, and the effect of the late administration of IKK16 (1.0 mg/kg s.c. days 7-13 post UUO). Contralateral: n=11; 7 days post UUO: n=6; 14 days post UUO + 10% DMSO vehicle days 7 - 13: n=8; 14 days post UUO + 1.0 mg/kg IKK16: n=9. Data are presented as mean ± SEM of n observations, ★P<0.05 vs. 14 days UUO + vehicle, unless otherwise stated.

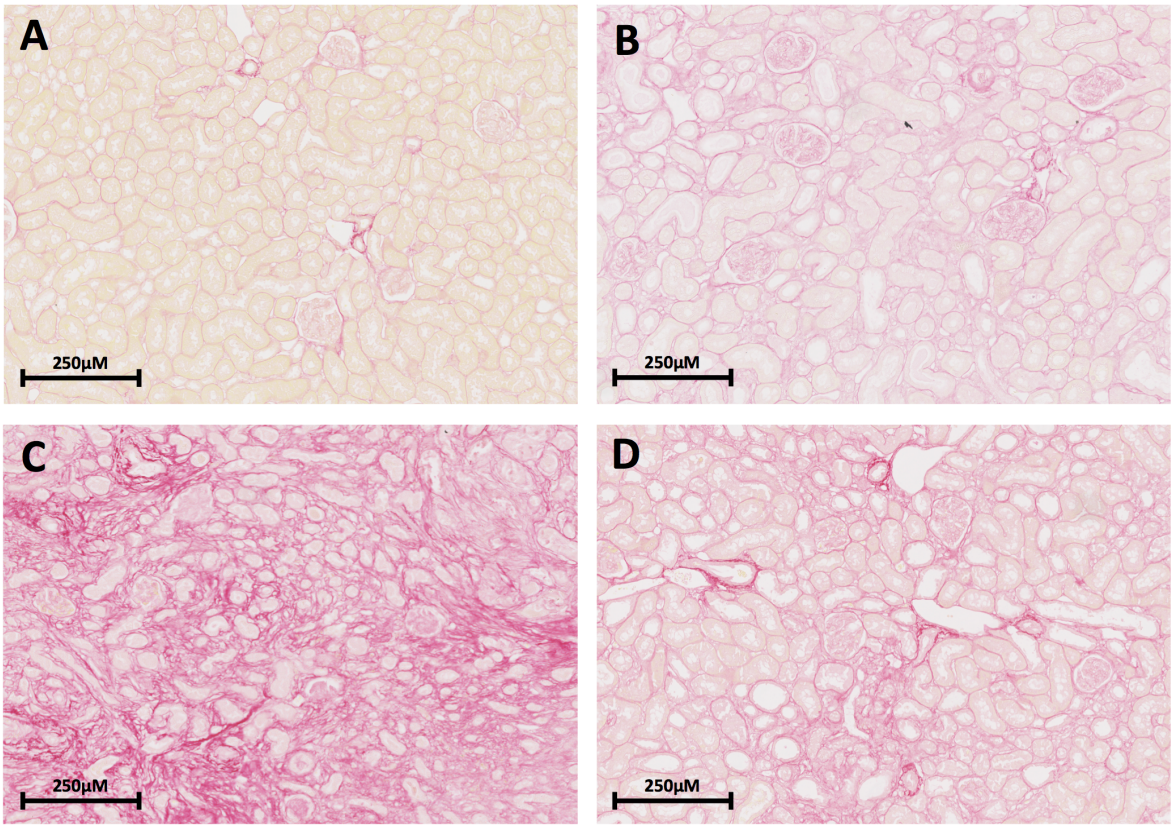

Figure 4.3 The time course of development of fibrosis (as measured by Sirius red for Collagen I and III) after unilateral ureteral obstruction (UUO) at 7 and 14 days, and the effect of the late administration of IKK16 (1.0 mg/kg s.c. days 7-13 post UUO). (A) Contralateral, (B) 7 days post UUO, (C) 14 days post UUO + 10% DMSO vehicle days 7 – 13, (D) 14 days post UUO + 1.0 mg/kg IKK16.

Effect of Late Inhibition of IKK on Myofibroblast Activation in the Rat Kidney after Unilateral Ureteral Obstruction

When compared to contralateral kidneys, kidneys subject to 14 days of UUO (+ vehicle) demonstrate significant increases in the % α-SMA per tissue field, indicating the activation of myofibroblasts (Figure 4.4). There was no significant increase in α-SMA staining at 7 days post UUO when compared to contralateral kidneys, indicating the activation of myofibroblasts from days 7-13. Administration of IKK16 (1.0 mg/kg) on days 7 – 13 post UUO significantly attenuated the increase in α-SMA staining for myofibroblasts when compared to vehicle treated animals after 14 days of UUO (Figure 4.4). Representative images of α-SMA stained sections are displayed in Figure 4.5.

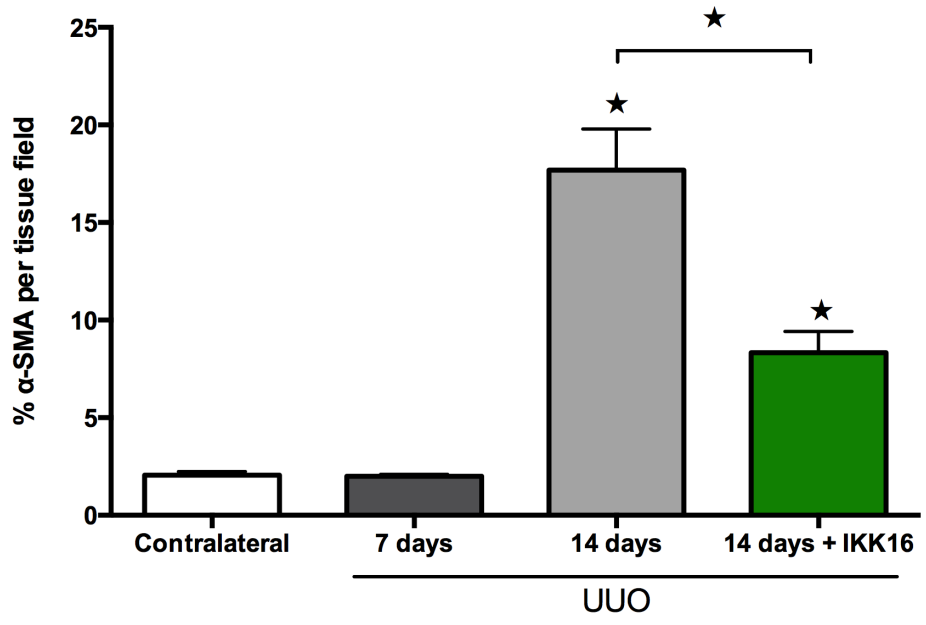

Figure 4.4 The effect of unilateral ureteral obstruction (UUO) at 7 and 14 days, and the effect of the late administration of IKK16 (1.0 mg/kg s.c. days 7-13 post UUO) on α-SMA staining for α-SMA-positive myofibroblasts. Contralateral: n=11; 7 days post UUO: n=6; 14 days post UUO + 10% DMSO vehicle days 7 - 13: n=8; 14 days post UUO + 1.0 mg/kg IKK16: n=9. Data are presented as mean ± SEM of n observations, ★P<0.05 vs. 14 days UUO + vehicle, unless otherwise stated.

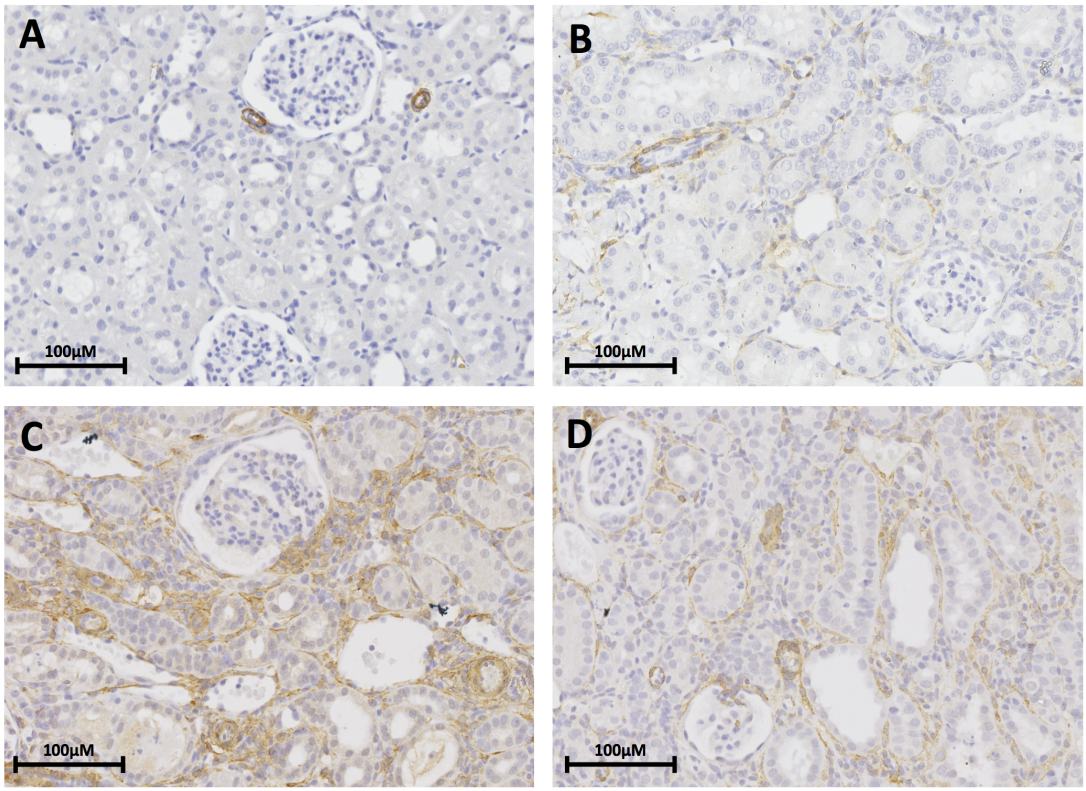

Figure 4.5 The effect of unilateral ureteral obstruction (UUO) at 7 and 14 days, and the effect of the late administration of IKK16 (1.0 mg/kg s.c. days 7-13 post UUO) on α-SMA staining for α-SMA-positive myofibroblasts. (A) Contralateral, (B) 7 days post UUO, (C) 14 days post UUO + 10% DMSO vehicle days 7 – 13, (D) 14 days post UUO + 1.0 mg/kg IKK16.

Effect of Late Inhibition of IKK on CD68$^+$ staining in the Rat Kidney after Unilateral Ureteral Obstruction

When compared to contralateral kidneys, kidneys subject to 14 days of UUO (+ vehicle) demonstrate significant increases in the % CD68$^+$ per tissue field, indicative of macrophages (Figure 4.6). There was no significant increase in CD68$^+$ staining at 7 days post UUO when compared to contralateral kidneys, indicating the infiltration of macrophages from days 7-13. Administration of IKK16 (1.0 mg/kg) on days 7 – 13 post UUO significantly attenuated the increase in CD68$^+$ staining for macrophages when compared to vehicle treated animals after 14 days of UUO (Figure 4.6). Representative images of CD68$^+$ stained sections are displayed in Figure 4.7.

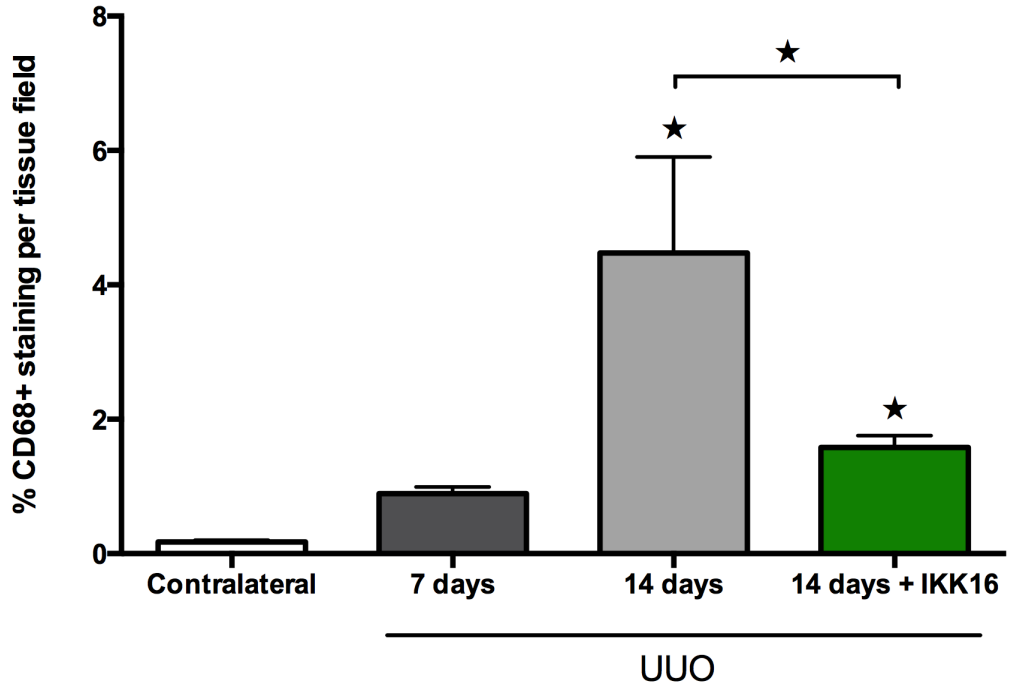

Figure 4.6 The effect of unilateral ureteral obstruction (UUO) at 7 and 14 days, and the effect of the late administration of IKK16 (1.0 mg/kg s.c. days 7-13 post UUO) on CD68$^+$ staining for macrophages. Contralateral: n=11; 7 days post UUO: n=6; 14 days post UUO + 10% DMSO vehicle days 7 - 13: n=8; 14 days post UUO + 1.0 mg/kg IKK16: n=9. Data are presented as mean ± SEM of n observations, ★P<0.05 vs. 14 days UUO + vehicle, unless otherwise stated.

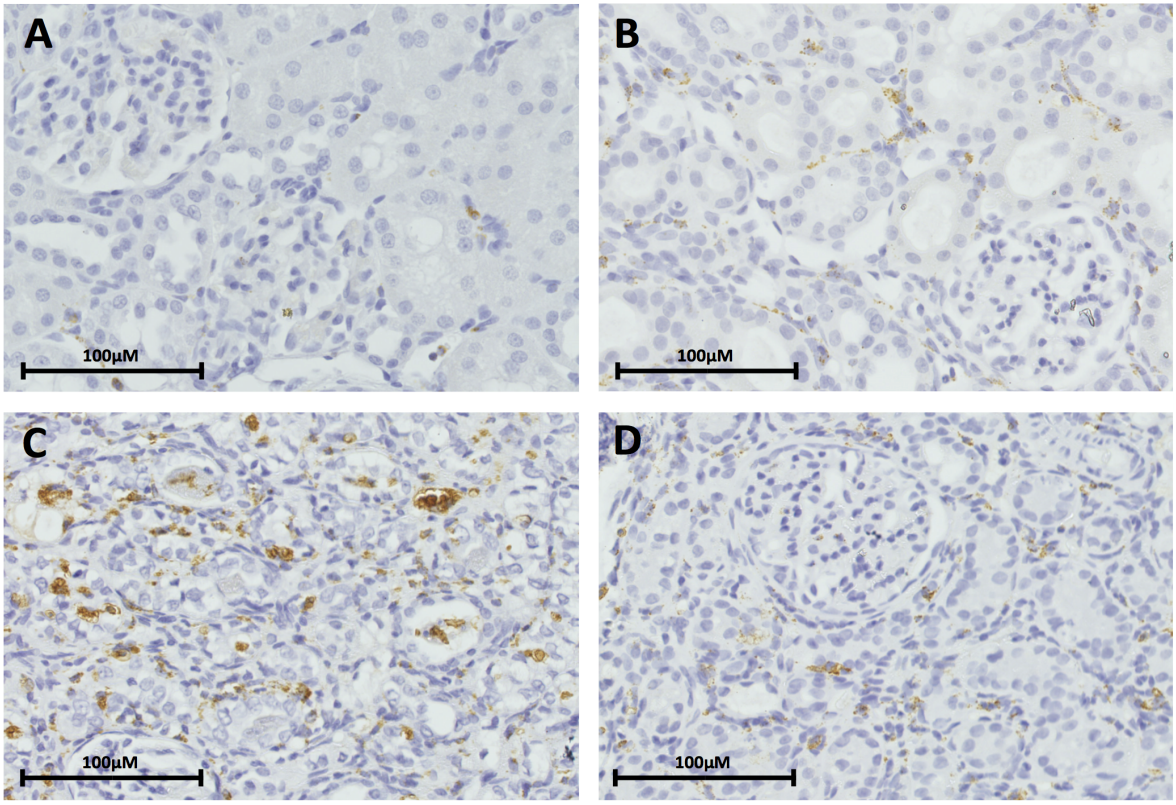

Figure 4.7 The effect of unilateral ureteral obstruction (UUO) at 7 and 14 days, and the effect of the late administration of IKK16 (1.0 mg/kg s.c. days 7-13 post UUO) on $CD68^{+}$ staining for macrophages. (A) Contralateral, (B) 7 days post UUO, (C) 14 days post UUO + 10% DMSO vehicle days 7 – 13, (D) 14 days post UUO + 1.0 mg/kg IKK16.

Effect of Unilateral Ureteral Obstruction and the Inhibition of IKK on the NF-κB Pathway in the Rat Kidney

When compared to contralateral kidneys, kidneys subject to 14 days of UUO (+ vehicle) exhibited significant phosphorylation of $Ser^{32/36}$ on IκBα (Figure 4.8A) and, hence, activation of the IKK complex (Figure 4.8B), as well as nuclear translocation of the p65 NF-κB subunit (Figure 4.8C). Administration of IKK16 (1.0 mg/kg) on days 7 – 13 post UUO significantly attenuated the increase in the phosphorylation of IκBα on $Ser^{32/36}$ (Figure 4.8A), consequently preventing the phosphorylation (and activation) of IKK at $Ser^{176/180}$ (Figure 4.8B) and therefore the subsequent nuclear translocation of the p65 NF-κB subunit (Figure 4.8C) when compared to vehicle treated animals after 14 days of UUO. There was also a significant increase in $Ser^{32/36}$ on IκBα (Figure 4.8A) activation of the IKK complex (Figure 4.8B), as well as nuclear translocation of the NF-κB subunit p65 (4.8C) in animals subject to 7 days of UUO when compared to contralateral animals.

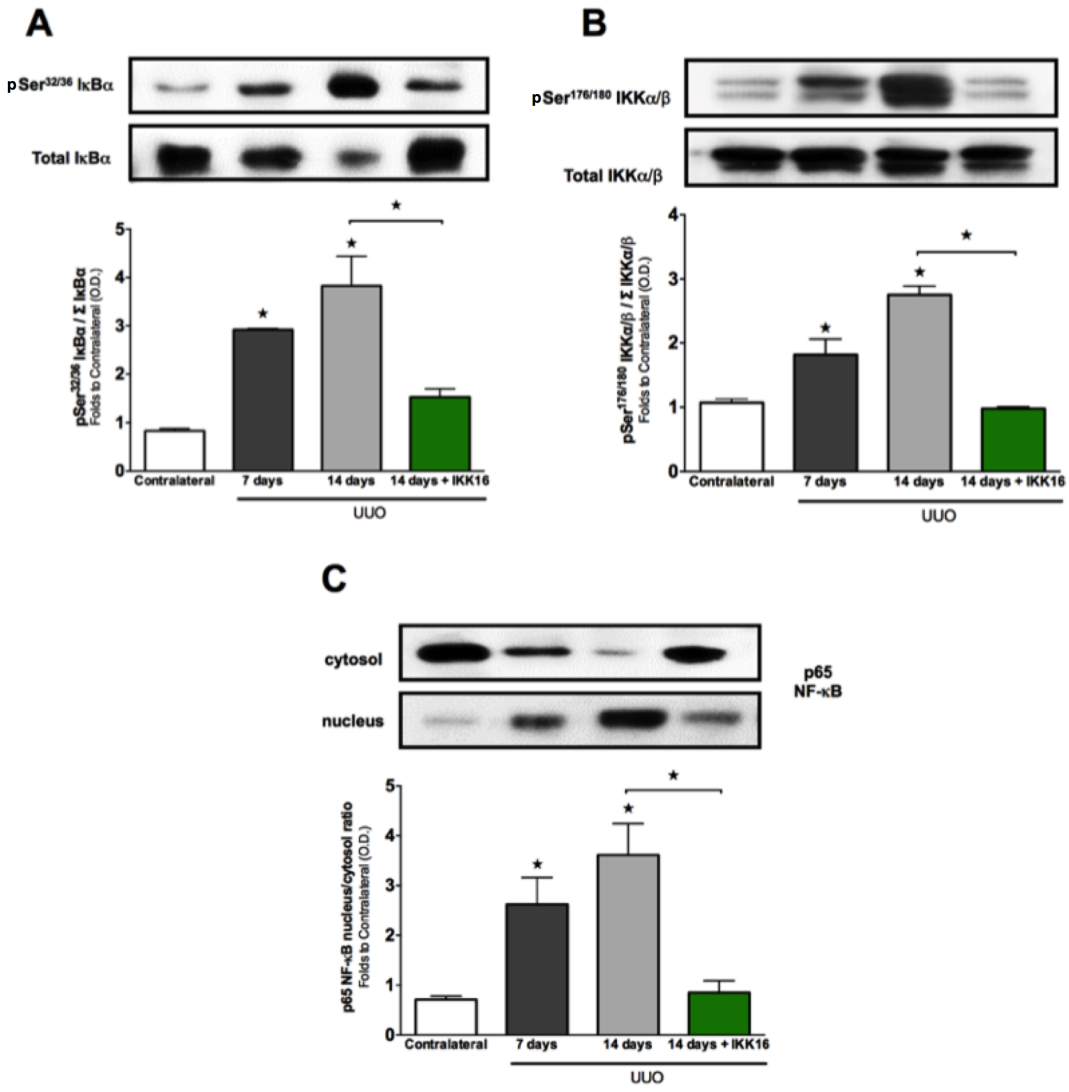

Figure 4.8 The effect of unilateral ureteral obstruction (UUO) at 7 and 14 days, and the effect of the late administration of IKK16 (1.0 mg/kg s.c. days 7-13 post UUO) on the activation of IκBα, IKKα/β and NF-κB. Activation of IκBα (A) was measured as phosphorylation of $Ser^{32/36}$ on IκBα. The activation of IκBα results in the activation of IKKα/β, measured as the phosphorylation of IKKα/β at $Ser^{176/180}$, which causes subsequent nuclear translocation of the p65 subunit of NF-κB (C). UUO; unilateral ureteral obstruction. Contralateral: n=8; 7 days post UUO: n=3; 14 days post UUO + 10% DMSO vehicle days 7 - 13: n=6; 14 days post UUO + 1.0 mg/kg IKK16: n=5. Densitometric analysis of the bands is expressed as relative optical density (OD) of IκBα phosphorylation at $Ser^{32/36}$ (A) or IKKα/β phosphorylation at $Ser^{176/180}$ (B), corrected for the corresponding total IκBα or IKKα/β content and normalised using the sham operated band. NF-κB nuclear translocation was evaluated by measuring NF-κB p65 subunit expression in both cytosolic and nuclear fractions, and expressing the results as nucleus/cytosol ratio. Each immunoblot is from a single experiment. Data are presented as mean ± SEM of n observations, ★P<0.05 vs. Contralateral, unless otherwise stated.

Effect of Late Inhibition of IKK on Pro-fibrotic Markers in the Rat Kidney after Unilateral Ureteral Obstruction

When compared to contralateral kidneys, kidneys subject to 14 days of UUO (+ vehicle) demonstrate significant increases in TGF-β expression (Figure 4.9). There was no significant increase in TGF-β at 7 days post UUO when compared to contralateral kidneys. Administration of IKK16 (1.0 mg/kg) on days 7 – 13 post UUO significantly attenuated the increase in TGF-β when compared to vehicle treated animals after 14 days of UUO (Figure 4.9).

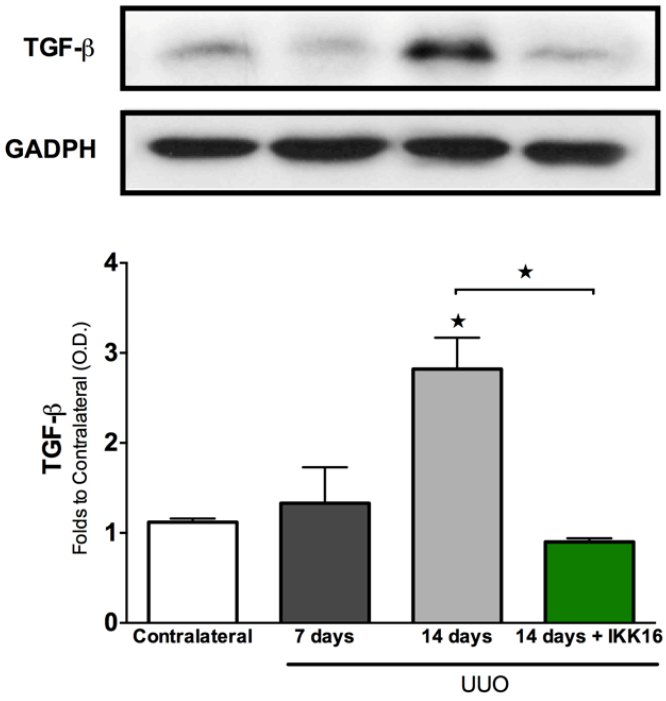

Figure 4.9 The effect of unilateral ureteral obstruction (UUO) at 7 and 14 days, and the effect of the late administration of IKK16 (1.0 mg/kg s.c. days 7-13 post UUO) on TGF-β expression. Contralateral: n=8; 7 days post UUO: n=4; 14 days post UUO + 10% DMSO vehicle days 7 - 13: n=5; 14 days post UUO + 1.0 mg/kg IKK16: n=5. Densitometric analysis of the bands is expressed as relative optical density (OD) of TGF-β, normalised using the sham operated band. Each immunoblot is from a single experiment. Data are presented as mean ± SEM of n observations, ★P<0.05 vs. Contralateral, unless otherwise stated.

When compared to contralateral kidneys, kidneys subject to 14 days of UUO (+ vehicle) demonstrate significant increases in Smad2/3 phosphorylation (Figure 4.10). There was no significant increase in Smad2/3 phosphorylation at 7 days post UUO when compared to contralateral kidneys. Administration of IKK16 (1.0 mg/kg) on days 7 – 13 post UUO significantly attenuated the increase in Smad2/3 phosphorylation when compared to vehicle treated animals after 14 days of UUO (Figure 4.10).

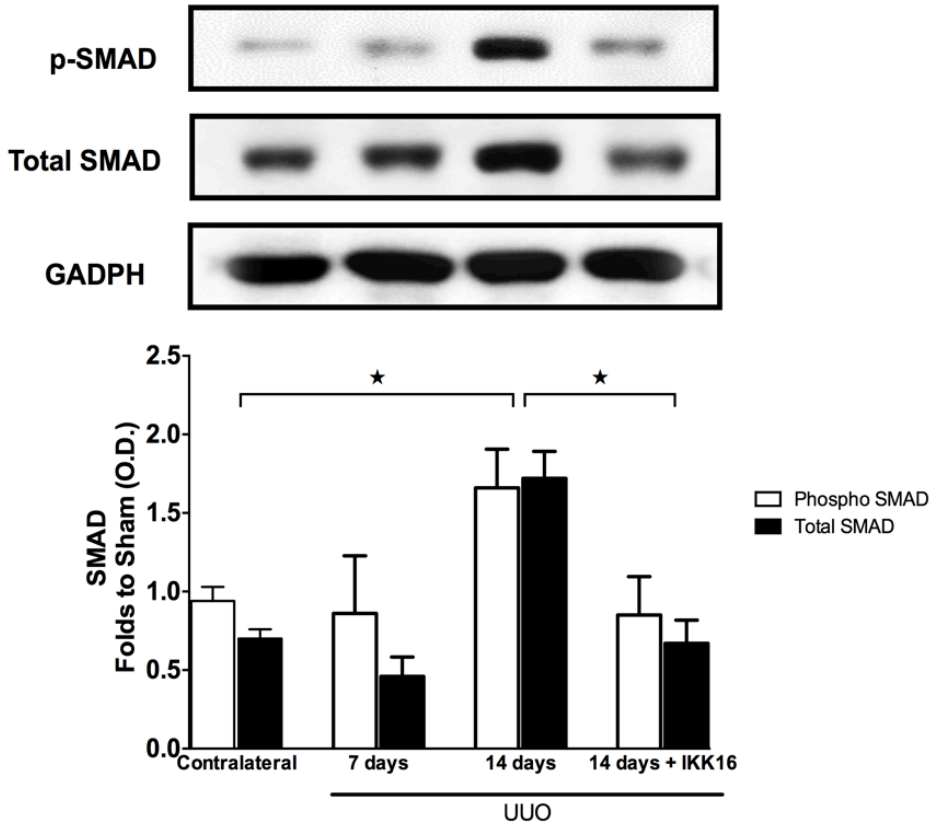

Figure 4.10 The effect of unilateral ureteral obstruction (UUO) at 7 and 14 days, and the effect of the late administration of IKK16 (1.0 mg/kg s.c. days 7-13 post UUO) on Smad2/3 phosphorylation. Contralateral: n=10; 7 days post UUO: n=6; 14 days post UUO + 10% DMSO vehicle days 7 - 13: n=6; 14 days post UUO + 1.0 mg/kg IKK16: n=6. Densitometric analysis of the bands is expressed as relative optical density (OD) phosphorylated Smad 2/3, corrected for the corresponding total Smad 2/3 content and normalised using the sham operated band. Each immunoblot is from a single experiment. Data are presented as mean ± SEM of n observations, ⋆P<0.05.

Effect of Late Inhibition of IKK on Extracellular Matrix Proteins in the Rat Kidney after Unilateral Ureteral Obstruction

When compared to contralateral kidneys, kidneys subject to 14 days of UUO (+ vehicle) demonstrate significant increases in vimentin expression (Figure 4.11). There was no significant increase in vimentin expression at 7 days post UUO when compared to contralateral kidneys. Administration of IKK16 (1.0 mg/kg) on days 7 – 13 post UUO significantly attenuated the increase in vimentin expression when compared to vehicle treated animals after 14 days of UUO (Figure 4.11).

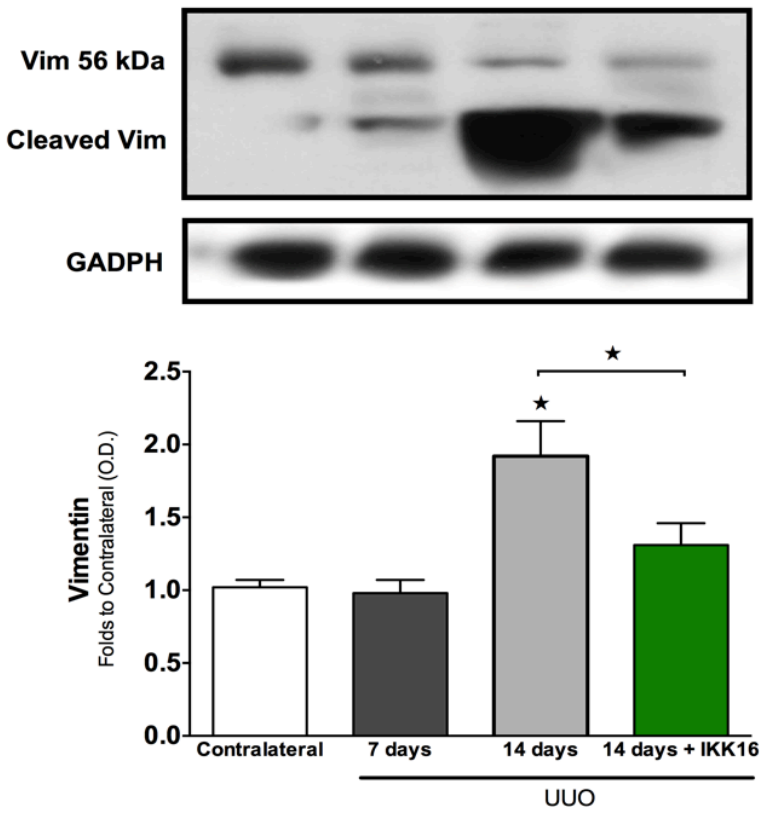

Figure 4.11 The effect of unilateral ureteral obstruction (UUO) at 7 and 14 days, and the effect of the late administration of IKK16 (1.0 mg/kg s.c. days 7-13 post UUO) on vimentin expression. Contralateral: n=6; 7 days post UUO: n=4; 14 days post UUO + 10% DMSO vehicle days 7 - 13: n=5; 14 days post UUO + 1.0 mg/kg IKK16: n=5. Densitometric analysis of the bands is expressed as relative optical density (OD) of total vimentin, normalised using the sham operated band. Each immunoblot is from a single experiment. Data are presented as mean ± SEM of n observations, ★P<0.05 vs. Contralateral, unless otherwise stated.

When compared to contralateral kidneys, kidneys subject to 14 days of UUO (+ vehicle) demonstrate significant increases in fibronectin expression (Figure 4.12). There was no significant increase in fibronectin expression at 7 days post UUO when compared to contralateral kidneys. Administration of IKK16 (1.0 mg/kg) on days 7 – 13 post UUO significantly attenuated the increase in fibronectin expression when compared to vehicle treated animals after 14 days of UUO (Figure 4.12).

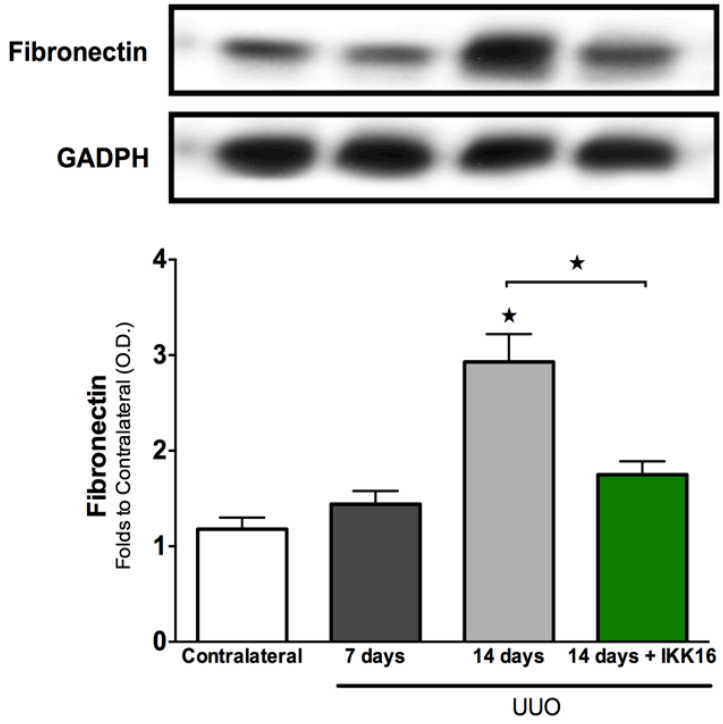

Figure 4.12 The effect of unilateral ureteral obstruction (UUO) at 7 and 14 days, and the effect of the late administration of IKK16 (1.0 mg/kg s.c. days 7-13 post UUO) on fibronectin expression. Contralateral: n=6; 7 days post UUO: n=4; 14 days post UUO + 10% DMSO vehicle days 7 - 13: n=5; 14 days post UUO + 1.0 mg/kg IKK16: n=5. Densitometric analysis of the bands is expressed as relative optical density (OD) of total fibronectin, normalised using the sham operated band. Each immunoblot is from a single experiment. Data are presented as mean ± SEM of n observations, ★P<0.05 vs. Contralateral, unless otherwise stated.

Discussion

Tubulointerstitial fibrosis is a major contributor to the loss of function in kidneys of patients with CKD, eventually leading to RRT-dependent ESRD. In this chapter, I have shown for the first time that the delayed inhibition of IKK, on days 7-13 in a rat model of UUO, resulted in a significant reduction in fibrosis and TGF-β expression.

UUO is a popular animal model of renal fibrosis as it is relatively short-term (in comparison to the 5/6 nephrectomy model, for example, which takes many months) and therefore inexpensive, modelling tubulointerstitial fibrosis similar to that of human CKD. UUO is not a functional model of renal fibrosis: UUO impairs the function of the ipsilateral kidney, and the contralateral kidney will compensate for this loss of function. The measurement of biochemical markers such as SCr and eCCL are unchanged and renal function cannot be used as a readout for disease severity. I have demonstrated in this chapter that rats subject to UUO have no significant changes in either SCr or eCCL over a period of 14 days. Tapmeier et al. (2008) developed a model of murine UUO in which the ureter was re-implanted up to 10 days post ureteral ligation, followed by contralateral nephrectomy (Tapmeier et al., 2008). Post re-implantation, the inflammatory process persisted and a functional assessment could then be made, making this model ideal for testing interventions, such as IKK16, to study the reversal of fibrosis, reduction of inflammation and/or the restoration of renal function. This model, however, is technically challenging due to the micro-suturing required to re-implant the ureter back into the bladder of the mouse.

In this chapter vehicle treated animals exhibit a significant increase in renal fibrosis when compared to contralateral (unligated) kidneys at 14 days post UUO, via the measurement of Sirius red staining for collagen I and III. At 7 days post UUO, there was no significant increase in any parameters associated with fibrosis (increased collagen I/III, increased α-SMA). Knowing that the development of fibrosis in this model occurred between 7 and 14 days post UUO, I decided to treat the animals in this period. The late inhibition of IKK (on days 7 – 13 s.c.) by IKK16 successfully reduced renal fibrosis caused by UUO.

In this chapter, I have demonstrated that the administration of IKK16 at days 7 – 13 significantly attenuates UUO-dependent increases in α-SMA, fibronectin and collagen I and III (as measured by Sirius red staining). Similarly, previous studies have demonstrated that IKK inhibition suppresses α-SMA and fibronectin expression as well as collagen type I production in dermal myofibroblasts via diminished nuclear translocation of NF-κB (Mia and Bank, 2015). I have shown here that the inhibition of IKK during days 7-13 post UUO reduces IKK activation and translocation of the NF-κB p65 subunit. The expression of the NF-κB p65 subunit and its nuclear translocation may be stimulated by TGF-β (Sun et al., 2015). Sun et al. (2015) described the increase in the p65 subunit in lung fibroblast differentiation when stimulated by TGF-β *in vitro*, and a further knockdown of Smad3 inhibited the TGF-β induced NF-κB p65 expression (Sun et al., 2015). In addition, NF-κB antisense oligonucleotide inhibits acquisition of the myofibroblast phenotype in lung fibroblasts after challenge with bleomycin (Zhou et al., 2014). TGF-β, therefore, may be important for the induction and translocation of NF-κB in

fibrosis, and NF-κB in turn may induce the myofibroblast phenotype (an increase in α-SMA) in renal fibroblasts.

Further to this, I have demonstrated that after 14 days post UUO, kidneys subject to UUO in vehicle treated animals exhibit a significant increase in staining for $CD68^+$, indicative of macrophages. After UUO, recruited macrophages are polarized from M1 (a subset whose functions include the removal of dead cells and debris) to M2 macrophages, which have the ability to stimulate tissue repair (Wang et al., 2015). M2 macrophages produce TGF-β1 to suppress bone morphogenetic protein 7 (BMP7), encouraging EMT. Depletion of M2 macrophages in UUO inhibits EMT and consequent fibrosis, however the same effect is not seen with M1 depletion (Pan et al., 2015). In various models of renal fibrosis, ablation of macrophages causes a considerable reduction in fibrosis (van Goor et al., 1992). Therefore, during chronic injury, prolonged infiltration of M2 macrophages may promote renal fibrosis (Pan et al., 2015).

I have shown here, for the first time, that the inhibition of IKK on days 7-13 post UUO resulted in a significant reduction in the staining for $CD68^+$, in kidneys subject to UUO when compared to vehicle-treated animals. Target genes of NF-κB include MCP-1, a monocyte chemoattractant (Guijarro and Egido, 2001). Inhibition of NF-κB with curcumin reduces MCP-1 expression, resulting in a reduction in immunostaining for macrophages (Kuwabara et al., 2006). Zhang et al. (2009) have described an increase in monocyte recruitment in vascular smooth muscle cells after vascular injury, through the activation of Smad2/3 and consequent gene transcription of MCP-1 (Zhang et al., 2009). Furthermore, overexpression of Smad 3 caused significant increases in MCP-1 and therefore monocyte recruitment

(Zhang et al., 2009). Moreover, neutralisation of MCP-1 in a mouse model of crescentic glomerulonephritis (producing a progressive fibrosis) dramatically reduced macrophage infiltration (by 47%) and collagen I (by 65%) when compared to untreated mice with crescentic glomerulonephritis (Lloyd et al., 1997). The increase in macrophage infiltration in animals subject to 14 days of UUO (+ vehicle) presented in this chapter, may therefore be due to the increase in TGF-β and Smad 2/3 signalling, and therefore increased MCP-1 gene transcription after 14 days of UUO (Zhang et al., 2009). IKK16 treated animals subject to UUO demonstrated a reduced macrophage infiltration when compared to vehicle control animals. It is possible that the inhibition of IKK, and a consequent inhibition of NF-κB translocation may prevent or reduce transcription of MCP-1, causing a reduction in macrophage influx into the renal tissue, however this is something I have yet to measure. Further experiments to explore MCP-1 expression would provide a greater insight into the mechanism of IKK-dependent macrophage activity.

In addition, macrophage-produced TGF-β1 causes local activation of myofibroblasts and EMT of tubular epithelial cells (Sutariya et al., 2016). These cells in turn produce their own source of TGF-β1, responsible for the production of ECM including fibronectin and vimentin. Mice over-expressing TGF-β1 develop renal fibrosis (Schnaper et al., 2003). Therefore, in this chapter, the reduction in TGF-β in IKK treated animals results in an attenuation of collagen I + III and ECM production (Sato et al., 2003). TGF-β binding TGF-β receptors activates Smads 2/3 to promote the production of pro-fibrotic genes. Smad3 -/- mice subject to UUO are protected against renal fibrosis, exhibiting reduced collagen, monocyte influx and reduced EMT, as Smad 3 is essential for TGF-β1-stimulated EMT (Sato et al., 2003). UUO caused a significant increase in the phosphorylation of Smad 2/3 at

day 14, which was successfully attenuated by the administration of IKK16 on days 7-13 post UUO. As Smad 2/3 is phosphorylated through TGF-β binding to the TGF-β receptor complex, attenuation in Smad 2/3 phosphorylation is due to reduced TGF-β receptor binding after IKK inhibition.

Finally, 14 days of UUO (+ vehicle) caused a significant increase in vimentin expression. Other than its role as an intermediate filament, vimentin is expressed in cells of mesenchymal origin and is used as a marker for EMT (Dave and Bayless, 2014). The western blots for vimentin in this chapter indicate that the vimentin has been 'cleaved' as there are two bands, one clear band at 56kDa ('normal' vimentin), and longer band at a lower molecular weight ('cleaved vimentin'). Intermediate filaments, including vimentin, can be cleaved and dismantled by various proteases, including calpain (Yoshida et al., 1984) and cysteine-dependent aspartate-directed proteases (caspases) (Byun et al., 2001). Caspases are a family of proteases that mediate apoptosis. Further to this, caspases 3 and 7 cleave vimentin at Asp^{85} producing a 48kDa fragment of vimentin (Byun et al., 2001), and caspase 6 to cleave vimentin at Asp^{259} producing lower molecular weight fragments from 20-30kDa (Byun et al., 2001). The cleavage of vimentin is initiated in apoptosis after caspase activation, and as there is strong evidence for the presence of apoptosis in UUO (Chevalier et al., 2009), this may provide an explanation for the cleavage of vimentin in both vehicle treated and IKK16 treated animals after 14 days of UUO in this chapter. Further experiments are required to assess the cleavage of vimentin and how it was reduced in IKK16 treated animals when compared to vehicle treated animals after 14 days of UUO. Further experiments

such as the study of caspase activation in UUO are required to further understand whether this is responsible for the cleavage of vimentin in this model.

In the UUO study I performed, rather than inhibiting IKK during the initial inflammatory stage (the first 7 days), I instead treated rats during the stage of collagen deposition and myofibroblast formation (the last 7 days). For the first time, I have identified that the late treatment of UUO with IKK16 prevents the deposition of collagen via reduction in TGF-β expression and formation of myofibroblasts, suggesting that the activation of IKK continues to be a critical component during the development of renal interstitial fibrosis.

Chapter V

General Discussion

AKI continues to be a great burden for the National Health Service, costing an estimated £500 million per annum (NHS Kidney Care, 2012). This figure is continually rising, due to the large increase in the number of patients suffering from AKI. Up to 7% of hospitalized patients present with AKI, and of these 7%, up to 60% will never regain full renal function (Uchino, 2006). Following AKI, a majority of patients will go on to later develop CKD, and with the increasing incidence of CKD comes an increase in ESRD, significant increases in treatment-associated costs and a large mortality rate (>1 million people per annum) (Hamer and El Nahas, 2006).

In this thesis, I have used a rat model of unilateral renal IRI (with contralateral nephrectomy). The literature contains models of both unilateral and bilateral renal IRI in a variety of species, most commonly rat or mouse. I chose the unilateral model of renal IRI as contralateral nephrectomy eliminates compensation of contralateral kidneys (as in the bilateral model of renal IRI) and, therefore, minimises variation in functional results (Skrypnyk et al., 2013). In the clinical setting, AKI may occur during or after transplantation in the recipient (Rao and Kjellstrand, 1983), and nephrectomised rats develop proteinuria, glomerulosclerosis, tubulointerstitial fibrosis and renal dysfunction after many months (Polichnowski et al., 2014). This is associated with the progression to CKD later in both pre-clinical models and in clinical studies (Nehus and Devarajan, 2012): another reason for using the unilateral renal IRI model. Previous publications by *Thiemermann and colleagues* have used a rat model of 30 min bilateral renal ischaemia and 48 h reperfusion, demonstrating significant renal and glomerular dysfunction (Patel et al., 2012). I adopted the same method, substituting

only the bilateral ischaemia for a unilateral ischaemia with contralateral nephrectomy.

In chapter II of this thesis, unilateral IRI with contralateral nephrectomy caused a significant increase in renal dysfunction, as measured by serum urea, glomerular dysfunction as measured by SCr and the eCCL and tubular dysfunction as measured by the $FENa^+$. All of these parameters were reversible, indicating an acute insult similar to that of human AKI. Serum urea is one of the most widely used tests for kidney function in the clinical setting and is elevated post AKI: as I have shown in animals subject to renal IRI in chapter II of this thesis. $FENa^+$ is useful in AKI evaluation: a high $FENa^+$ represents Na^+ loss and therefore tubular damage, which is useful in the diagnosis ATN or intrinsic renal failure.

In patients, AKI is diagnosed as a rise in SCr occurring between 24 and 72 h post AKI, a major flaw in the clinical diagnosis process as nephron damage occurs before this period. Both serum urea and SCr may also be affected by factors not relating to AKI, highlighting the need for early detection of injury with biomarkers, such as troponin in myocardial ischaemia. Measurement of early renal biomarkers requires further development and refinement: the ideal biomarker would predict long term outcomes such as mortality and potential CKD development as well as short term outcomes such as dialysis post AKI. Biomarkers such as NGAL and kidney injury molecule-1 (KIM-1) are highly sensitive and renal-specific but have not yet been developed for clinical use. However, despite the need for the earlier detection of AKI, I have shown here for the first time that it is possible to treat animals subject to renal IRI at peak SCr (24 h), demonstrating that a clinically relevant treatment strategy in relation to SCr elevation is possible.

There is good evidence that NF-κB plays a detrimental role in renal IRI. In this thesis, I have demonstrated that kidneys of rats subject to 30 min/48 h renal IRI, the activation of NF-κB is significantly elevated compared to sham animals. Similar data by Patel et al. (2012) demonstrates an increased p65 NF-κB nucleus to cytosol ratio at 48 h post reperfusion after 30 min bilateral renal IRI (Patel et al., 2012). Further to this, the phosphorylation of IκBα (this thesis) was also elevated at 48 h post reperfusion. With these data in mind, I treated the animals at 24 h post reperfusion at peak SCr and prior to NF-κB activation. In this thesis, I have demonstrated for the first time that the delayed inhibition of IKK (at 24 h), using the IKK inhibitor IKK16, in a rat model of unilateral renal IRI and contralateral nephrectomy attenuates IRI-dependent changes in biochemical markers (namely serum urea, SCr, eCCL and $FENa^{+}$), indicating improvement in renal, glomerular and tubular function when compared to control animals. In addition, IKK inhibition (at 24 h) successfully attenuated IκBα phosphorylation and consequent NF-κB translocation to the nucleus.

NF-κB mediates many inflammatory states, including AKI, playing a fundamental role in the production of pro-inflammatory cytokines such as IL-6, IL-1β, and IL-8, to name a few (Bonizzi and Karin, 2004). It has previously been proven that the early inhibition of NF-κB in inflammatory disease states successfully attenuates inflammation. López-Franco et al. (2002) have previously shown that in an animal model of glomerulonephritis, early NF-κB inhibition reduced proteinuria, glomerular lesions and monocyte/macrophage infiltration (López-Franco et al., 2002). The inhibition of IKK at 24 h post reperfusion most likely reduced IRI-associated inflammation, restoring both functional and structural injury to sham-like levels.

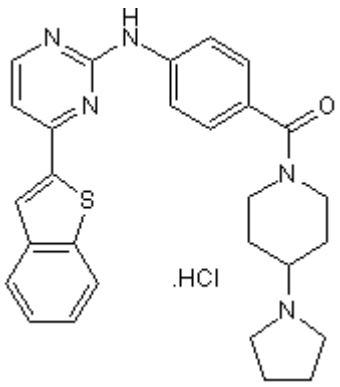

Figure 5.1 The structure of IKK16, a 2-benzomido-pyrimidine, with selectivity for IKKβ. Taken from (Waelchli et al., 2006)

The compound used in this thesis, IKK16, was screened from a Novartis compound archive for 'hits' with a typical kinase inhibitor motif (Figure 5.1) (Waelchli et al., 2006). IKK16 is a tertiary 2-benzamido-pyrimidine with selectivity for IKKβ, and of all the compounds screened in this paper, IKK16 was the most potent. This was confirmed by an IκBα degradation assay, from which the IC_{50} value was calculated (Waelchli et al., 2006). IKK16 was among several compounds tested and was further used in *in vivo* efficacy studies. Firstly, IKK16 was used in a rat model of lipopolysaccharide (LPS)-induced TNF-α release, where both p.o. (30 mg/kg) and s.c. (30 mg/kg) IKK16 administered 1 h prior to LPS challenge produced a significant attenuation of plasma TNF-α, and inhibited the expression of adhesion molecules E-selectin, ICAM and VCAM (Waelchli et al., 2006). In a second animal model, IKK16 (10 mg/kg s.c.) inhibited neutrophil extravasation in thioglycollate-induced peritonitis (Waelchli et al., 2006).

Previous *in vivo* studies by Waelchli et al. (2006) administered 30 mg/kg IKK16 via p.o. and s.c. routes of administration (Waelchli et al., 2006), so the decision was to lower the dose based on a i.v. route of administration, with a dose response from 0.1 mg/kg to 1.0 mg/kg. I demonstrate in this thesis that the two lowest concentrations of IKK16 (0.1 mg/kg and 0.3 mg/kg) administered at 24 h post reperfusion had no significant effect on any of the biochemical parameters measured (serum urea, SCr, eCCL and $FENa^+$). Assuming a blood volume of

17.5ml per 250 g rat, 0.1 mg/kg and 0.3 mg/kg would result in a plasma concentration of approximately 2.75 μM and 9.15 μM, respectively. The IC_{50} values for IKK16 are as follows: IKKβ, 40 nM; IKK complex, 70 nM; IKKα, 200 nM. Despite the calculated plasma concentrations for both 0.1 mg/kg and 0.3 mg/kg being sufficient to inhibit the IKK complex, the plasma concentration of IKK16 will realistically be lower than this for two reasons: 1) tissue distribution of the compound and 2) elimination of the compound by metabolism or excretion. Pharmacokinetic studies are required to determine the half-life of the compound and the concentration of IKK16 in the kidney after administration. IKK16 may have a short pharmacodynamic profile that may result in a reduced plasma concentration. Based on the assumptions previously described, 1.0 mg/kg would result in a plasma concentration of 27.5 μM, likely to result in a sufficient plasma concentration to inhibit IKK. 1.0 mg/kg IKK16 successfully inhibited the IKK complex (as demonstrated in chapter II by the attenuation of renal IRI-dependent increases in the phosphorylation of $Ser^{176/180}$ on IKK and therefore its activation, and further confirmed by the attenuation of the phosphorylation of $Ser^{32/36}$ on IκBα and the p65 NF-κB nucleus to cytosol ratio).

I decided to use IKK as a target, as it is just upstream from NF-κB. The debate surrounding NF-κB inhibition is very much a 'hot' topic and the dilemma surrounding when to inhibit NF-κB is still being elucidated given that more than 800 synthetic and naturally occurring compounds partly mediate their effects through the modulation of NF-κB activation (Gilmore and Herscovitch, 2006). I propose that the initial activation of NF-κB for the onset of inflammation is critical for the induction of subsequent tissue-repair mechanisms by a complex system of

gene expression for molecular regulators such as various growth factors, adhesion molecules and cell cycle regulators. It is the over-activation of NF-κB that must be limited in order to allow such tissue-repair mechanisms to be initiated.

The use of knockout animals would help to further elucidate the role of IKK in renal IRI and the development of fibrosis. IKK-/- animals die in utero; IKKα-/- animals die shortly after birth, and display defective keratinocyte differentiation and skeletal abnormalities (Sil et al., 2004), whereas IKKβ-/- mice experience liver injury and apoptosis during embryonic development around day 14 (Tanaka et al., 1999). A similar phenotype is seen with IKKγ knockout animals, which are also embryonically lethal (Rudolph et al., 2000). Despite this, conditional deletion of IKKβ is possible via cre-loxP technology. In a mouse model of stroke, IKKβ gene deletion by crossing mice carrying *Ikbkb* alleles flanked by loxP sites markedly reduced ischaemic death in neuronal cells (Herrmann et al., 2005). Again, this technique could be used to further confirm the role of IKK in both renal IRI and the subsequent development of fibrosis.

Recent clinical research has highlighted the dramatic link between AKI severity and progression to CKD (Belayev and Palevsky, 2014). In chapter III of this thesis, I extended the reperfusion period to 28 days following unilateral renal IRI (with contralateral nephrectomy), to simulate the development of CKD. The extension of the renal IRI model did not result in a reduction in renal function as seen in CKD patients post AKI, however after excision of the kidney, it was found that there was significant development of fibrosis in vehicle-treated rats. Furthermore, this was ameliorated by the inhibition of IKK with one single bolus of IKK16, at 24 h post

reperfusion, at peak SCr. Basile et al. (2015) have recently described repair after AKI as 'adaptive' or 'maladaptive' (Basile et al., 2015). Adaptive repair describes the return of 'normal' structure and function at 90 days post AKI, characterised by rapid restoration of renal function, proliferation of tubular cells, and resolution of pathology, inflammation and damage biomarkers (Figure 5.2A). Conversely, maladaptive repair consists of a reduction in kidney function associated with a change in renal structure, expression of pro-fibrotic factors, delayed resolution of inflammation and damage biomarkers (Figure 5.2B) (Basile et al., 2015). Maladaptive repair occurs within the tubules, vasculature and the interstitial space post AKI, therefore promoting the deposition of collagen in the interstitium. Figure 5.2 demonstrates these types of repair, and suggests that the repair in this chapter may be either adaptive or maladaptive, due to the restoration of original renal function 7 days post renal IRI (adaptive) and the persistence of pro-fibrotic markers at day 28 (maladaptive). For future studies, modelling more severe maladaptive repair may be more suitable due to the development of permanent fibrosis and a persistent decline in renal function. It is the balance between these two repair states that predicts fibrosis and CKD development. In clinical situations, the probability of progressing to CKD from AKI increases proportionally with the number of episodes of AKI (Belayev and Palevsky, 2014); therefore future work to develop an animal model to include multiple sessions of renal IRI *in vivo* may be of more clinical relevance. Delivering more severe injury to promote fibroblast activation, fibrosis development and functional decline would provide a more accurate model to study the AKI to CKD phenomena, and indeed the inhibition of IKK.

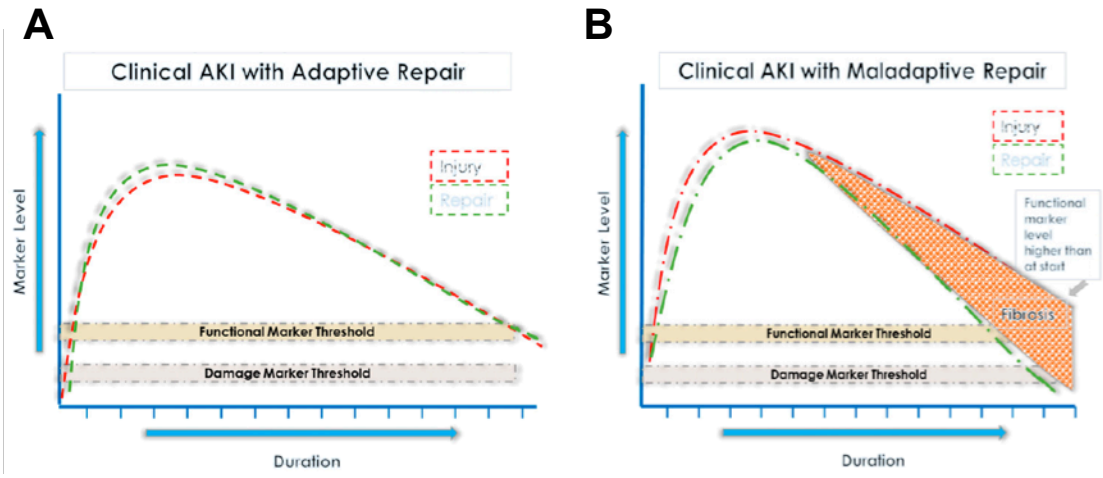

Figure 5 Clinical AKI with (A) adaptive and (B) maladaptive repair. Adaptive repair is injury causing an increase in both damage and functional markers, in which repair matches injury and therefore resolution of AKI. Maladaptive repair sees injury levels higher than repair rate and therefore fibrosis is produced, leading to chronic damage and non-recovery (to CKD). Image adapted from Basile et al. (2015).

I have demonstrated for the first time that the inhibition of IKK at peak SCr not only reduces both structural and functional injury at 48 h post reperfusion, but also surprisingly causes a significant reduction in fibrosis at 28 days post reperfusion when compared to control animals. I have further found a significant increase of TGF-β and α-SMA at 7 days post reperfusion in vehicle treated animals. This data indicates the beginning of the fibrotic process in this model, however may also be used as a timeline of when to use certain compounds to target fibrosis, e.g. the administration of a TGF-β inhibitor at 7 days post IRI. Studying activation of particular markers at different times in the progression may open a whole new door to accurate initiation of therapies to combat impending CKD. Clinically, it is difficult to know when to intervene, what to intervene with, and when previous episodes of AKI have occurred. Such issues require a better understanding of biomarkers involved in the progression of AKI to CKD, and better animal models to deal with this.

Fibrotic disease is responsible for 45% mortality in the developed world (Wynn, 2008), and yet there are still no effective, approved anti-fibrotic treatments. Finally, in chapter IV of this thesis, I have demonstrated that the inhibition of IKK on days 7-13 in a rat UUO model successfully attenuated renal fibrosis formation, myofibroblast activation and macrophage infiltration. Previous studies inhibiting IKK in a variety of different animal models of lung (Ogawa et al., 2011), liver (Wei et al., 2011) and heart (Maier et al., 2012) have proven the importance of the role of IKK in the fibrotic process. In reality, treating fibrosis in patients is likely to be far more complex than the sole inhibition of IKK; fibrosis involves multiple interconnecting pathways, each molecule playing a similarly important role to the next. Realistically, inhibition of a single pathway in the fibrotic process will not sufficiently completely eradicate/halt fibrosis, therefore in future, combination therapies targeting multiple pathways should be considered.

In conclusion, it is evident that NF-κB and the activation of IKK affect functional and structural outcomes after both renal IRI and the subsequent development of fibrosis. In this thesis, I have mapped the time course of NF-κB in an acute model of renal IRI, finding the inhibition of IKK at 24 h post reperfusion to be of both functional and structural benefit to the kidney. The successful inhibition of IKK at peak SCr demonstrates that it is possible to intervene in patients with AKI at such a late stage (i.e. peak SCr), providing hope for the development of such therapies. Furthermore, the amelioration of functional and structural damage via the inhibition of IKK at 24 h successfully ameliorates the subsequent development of fibrosis, pro-fibrotic markers and over-production of ECM components at 28 days post renal

IRI. In addition, the inhibition of IKK in a model of UUO, modelling tubulointerstitial fibrosis, successfully attenuates the production of fibrosis, pro-fibrotic markers and over-production of ECM components after 14 days of UUO. These data indicate that the activation of the IKK complex drives tubulointerstitial fibrosis, and suggests that the inhibition of IKK could be a useful pharmacological tool for the creation of therapies to combat AKI and the subsequent development of fibrosis, via the reduction of both inflammation and the prevention of the expression of pro-fibrotic markers.

Suggestions for Future Research

- To measure early damage biomarkers (such as KIM-1, cystatin C, NGAL) in the rat model of renal IRI (30 min ischaemia/28 day reperfusion) throughout the timecourse, to assess whether the development of fibrosis in vehicle control animals correlates with biomarker expression at any time point. If so, does the inhibition of IKK with IKK16 reduce biomarker expression?
- To extend the reperfusion period (after 30 min ischaemia) to 90 days to assess whether the fibrosis developed in vehicle control animals reverses, persists or worsens, and to see the effect that IKK inhibition (at 24 h post reperfusion) has on fibrosis in the kidney after a 90 day reperfusion period.
- To develop a new rat model of unilateral renal IRI (45-60 min) with no contralateral nephrectomy. The renal function will remain sham-like in injured animals due to the functioning contralateral kidney; however, this model would deliver a more severe renal insult, resulting in a more severe fibrosis, and may also result in persistent myofibroblast activation and macrophage infiltration at 28 days. Additionally, this model could be used to see whether the inhibition of IKK with IKK16 at 24 h post reperfusion causes a reduction in renal fibrosis developed at 28 days post renal IRI.
- To investigate the activation of other transcription factors post renal IRI in the rat, e.g. peroxisome proliferator-activated receptor-γ (PPAR-γ). PPAR-γ agonism prior to, and during reperfusion, has shown to be beneficial in renal IRI (Sivarajah et al., 2003). Many insulin-sensitizing drugs target PPAR-γ and are already approved as pharmacological therapies for type II diabetes. Using therapies already approved for human use in pre-clinical studies therefore increases the translatability of the intervention (if successful in renal IRI).

Conclusions

- In the first chapter of this thesis, I studied the timecourse of AKI in a rat model of IRI (30 minutes ischaemia, 24, 48 and 72 h reperfusion). During the time course, renal dysfunction (maximal SCr) was most significant at 24 h post reperfusion, and NF-κB activation was at 48 h post reperfusion. Using these data I treated animals at 24 h post reperfusion with the IKK inhibitor, IKK16.
- IKK inhibition at 24 h post reperfusion successfully attenuated renal dysfunction and histological changes associated with AKI, whilst also inhibiting IKK activation and subsequent NF-κB translocation. These data indicate that renal IRI may be successfully treated at 24 h post reperfusion, during peak SCr, at which time AKI is diagnosed. This may be a step forward into research aimed at therapy initiation post-AKI diagnosis.
- Furthermore, IKK inhibition at 24 h post renal IRI successfully reduced the development of fibrosis associated with 30 min ischaemia and 28 days of reperfusion in a rat model of IRI. IKK inhibition also reduced the activation of myofibroblasts and the infiltration of macrophages at 7 days post reperfusion. This indicates that the early amelioration of AKI post-diagnosis may reduce/retard/prevent the development of fibrosis and therefore the progression to CKD after AKI.
- IKK inhibition also reduced fibrosis development, myofibroblast activation and macrophage infiltration associated with UUO.
- These data indicate that the activation of the IKK complex drives fibrosis, and suggests that the inhibition of IKK could be a useful pharmacological tool for the creation of therapies to combat AKI and the subsequent development of fibrosis.

References

Acikgoz, Y., Can, B., Bek, K., Acikgoz, A., Ozkaya, O., Genç, G., et al. (2014). The effect of simvastatin and erythropoietin on renal fibrosis in rats with unilateral ureteral obstruction. Ren. Fail. *36*: 252–7.

Ali, T., Khan, I., Simpson, W., Prescott, G., Townend, J., Smith, W., et al. (2007). Incidence and outcomes in acute kidney injury: a comprehensive population-based study. J Am Soc Nephrol *18*: 1292–1298.

Anders, H.-J., and Ryu, M. (2011). Renal microenvironments and macrophage phenotypes determine progression or resolution of renal inflammation and fibrosis. Kidney Int. *80*: 915–25.

Ansaldi, D., Hod, E.A., Stellari, F., Kim, J.-B., Lim, E., Roskey, M., et al. (2011). Imaging pulmonary NF-kappaB activation and therapeutic effects of MLN120B and TDZD-8. PLoS One *waek6*: e25093.

Arfian, N., Emoto, N., Vignon-Zellweger, N., Nakayama, K., Yagi, K., and Hirata, K. (2012). ET-1 deletion from endothelial cells protects the kidney during the extension phase of ischemia/reperfusion injury. Biochem Biophys Res Commun *425*: 443–449.

Association, U.K.R. (2015). Clinical Practice Guidelines (http://www.renal.org/guidelines/modules/acute-kidney-injury).

Atthe, B.K., Babsky, A.M., Hopewell, P.N., Phillips, C.L., Molitoris, B.A., and Bansal, N. (2009). Early monitoring of acute tubular necrosis in the rat kidney by 23Na-MRI. Am J Physiol Ren. Physiol *297*: F1288–98.

Azuma, H., Nadeau, K., Takada, M., and Tilney, N.L. (2007) Initial ischemia/reperfusion injury influences late functional and structural changes in the kidney. Transplant. Proc. *29*: 1528–9.

Baek, J.-H., Zeng, R., Weinmann-Menke, J., Valerius, M.T., Wada, Y., Ajay, A.K., et al. (2015). IL-34 mediates acute kidney injury and worsens subsequent chronic kidney disease. J. Clin. Invest. *125*: 3198–214.

Bagshaw, S.M., Bellomo, R., Devarajan, P., Johnson, C., Karvellas, C.J., Kutsiogiannis, D.J., et al. (2010). Acute kidney injury in critical illness. Can. J. Anaesth. *57*: 985–98.

Barnes, J.L., and Glass, W.F. (2011). Renal interstitial fibrosis: a critical evaluation

of the origin of myofibroblasts. Contrib. Nephrol. *169*: 73–93.

Barrera-Chimal, J., Pérez-Villalva, R., Rodríguez-Romo, R., Reyna, J., Uribe, N., Gamba, G., et al. (2013). Spironolactone prevents chronic kidney disease caused by ischemic acute kidney injury. Kidney Int. *83*: 93–103.

Basile, D.P., Bonventre, J. V, Mehta, R., Nangaku, M., Unwin, R., Rosner, M.H., et al. (2015). Progression after AKI: Understanding Maladaptive Repair Processes to Predict and Identify Therapeutic Treatments. J. Am. Soc. Nephrol. *27*: 687–97.

Basile, D.P., Donohoe, D., Roethe, K., and Osborn, J.L. (2001). Renal ischemic injury results in permanent damage to peritubular capillaries and influences long-term function. Am J Physiol Ren. Physiol *281*: F887–99.

Basile, D.P., Fredrich, K., Chelladurai, B., Leonard, E.C., and Parrish, A.R. (2008). Renal ischemia reperfusion inhibits VEGF expression and induces ADAMTS-1, a novel VEGF inhibitor. Am J Physiol Ren. Physiol *294*: F928–36.

Belayev, L.Y., and Palevsky, P.M. (2014). The link between acute kidney injury and chronic kidney disease. Curr. Opin. Nephrol. Hypertens. *23*: 149–54.

Biesen, W. Van, Vanholder, R., and Lameire, N. (2006). Defining acute renal failure: RIFLE and beyond. Clin J Am Soc Nephrol *1*: 1314–1319.

Bilge, U., Sahin, G., Unluoglu, I., Ipek, M., Durdu, M., and Keskin, A. (2013). Inappropriate use of nonsteroidal anti-inflammatory drugs and other drugs in chronic kidney disease patients without renal replacement therapy. Ren Fail *35*: 906–910.

Bonizzi, G., and Karin, M. (2004). The two NF-kappaB activation pathways and their role in innate and adaptive immunity. Trends Immunol *25*: 280–288.

Bonventre, J. V, and Weinberg, J.M. (2003). Recent advances in the pathophysiology of ischemic acute renal failure. J Am Soc Nephrol *14*: 2199–2210.

Boor, P., Ostendorf, T., and Floege, J. (2010). Renal fibrosis: novel insights into mechanisms and therapeutic targets. Nat. Rev. Nephrol. *6*: 643–56.

Boron, W., and Boulpaep, E. (2008). Medical Physiology (Elsevier Health Sciences).

Braga, T.T., Agudelo, J.S.H., and Camara, N.O.S. (2015). Macrophages During the Fibrotic Process: M2 as Friend and Foe. Front. Immunol. *6*: 602.

Bucaloiu, I.D., Kirchner, H.L., Norfolk, E.R., Hartle, J.E., and Perkins, R.M. (2012). Increased risk of death and de novo chronic kidney disease following reversible acute kidney injury. Kidney Int. *81*: 477–85.

Byun, Y., Chen, F., Chang, R., Trivedi, M., Green, K.J., and Cryns, V.L. (2001). Caspase cleavage of vimentin disrupts intermediate filaments and promotes apoptosis. Cell Death Differ. *8*: 443–50.

Cachat, F., Lange-Sperandio, B., Chang, A.Y., Kiley, S.C., Thornhill, B.A., Forbes, M.S., et al. (2003). Ureteral obstruction in neonatal mice elicits segment-specific tubular cell responses leading to nephron loss. Kidney Int. *63*: 564–75.

Cai, G., Zhang, X., Hong, Q., Shao, F., Shang, X., Fu, B., et al. (2008). Tissue inhibitor of metalloproteinase-1 exacerbated renal interstitial fibrosis through enhancing inflammation. Nephrol Dial Transpl. *23*: 1861–1875.

Cao, C.C., Ding, X.Q., Ou, Z. Lou, Liu, C.F., Li, P., Wang, L., et al. (2004). In vivo transfection of NF-kappaB decoy oligodeoxynucleotides attenuate renal ischemia/reperfusion injury in rats. Kidney Int. *65*: 834–45.

Carlstrom, M., Wilcox, C.S., and Arendshorst, W.J. (2015). Renal autoregulation in health and disease. Physiol Rev *95*: 405–511.

Chandraker, A., Takada, M., Nadeau, K.C., Peach, R., Tilney, N.L., and Sayegh, M.H. (1997). CD28-b7 blockade in organ dysfunction secondary to cold ischemia/reperfusion injury. Kidney Int *52*: 1678–1684.

Channon, K.M. (2004). Tetrahydrobiopterin: regulator of endothelial nitric oxide synthase in vascular disease. Trends Cardiovasc. Med. *14*: 323–7.

Chawla, L.S., Amdur, R.L., Amodeo, S., Kimmel, P.L., and Palant, C.E. (2011). The severity of acute kidney injury predicts progression to chronic kidney disease. Kidney Int *79*: 1361–1369.

Chen, G., Cao, P., and Goeddel, D. V (2002). TNF-induced recruitment and activation of the IKK complex require Cdc37 and Hsp90. Mol. Cell *9*: 401–10.

Chen, X., Liu, X., Wan, X., Wu, Y., Chen, Y., and Cao, C. (2009). Ischemic preconditioning attenuates renal ischemia-reperfusion injury by inhibiting activation of IKKbeta and inflammatory response. Am. J. Nephrol. *30*: 287–94.

Chen, Y.R., and Tan, T.H. (1998). Inhibition of the c-Jun N-terminal kinase (JNK) signaling pathway by curcumin. Oncogene *17*: 173–8.

Chen, Z.P., Mitchelhill, K.I., Michell, B.J., Stapleton, D., Rodriguez-Crespo, I., Witters, L.A., et al. (1999). AMP-activated protein kinase phosphorylation of endothelial NO synthase. FEBS Lett. *443*: 285–9.

Chevalier, R.L., Forbes, M.S., and Thornhill, B.A. (2009). Ureteral obstruction as a model of renal interstitial fibrosis and obstructive nephropathy. Kidney Int *75*: 1145–1152.

Clements, M.E., Chaber, C.J., Ledbetter, S.R., and Zuk, A. (2013). Increased cellular senescence and vascular rarefaction exacerbate the progression of kidney fibrosis in aged mice following transient ischemic injury. PLoS One *8*: e70464.

Coca, S.G., Singanamala, S., and Parikh, C.R. (2012). Chronic kidney disease after acute kidney injury: a systematic review and meta-analysis. Kidney Int. *81*: 442–8.

Coca, S.G., Zabetian, A., Ferket, B.S., Zhou, J., Testani, J.M., Garg, A.X., et al. (2015). Evaluation of Short-Term Changes in Serum Creatinine Level as a Meaningful End Point in Randomized Clinical Trials. J. Am. Soc. Nephrol. [EPub ahead of print].

Coldewey, S.M., Rogazzo, M., Collino, M., Patel, N.S.A., and Thiemermann, C. (2013). Inhibition of IκB kinase reduces the multiple organ dysfunction caused by sepsis in the mouse. Dis. Model. Mech. *6*: 1031–42.

Collino, M., Aragno, M., Mastrocola, R., Gallicchio, M., Rosa, A.C., Dianzani, C., et al. (2006). Modulation of the oxidative stress and inflammatory response by PPAR-gamma agonists in the hippocampus of rats exposed to cerebral ischemia/reperfusion. Eur. J. Pharmacol. *530*: 70–80.

Conger, J.D., and Schrier, R.W. (1980). Renal hemodynamics in acute renal failure. Annu Rev Physiol *42*: 603–614.

Costa, M.F.B. da, Libório, A.B., Teles, F., Martins, C. da S., Soares, P.M.G., Meneses, G.C., et al. (2015). Red propolis ameliorates ischemic-reperfusion acute kidney injury. Phytomedicine *22*: 787–95.

Cruthirds, D.L., Novak, L., Akhi, K.M., Sanders, P.W., Thompson, J.A., and MacMillan-Crow, L.A. (2003). Mitochondrial targets of oxidative stress during renal ischemia/reperfusion. Arch Biochem Biophys *412*: 27–33.

Cruz, D.N., Ricci, Z., and Ronco, C. (2009). Clinical review: RIFLE and AKIN--time for reappraisal. Crit Care *13*: 211.

Dave, J.M., and Bayless, K.J. (2014). Vimentin as an integral regulator of cell

adhesion and endothelial sprouting. Microcirculation *21*: 333–44.

Dendooven, A., Ishola, D.A., Nguyen, T.Q., Giezen, D.M. Van der, Kok, R.J., Goldschmeding, R., et al. (2011). Oxidative stress in obstructive nephropathy. Int. J. Exp. Pathol. *92*: 202–10.

Derynck, R., and Zhang, Y.E. (2003). Smad-dependent and Smad-independent pathways in TGF-beta family signalling. Nature *425*: 577–84.

Desai, A., Singh, N., and Raghubir, R. (2010). Neuroprotective potential of the NF-κB inhibitor peptide IKK-NBD in cerebral ischemia-reperfusion injury. Neurochem. Int. *57*: 876–83.

Docherty, N.G., Perez-Barriocanal, F., Balboa, N.E., and Lopez-Novoa, J.M. (2002). Transforming growth factor-beta1 (TGF-beta1): a potential recovery signal in the post-ischemic kidney. Ren Fail *24*: 391–406.

Donnahoo, K.K., Meldrum, D.R., Shenkar, R., Chung, C.S., Abraham, E., and Harken, A.H. (2000). Early renal ischemia, with or without reperfusion, activates NFkappaB and increases TNF-alpha bioactivity in the kidney. J. Urol. *163*: 1328–32.

Duffield, J.S. (2010). Macrophages and immunologic inflammation of the kidney. Semin Nephrol *30*: 234–254.

Eardley, K.S., Zehnder, D., Quinkler, M., Lepenies, J., Bates, R.L., Savage, C.O., et al. (2006). The relationship between albuminuria, MCP-1/CCL2, and interstitial macrophages in chronic kidney disease. Kidney Int. *69*: 1189–97.

Eddy, A.A. (2000). Molecular basis of renal fibrosis. Pediatr Nephrol *15*: 290–301.

Eddy, A.A., López-Guisa, J.M., Okamura, D.M., and Yamaguchi, I. (2012). Investigating mechanisms of chronic kidney disease in mouse models. Pediatr. Nephrol. *27*: 1233–47.

Filippo, K. De, Dudeck, A., Hasenberg, M., Nye, E., Rooijen, N. van, Hartmann, K., et al. (2013). Mast cell and macrophage chemokines CXCL1/CXCL2 control the early stage of neutrophil recruitment during tissue inflammation. Blood *121*: 4930–4937.

Fine, L.G., Orphanides, C., and Norman, J.T. (1998). Progressive renal disease: the chronic hypoxia hypothesis. Kidney Int Suppl *65*: S74–8.

Firth, J.D., Ratcliffe, P.J., Raine, A.E., and Ledingham, J.G. (1988). Endothelin: an

important factor in acute renal failure? Lancet *2*: 1179–1182.

Fontana, J., Fulton, D., Chen, Y., Fairchild, T.A., McCabe, T.J., Fujita, N., et al. (2002). Domain mapping studies reveal that the M domain of hsp90 serves as a molecular scaffold to regulate Akt-dependent phosphorylation of endothelial nitric oxide synthase and NO release. Circ. Res. *90*: 866–73.

Forbes, J.M., Hewitson, T.D., Becker, G.J., and Jones, C.L. (2001). Simultaneous blockade of endothelin A and B receptors in ischemic acute renal failure is detrimental to long-term kidney function. Kidney Int *59*: 1333–1341.

Fujii, T., Kurata, H., Takaoka, M., Muraoka, T., Fujisawa, Y., Shokoji, T., et al. (2003). The role of renal sympathetic nervous system in the pathogenesis of ischemic acute renal failure. Eur J Pharmacol *481*: 241–248.

Fukai, T., and Ushio-Fukai, M. (2011). Superoxide dismutases: role in redox signaling, vascular function, and diseases. Antioxid Redox Signal *15*: 1583–1606.

Gaedeke, J., Noble, N.A., and Border, W.A. (2004). Curcumin blocks multiple sites of the TGF-beta signaling cascade in renal cells. Kidney Int. *66*: 112–20.

Gao, H.-K., Yin, Z., Zhang, R.-Q., Zhang, J., Gao, F., and Wang, H.-C. (2009). GSK-3beta inhibitor modulates TLR2/NF-kappaB signaling following myocardial ischemia-reperfusion. Inflamm. Res. *58*: 377–83.

Gharib, S.A., Johnston, L.K., Huizar, I., Birkland, T.P., Hanson, J., Wang, Y., et al. (2014). MMP28 promotes macrophage polarization toward M2 cells and augments pulmonary fibrosis. J. Leukoc. Biol. *95*: 9–18.

Ghosh, S., May, M.J., and Kopp, E.B. (1998). NF-kappa B and Rel proteins: evolutionarily conserved mediators of immune responses. Annu Rev Immunol *16*: 225–260.

Gilmore, T.D., and Herscovitch, M. (2006). Inhibitors of NF-κB signaling: 785 and counting. Oncogene *25*: 6887–6899.

Go, A.S., Chertow, G.M., Fan, D., McCulloch, C.E., and Hsu, C.Y. (2004). Chronic kidney disease and the risks of death, cardiovascular events, and hospitalization. N Engl J Med *351*: 1296–1305.

Gobe, G.C., Bennett, N.C., West, M., Colditz, P., Brown, L., Vesey, D.A., et al. (2014). Increased progression to kidney fibrosis after erythropoietin is used as a treatment for acute kidney injury. Am. J. Physiol. Renal Physiol. *306*: F681–92.

Goligorsky, M.S., Lieberthal, W., Racusen, L., and Simon, E.E. (1993). Integrin receptors in renal tubular epithelium: new insights into pathophysiology of acute renal failure. Am J Physiol *264*: F1–8.

Gonçalves, J.G., Bragança, A.C. de, Canale, D., Shimizu, M.H.M., Sanches, T.R., Moysés, R.M.A., et al. (2014). Vitamin D deficiency aggravates chronic kidney disease progression after ischemic acute kidney injury. PLoS One *9*: e107228.

Gonzalez-Flecha, B., and Boveris, A. (1995). Mitochondrial sites of hydrogen peroxide production in reperfused rat kidney cortex. Biochim Biophys Acta *1243*: 361–366.

Goor, H. van, Horst, M.L. van der, Fidler, V., and Grond, J. (1992). Glomerular macrophage modulation affects mesangial expansion in the rat after renal ablation. Lab. Invest. *66*: 564–71.

Grande, M.T., and López-Novoa, J.M. (2009). Fibroblast activation and myofibroblast generation in obstructive nephropathy. Nat. Rev. Nephrol. *5*: 319–28.

Gratton, J.P., Fontana, J., O'Connor, D.S., Garcia-Cardena, G., McCabe, T.J., and Sessa, W.C. (2000). Reconstitution of an endothelial nitric-oxide synthase (eNOS), hsp90, and caveolin-1 complex in vitro. Evidence that hsp90 facilitates calmodulin stimulated displacement of eNOS from caveolin-1. J. Biol. Chem. *275*: 22268–72.

Gröne, H.J., Weber, K., Gröne, E., Helmchen, U., and Osborn, M. (1987). Coexpression of keratin and vimentin in damaged and regenerating tubular epithelia of the kidney. Am. J. Pathol. *129*: 1–8.

Guijarro, C., and Egido, J. (2001). Transcription factor-kappa B (NF-kappa B) and renal disease. Kidney Int. *59*: 415–24.

Hamer, R.A., and Nahas, A.M. El (2006). The burden of chronic kidney disease. BMJ *332*: 563–4.

Herrmann, O., Baumann, B., Lorenzi, R. de, Muhammad, S., Zhang, W., Kleesiek, J., et al. (2005). IKK mediates ischemia-induced neuronal death. Nat. Med. *11*: 1322–9.

Heung, M., and Chawla, L.S. (2012). Predicting progression to chronic kidney disease after recovery from acute kidney injury. Curr. Opin. Nephrol. Hypertens. *21*: 628–34.

Hsu, C.Y. (2012). Yes, AKI truly leads to CKD. J Am Soc Nephrol *23*: 967–969.

Huang, X.R., Chung, A.C., Wang, X.J., Lai, K.N., and Lan, H.Y. (2008). Mice overexpressing latent TGF-beta1 are protected against renal fibrosis in obstructive kidney disease. Am J Physiol Ren. Physiol *295*: F118–27.

Inayama, M., Nishioka, Y., Azuma, M., Muto, S., Aono, Y., Makino, H., et al. (2006). A novel IkappaB kinase-beta inhibitor ameliorates bleomycin-induced pulmonary fibrosis in mice. Am. J. Respir. Crit. Care Med. *173*: 1016–22.

Isaac, J., Togel, F.E., and Westenfelder, C. (2007). Extent of glomerular tubularization is an indicator of the severity of experimental acute kidney injury in mice. Nephron Exp Nephrol *105*: e33–40.

Ishani, A., Nelson, D., Clothier, B., Schult, T., Nugent, S., Greer, N., et al. (2011). The magnitude of acute serum creatinine increase after cardiac surgery and the risk of chronic kidney disease, progression of kidney disease, and death. Arch. Intern. Med. *171*: 226–33.

Ishani, A., Xue, J.L., Himmelfarb, J., Eggers, P.W., Kimmel, P.L., Molitoris, B.A., et al. (2009). Acute kidney injury increases risk of ESRD among elderly. J Am Soc Nephrol *20*: 223–228.

Izmailova, E.S., Paz, N., Alencar, H., Chun, M., Schopf, L., Hepperle, M., et al. (2007). Use of molecular imaging to quantify response to IKK-2 inhibitor treatment in murine arthritis. Arthritis Rheum. *56*: 117–28.

Johnson, T.S., Skill, N.J., Nahas, A.M. El, Oldroyd, S.D., Thomas, G.L., Douthwaite, J.A., et al. (1999). Transglutaminase transcription and antigen translocation in experimental renal scarring. J Am Soc Nephrol *10*: 2146–2157.

Jope, R.S., and Johnson, G.V.W. (2004). The glamour and gloom of glycogen synthase kinase-3. Trends Biochem. Sci. *29*: 95–102.

Kaissling, B., and Hir, M. Le (2008). The renal cortical interstitium: morphological and functional aspects. Histochem Cell Biol *130*: 247–262.

Kalluri, R., and Neilson, E.G. (2003). Epithelial-mesenchymal transition and its implications for fibrosis. J. Clin. Invest. *112*: 1776–1784.

Karin, M., and Ben-Neriah, Y. (2000). Phosphorylation meets ubiquitination: the control of NF-[kappa]B activity. Annu Rev Immunol *18*: 621–663.

K/DOQI clinical practice guidelines for chronic kidney disease: evaluation, classification and stratification. (2002) Am J Kidney Dis *39*: S1–266.

Keir, I., and Kellum, J.A. (2015). Acute kidney injury in severe sepsis: pathophysiology, diagnosis, and treatment recommendations. J Vet Emerg Crit Care (San Antonio) *25*: 200–209.

Kellerman, P.S., and Bogusky, R.T. (1992). Microfilament disruption occurs very early in ischemic proximal tubule cell injury. Kidney Int *42*: 896–902.

Kelly, K.J., Williams Jr., W.W., Colvin, R.B., Meehan, S.M., Springer, T.A., Gutierrez-Ramos, J.C., et al. (1996). Intercellular adhesion molecule-1-deficient mice are protected against ischemic renal injury. J Clin Invest *97*: 1056–1063.

Khanna, A., and McCullough, P.A. (2003). Malignant hypertension presenting as hemolysis, thrombocytopenia, and renal failure. Rev Cardiovasc Med *4*: 255–259.

Khosla, N., Soroko, S.B., Chertow, G.M., Himmelfarb, J., Ikizler, T.A., Paganini, E., et al. (2009). Preexisting chronic kidney disease: a potential for improved outcomes from acute kidney injury. Clin J Am Soc Nephrol *4*: 1914–1919.

Kim, M.-G., Kim, S.C., Ko, Y.S., Lee, H.Y., Jo, S.-K., and Cho, W. (2015). The Role of M2 Macrophages in the Progression of Chronic Kidney Disease following Acute Kidney Injury. PLoS One *10*: e0143961.

Kinsey, G.R. (2014). Macrophage dynamics in AKI to CKD progression. J Am Soc Nephrol *25*: 209–211.

Ko, G.J., Boo, C.S., Jo, S.K., Cho, W.Y., and Kim, H.K. (2008). Macrophages contribute to the development of renal fibrosis following ischaemia/reperfusion-induced acute kidney injury. Nephrol Dial Transpl. *23*: 842–852.

Kuwabara, N., Tamada, S., Iwai, T., Teramoto, K., Kaneda, N., Yukimura, T., et al. (2006). Attenuation of renal fibrosis by curcumin in rat obstructive nephropathy. Urology *67*: 440–6.

Lan, H.Y. (2003). Tubular epithelial-myofibroblast transdifferentiation mechanisms in proximal tubule cells. Curr. Opin. Nephrol. Hypertens. *12*: 25–9.

LeBleu, V.S., Taduri, G., O'Connell, J., Teng, Y., Cooke, V.G., Woda, C., et al. (2013). Origin and function of myofibroblasts in kidney fibrosis. Nat. Med. *19*: 1047–53.

Lee, S., Huen, S., Nishio, H., Nishio, S., Lee, H.K., Choi, B.-S., et al. (2011). Distinct macrophage phenotypes contribute to kidney injury and repair. J. Am. Soc. Nephrol. *22*: 317–26.

Lee, S.B., and Kalluri, R. (2010). Mechanistic connection between inflammation and fibrosis. Kidney Int. Suppl. S22–6.

Levey, A.S., Eckardt, K.U., Tsukamoto, Y., Levin, A., Coresh, J., Rossert, J., et al. (2005). Definition and classification of chronic kidney disease: a position statement from Kidney Disease: Improving Global Outcomes (KDIGO). Kidney Int *67*: 2089–2100.

Li, L., Huang, L., Sung, S.S., Vergis, A.L., Rosin, D.L., Rose Jr., C.E., et al. (2008). The chemokine receptors CCR2 and CX3CR1 mediate monocyte/macrophage trafficking in kidney ischemia-reperfusion injury. Kidney Int *74*: 1526–1537.

Lieberthal, W., Koh, J.S., and Levine, J.S. (1998). Necrosis and apoptosis in acute renal failure. Semin Nephrol *18*: 505–518.

Lin, L.-Y., Lin, C.-Y., Ho, F.-M., and Liau, C.S. (2005). Up-regulation of the association between heat shock protein 90 and endothelial nitric oxide synthase prevents high glucose-induced apoptosis in human endothelial cells. J. Cell. Biochem. *94*: 194–201.

Liu, Y. (2006). Renal fibrosis: new insights into the pathogenesis and therapeutics. Kidney Int *69*: 213–217.

Liu, Y. (2011). Cellular and molecular mechanisms of renal fibrosis. Nat Rev Nephrol *7*: 684–696.

Lloyd, C.M., Minto, A.W., Dorf, M.E., Proudfoot, A., Wells, T.N., Salant, D.J., et al. (1997). RANTES and monocyte chemoattractant protein-1 (MCP-1) play an important role in the inflammatory phase of crescentic nephritis, but only MCP-1 is involved in crescent formation and interstitial fibrosis. J. Exp. Med. *185*: 1371–80.

López-Franco, O., Suzuki, Y., Sanjuán, G., Blanco, J., Hernández-Vargas, P., Yo, Y., et al. (2002). Nuclear factor-kappa B inhibitors as potential novel anti-inflammatory agents for the treatment of immune glomerulonephritis. Am. J. Pathol. *161*: 1497–505.

López-Hernández, F.J., and López-Novoa, J.M. (2012). Role of TGF-β in chronic kidney disease: an integration of tubular, glomerular and vascular effects. Cell Tissue Res. *347*: 141–54.

Luedde, T., Assmus, U., Wüstefeld, T., Meyer zu Vilsendorf, A., Roskams, T., Schmidt-Supprian, M., et al. (2005). Deletion of IKK2 in hepatocytes does not sensitize these cells to TNF-induced apoptosis but protects from

ischemia/reperfusion injury. J. Clin. Invest. *115*: 849–59.

Luque Contreras, D., Vargas Robles, H., Romo, E., Rios, A., and Escalante, B. (2006). The role of nitric oxide in the post-ischemic revascularization process. Pharmacol. Ther. *112*: 553–63.

Macedo, E., and Mehta, R.L. (2010). Early vs late start of dialysis: it's all about timing. Crit. Care *14*: 112.

Mack, M., and Yanagita, M. (2015). Origin of myofibroblasts and cellular events triggering fibrosis. Kidney Int. *87*: 297–307.

Maier, H.J., Schips, T.G., Wietelmann, A., Krüger, M., Brunner, C., Sauter, M., et al. (2012). Cardiomyocyte-specific IκB kinase (IKK)/NF-κB activation induces reversible inflammatory cardiomyopathy and heart failure. Proc. Natl. Acad. Sci. U. S. A. *109*: 11794–9.

Marcussen, N. (2000). Tubulointerstitial damage leads to atubular glomeruli: significance and possible role in progression. Nephrol Dial Transpl. *15 Suppl 6*: 74–75.

Meguid El Nahas, A., and Bello, A.K. (2005). Chronic kidney disease: the global challenge. Lancet *365*: 331–340.

Mehta, R.L., Kellum, J.A., Shah, S. V, Molitoris, B.A., Ronco, C., Warnock, D.G., et al. (2007). Acute Kidney Injury Network: report of an initiative to improve outcomes in acute kidney injury. Crit Care *11*: R31.

Meng, X.-M., Tang, P.M.-K., Li, J., and Lan, H.Y. (2015). TGF-β/Smad signaling in renal fibrosis. Front. Physiol. *6*: 82.

Mia, M.M., and Bank, R.A. (2015). The IκB kinase inhibitor ACHP strongly attenuates TGFβ1-induced myofibroblast formation and collagen synthesis. J. Cell. Mol. Med. *19*: 2780–92.

Miyajima, A., Chen, J., Lawrence, C., Ledbetter, S., Soslow, R.A., Stern, J., et al. (2000). Antibody to transforming growth factor-beta ameliorates tubular apoptosis in unilateral ureteral obstruction. Kidney Int. *58*: 2301–13.

Mohan, S., Konopinski, R., Yan, B., Centonze, V.E., and Natarajan, M. (2009). High glucose-induced IKK-Hsp-90 interaction contributes to endothelial dysfunction. Am. J. Physiol. Cell Physiol. *296*: C182–92.

Molitoris, B.A., and Marrs, J. (1999). The role of cell adhesion molecules in

ischemic acute renal failure. Am J Med *106*: 583–592.

Moss, N.C., Stansfield, W.E., Willis, M.S., Tang, R.-H., and Selzman, C.H. (2007). IKKbeta inhibition attenuates myocardial injury and dysfunction following acute ischemia-reperfusion injury. Am. J. Physiol. Heart Circ. Physiol. *293*: H2248–53.

Moynagh, P.N. (2005). The NF-kappaB pathway. J Cell Sci *118*: 4589–4592.

Mudaliar, H., Pollock, C., Komala, M.G., Chadban, S., Wu, H., and Panchapakesan, U. (2013). The role of Toll-like receptor proteins (TLR) 2 and 4 in mediating inflammation in proximal tubules. Am. J. Physiol. Renal Physiol. *305*: F143–54.

Nakamura, M., Seki, G., Iwadoh, K., Nakajima, I., Fuchinoue, S., Fujita, T., et al. (2012). Acute kidney injury as defined by the RIFLE criteria is a risk factor for kidney transplant graft failure. Clin Transpl. *26*: 520–528.

Nath, K.A., and Norby, S.M. (2000). Reactive oxygen species and acute renal failure. Am J Med *109*: 665–678.

Navar, L.G., and Mitchell, K.D. (1990). Contribution of the tubuloglomerular feedback mechanism to sodium homeostasis and interaction with the renin-angiotensin system. Acta Physiol Scand Suppl *591*: 66–73.

Nehus, E.J., and Devarajan, P. (2012). Acute kidney injury: AKI in kidney transplant recipients--here to stay. Nat. Rev. Nephrol. *8*: 198–9.

Nelson, P.J., and Cantley, L. (2010). GSK3beta plays dirty in acute kidney injury. J. Am. Soc. Nephrol. *21*: 199–200.

NHS Choices. ‘One million people’ with ‘undiagnosed’ chronic kidney disease - Health news. NHS.

Noiri, E., Nakao, A., Uchida, K., Tsukahara, H., Ohno, M., Fujita, T., et al. (2001). Oxidative and nitrosative stress in acute renal ischemia. Am J Physiol Ren. Physiol *281*: F948–57.

Nowling, T.K., and Gilkeson, G.S. (2011). Mechanisms of tissue injury in lupus nephritis. Arthritis Res Ther *13*: 250.

Ogawa, H., Azuma, M., Muto, S., Nishioka, Y., Honjo, A., Tezuka, T., et al. (2011). IκB kinase β inhibitor IMD-0354 suppresses airway remodelling in a Dermatophagoides pteronyssinus-sensitized mouse model of chronic asthma. Clin. Exp. Allergy *41*: 104–15.

Oh, D.J., Dursun, B., He, Z., Lu, L., Hoke, T.S., Ljubanovic, D., et al. (2008). Fractalkine receptor (CX3CR1) inhibition is protective against ischemic acute renal failure in mice. Am J Physiol Ren. Physiol *294*: F264–71.

Okusa, M.D., Chertow, G.M., Portilla, D., and Acute Kidney Injury Advisory Group of the American Society of, N. (2009). The nexus of acute kidney injury, chronic kidney disease, and World Kidney Day 2009. Clin J Am Soc Nephrol *4*: 520–522.

Ono, M., Sakao, Y., Tsuji, T., Ohashi, N., Yasuda, H., Nishiyama, A., et al. (2015). Role of intrarenal (pro)renin receptor in ischemic acute kidney injury in rats. Clin. Exp. Nephrol. *19*: 185–96.

Padanilam, B.J. (2003). Cell death induced by acute renal injury: a perspective on the contributions of apoptosis and necrosis. Am J Physiol Ren. Physiol *284*: F608–27.

Palm, F., and Nordquist, L. (2011). Renal tubulointerstitial hypoxia: cause and consequence of kidney dysfunction. Clin. Exp. Pharmacol. Physiol. *38*: 474–80.

Pan, B., Liu, G., Jiang, Z., and Zheng, D. (2015). Regulation of renal fibrosis by macrophage polarization. Cell. Physiol. Biochem. *35*: 1062–9.

Patel, N.S.A., Kerr-Peterson, H.L., Brines, M., Collino, M., Rogazzo, M., Fantozzi, R., et al. (2012). Delayed administration of pyroglutamate helix B surface peptide (pHBSP), a novel nonerythropoietic analog of erythropoietin, attenuates acute kidney injury. Mol. Med. *18*: 719–27.

Perazella, M.A., and Markowitz, G.S. (2010). Drug-induced acute interstitial nephritis. Nat Rev Nephrol *6*: 461–470.

Piera-Velazquez, S., Li, Z., and Jimenez, S.A. (2011). Role of endothelial-mesenchymal transition (EndoMT) in the pathogenesis of fibrotic disorders. Am. J. Pathol. *179*: 1074–80.

Polichnowski, A.J., Lan, R., Geng, H., Griffin, K.A., Venkatachalam, M.A., and Bidani, A.K. (2014). Severe renal mass reduction impairs recovery and promotes fibrosis after AKI. J. Am. Soc. Nephrol. *25*: 1496–507.

Rabb, H., O'Meara, Y.M., Maderna, P., Coleman, P., and Brady, H.R. (1997). Leukocytes, cell adhesion molecules and ischemic acute renal failure. Kidney Int *51*: 1463–1468.

Raman, C.S., Li, H., Martásek, P., Král, V., Masters, B.S., and Poulos, T.L. (1998). Crystal structure of constitutive endothelial nitric oxide synthase: a paradigm for pterin function involving a novel metal center. Cell *95*: 939–50.

Rang, H., Dale, M., Ritter, J., and Flower, R. (2007). Rang and Dale's Pharmacology (Churchill Livingstone).

Rao, K. V, and Kjellstrand, C.M. (1983). Post transplant acute renal failure: a review. Clin. Exp. Dial. Apheresis *7*: 127–43.

Rodriguez-Moran, M., Gonzalez-Gonzalez, G., Bermudez-Barba, M. V, Medina de la Garza, C.E., Tamez-Perez, H.E., Martinez-Martinez, F.J., et al. (2006). Effects of pentoxifylline on the urinary protein excretion profile of type 2 diabetic patients with microproteinuria: a double-blind, placebo-controlled randomized trial. Clin Nephrol *66*: 3–10.

Rogers, N.M., Stephenson, M.D., Kitching, A.R., Horowitz, J.D., and Coates, P.T.H. (2012). Amelioration of renal ischaemia-reperfusion injury by liposomal delivery of curcumin to renal tubular epithelial and antigen-presenting cells. Br. J. Pharmacol. *166*: 194–209.

Rudolph, D., Yeh, W.C., Wakeham, A., Rudolph, B., Nallainathan, D., Potter, J., et al. (2000). Severe liver degeneration and lack of NF-kappaB activation in NEMO/IKKgamma-deficient mice. Genes Dev. *14*: 854–62.

Rydén, L., Sartipy, U., Evans, M., and Holzmann, M.J. (2014). Acute kidney injury after coronary artery bypass grafting and long-term risk of end-stage renal disease. Circulation *130*: 2005–11.

Safran, M., Kim, W.Y., O'Connell, F., Flippin, L., Gunzler, V., Horner, J.W., et al. (2006). Mouse model for noninvasive imaging of HIF prolyl hydroxylase activity: assessment of an oral agent that stimulates erythropoietin production. Proc Natl Acad Sci U S A *103*: 105–110.

Sakairi, T., Hiromura, K., Yamashita, S., Takeuchi, S., Tomioka, M., Ideura, H., et al. (2007). Nestin expression in the kidney with an obstructed ureter. Kidney Int *72*: 307–318.

Sanz, A.B., Sanchez-Nino, M.D., Ramos, A.M., Moreno, J.A., Santamaria, B., Ruiz-Ortega, M., et al. (2010). NF-kappaB in renal inflammation. J Am Soc Nephrol *21*: 1254–1262.

Sanz, A.B., Santamaria, B., Ruiz-Ortega, M., Egido, J., and Ortiz, A. (2008). Mechanisms of renal apoptosis in health and disease. J Am Soc Nephrol *19*: 1634–

1642.

Sato, M., Muragaki, Y., Saika, S., Roberts, A.B., and Ooshima, A. (2003). Targeted disruption of TGF-beta1/Smad3 signaling protects against renal tubulointerstitial fibrosis induced by unilateral ureteral obstruction. J. Clin. Invest. *112*: 1486–94.

Schmid, J.A., and Birbach, A. (2008). IkappaB kinase beta (IKKbeta/IKK2/IKBKB)--a key molecule in signaling to the transcription factor NF-kappaB. Cytokine Growth Factor Rev *19*: 157–165.

Schmidt, T.S., and Alp, N.J. (2007). Mechanisms for the role of tetrahydrobiopterin in endothelial function and vascular disease. Clin. Sci. (Lond). *113*: 47–63.

Schnaper, H.W., Hayashida, T., Hubchak, S.C., and Poncelet, A.-C. (2003). TGF-beta signal transduction and mesangial cell fibrogenesis. Am. J. Physiol. Renal Physiol. *284*: F243–52.

Schumer, M., Colombel, M.C., Sawczuk, I.S., Gobe, G., Connor, J., O'Toole, K.M., et al. (1992). Morphologic, biochemical, and molecular evidence of apoptosis during the reperfusion phase after brief periods of renal ischemia. Am J Pathol *140*: 831–838.

Senftleben, U., Cao, Y., Xiao, G., Greten, F.R., Krahn, G., Bonizzi, G., et al. (2001). Activation by IKKalpha of a second, evolutionary conserved, NF-kappa B signaling pathway. Science (80-.). *293*: 1495–1499.

Sharfuddin, A.A., and Molitoris, B.A. (2011). Pathophysiology of ischemic acute kidney injury. Nat Rev Nephrol *7*: 189–200.

Sharples, E.J. (2007). Acute kidney injury: stimulation of repair. Curr Opin Crit Care *13*: 652–655.

Shen, B., Liu, X., Fan, Y., and Qiu, J. (2014a). Macrophages regulate renal fibrosis through modulating TGFbeta superfamily signaling. Inflammation *37*: 2076–2084.

Shen, H., Sheng, L., Chen, Z., Jiang, L., Su, H., Yin, L., et al. (2014b). Mouse hepatocyte overexpression of NF-kappaB-inducing kinase (NIK) triggers fatal macrophage-dependent liver injury and fibrosis. Hepatology *60*: 2065–2076.

Shi, M., Flores, B., Gillings, N., Bian, A., Cho, H.J., Yan, S., et al. (2015). αKlotho Mitigates Progression of AKI to CKD through Activation of Autophagy. J. Am. Soc. Nephrol. [EPub ahead of print]

Shiao, C.-C., Wu, V.-C., Li, W.-Y., Lin, Y.-F., Hu, F.-C., Young, G.-H., et al.

(2009). Late initiation of renal replacement therapy is associated with worse outcomes in acute kidney injury after major abdominal surgery. Crit. Care *13*: R171.

Shoskes, D.A., Xie, Y., and Gonzalez-Cadavid, N.F. (1997). Nitric oxide synthase activity in renal ischemia-reperfusion injury in the rat: implications for renal transplantation. Transplantation *63*: 495–500.

Sil, A.K., Maeda, S., Sano, Y., Roop, D.R., and Karin, M. (2004). IkappaB kinase-alpha acts in the epidermis to control skeletal and craniofacial morphogenesis. Nature *428*: 660–4.

Singh, P., and Okusa, M.D. (2011). The role of tubuloglomerular feedback in the pathogenesis of acute kidney injury. Contrib Nephrol *174*: 12–21.

Singh, S., and Aggarwal, B.B. (1995). Activation of transcription factor NF-kappa B is suppressed by curcumin (diferuloylmethane) [corrected]. J. Biol. Chem. *270*: 24995–5000.

Singh, S.P., Tao, S., Fields, T.A., Webb, S., Harris, R.C., and Rao, R. (2015). Glycogen synthase kinase-3 inhibition attenuates fibroblast activation and development of fibrosis following renal ischemia-reperfusion in mice. Dis. Model. Mech. *8*: 931–40.

Sivarajah, A., Chatterjee, P.K., Patel N.S., Todorovic, Z., Hattori, Y., Brown, P.A., et al. (2003). Agonists or peroxisome-proliferator activated receptor-gamma reduce renal ischemia/reperfusion injury. Am. J. Nephrol. *23*: 267-276

Skrypnyk, N.I., Harris, R.C., and Caestecker, M.P. de (2013). Ischemia-reperfusion model of acute kidney injury and post injury fibrosis in mice. J. Vis. Exp. *78*

Sordi, R., Chiazza, F., Johnson, F.L., Patel, N.S.A., Brohi, K., Collino, M., et al. (2015). Inhibition of IκB Kinase Attenuates the Organ Injury and Dysfunction Associated with Hemorrhagic Shock. Mol. Med. *21*: 563–75.

Steenkamp, R., Castledine, C., Feest, T., and Fogarty, D. (2011). UK Renal Registry 13th Annual Report (December 2010): Chapter 2: UK RRT prevalence in 2009: national and centre-specific analyses. Nephron Clin Pr. *119 Suppl* : c27–52.

Sun, X., Chen, E., Dong, R., Chen, W., and Hu, Y. (2015). Nuclear factor (NF)-κB p65 regulates differentiation of human and mouse lung fibroblasts mediated by TGF-β. Life Sci. *122*: 8–14.

Sutariya, B., Jhonsa, D., and Saraf, M.N. (2016). TGF-β: the connecting link

between nephropathy and fibrosis. Immunopharmacol. Immunotoxicol. *38*: 39–49.

Sutton, T.A., Fisher, C.J., and Molitoris, B.A. (2002). Microvascular endothelial injury and dysfunction during ischemic acute renal failure. Kidney Int *62*: 1539–1549.

Tanaka, M., Fuentes, M.E., Yamaguchi, K., Durnin, M.H., Dalrymple, S.A., Hardy, K.L., et al. (1999). Embryonic lethality, liver degeneration, and impaired NF-kappa B activation in IKK-beta-deficient mice. Immunity *10*: 421–9.

Tapmeier, T.T., Brown, K.L., Tang, Z., Sacks, S.H., Sheerin, N.S., and Wong, W. (2008). Reimplantation of the ureter after unilateral ureteral obstruction provides a model that allows functional evaluation. Kidney Int. *73*: 885–9.

Tashiro, K., Tamada, S., Kuwabara, N., Komiya, T., Takekida, K., Asai, T., et al. (2003). Attenuation of renal fibrosis by proteasome inhibition in rat obstructive nephropathy: possible role of nuclear factor kappaB. Int. J. Mol. Med. *12*: 587–92.

Thakar, C. V, Christianson, A., Himmelfarb, J., and Leonard, A.C. (2011). Acute kidney injury episodes and chronic kidney disease risk in diabetes mellitus. Clin J Am Soc Nephrol *6*: 2567–2572.

Thiele, R.H., Isbell, J.M., and Rosner, M.H. (2015). AKI associated with cardiac surgery. Clin J Am Soc Nephrol *10*: 500–514.

Thornton, M.A., Winn, R., Alpers, C.E., and Zager, R.A. (1989). An evaluation of the neutrophil as a mediator of in vivo renal ischemic-reperfusion injury. Am J Pathol *135*: 509–515.

Trachtman, H., Fervenza, F.C., Gipson, D.S., Heering, P., Jayne, D.R., Peters, H., et al. (2011). A phase 1, single-dose study of fresolimumab, an anti-TGF-beta antibody, in treatment-resistant primary focal segmental glomerulosclerosis. Kidney Int *79*: 1236–1243.

Traynor, J., Mactier, R., Geddes, C.C., and Fox, J.G. (2006). How to measure renal function in clinical practice. BMJ *333*: 733–737.

Tsukamoto, T., and Nigam, S.K. (1997). Tight junction proteins form large complexes and associate with the cytoskeleton in an ATP depletion model for reversible junction assembly. J Biol Chem *272*: 16133–16139.

Turner, J.M., Bauer, C., Abramowitz, M.K., Melamed, M.L., and Hostetter, T.H. (2012). Treatment of chronic kidney disease. Kidney Int *81*: 351–362.

Uchino, S. (2006). The epidemiology of acute renal failure in the world. Curr Opin Crit Care *12*: 538–543.

Vaziri, N.D., Liu, S.-M., Lau, W.L., Khazaeli, M., Nazertehrani, S., Farzaneh, S.H., et al. (2014). High amylose resistant starch diet ameliorates oxidative stress, inflammation, and progression of chronic kidney disease. PLoS One *9*: e114881.

Venkatachalam, M.A., Bernard, D.B., Donohoe, J.F., and Levinsky, N.G. (1978). Ischemic damage and repair in the rat proximal tubule: differences among the S1, S2, and S3 segments. Kidney Int *14*: 31–49.

Venkatachalam, M.A., Griffin, K.A., Lan, R., Geng, H., Saikumar, P., and Bidani, A.K. (2010). Acute kidney injury: a springboard for progression in chronic kidney disease. Am J Physiol Ren. Physiol *298*: F1078–94.

Venkatachalam, M.A., Weinberg, J.M., Kriz, W., and Bidani, A.K. (2015). Failed Tubule Recovery, AKI-CKD Transition, and Kidney Disease Progression. J. Am. Soc. Nephrol. *26*: 1765–76.

Waelchli, R., Bollbuck, B., Bruns, C., Buhl, T., Eder, J., Feifel, R., et al. (2006). Design and preparation of 2-benzamido-pyrimidines as inhibitors of IKK. Bioorg. Med. Chem. Lett. *16*: 108–12.

Wan, X., Fan, L., Hu, B., Yang, J., Li, X., Chen, X., et al. (2011a). Small interfering RNA targeting IKKbeta prevents renal ischemia-reperfusion injury in rats. Am J Physiol Ren. Physiol *300*: F857–63.

Wan, X., Yang, J., Xing, L., Fan, L., Hu, B., Chen, X., et al. (2011b). Inhibition of IκB Kinase β attenuates hypoxia-induced inflammatory mediators in rat renal tubular cells. Transplant. Proc. *43*: 1503–10.

Wang, Y., Chang, J., Yao, B., Niu, A., Kelly, E., Breeggemann, M.C., et al. (2015). Proximal tubule-derived colony stimulating factor-1 mediates polarization of renal macrophages and dendritic cells, and recovery in acute kidney injury. Kidney Int. *88*: 1274–1282.

Wang, Y., Wang, Y.P., Zheng, G., Lee, V.W.S., Ouyang, L., Chang, D.H.H., et al. (2007). Ex vivo programmed macrophages ameliorate experimental chronic inflammatory renal disease. Kidney Int. *72*: 290–9.

Wei, J., Shi, M., Wu, W.Q., Xu, H., Wang, T., Wang, N., et al. (2011). IkappaB kinase-beta inhibitor attenuates hepatic fibrosis in mice. World J Gastroenterol *17*: 5203–5213.

Weight, S.C., Bell, P.R., and Nicholson, M.L. (1996). Renal ischaemia--reperfusion injury. Br J Surg *83*: 162–170.

Wenzel, R.R., Littke, T., Kuranoff, S., Jurgens, C., Bruck, H., Ritz, E., et al. (2009). Avosentan reduces albumin excretion in diabetics with macroalbuminuria. J Am Soc Nephrol *20*: 655–664.

Whitehouse, T., Stotz, M., Taylor, V., Stidwill, R., and Singer, M. (2006). Tissue oxygen and hemodynamics in renal medulla, cortex, and corticomedullary junction during hemorrhage-reperfusion. Am J Physiol Ren. Physiol *291*: F647–53.

Widmaier, E., Raff, H., and Strang, K. (2007). Vander's Human Physiology (McGraw-Hill).

Wiegele, G., Brandis, M., and Zimmerhackl, L.B. (1998). Apoptosis and necrosis during ischaemia in renal tubular cells (LLC-PK1 and MDCK). Nephrol Dial Transpl. *13*: 1158–1167.

Wilson, H.M., Chettibi, S., Jobin, C., Walbaum, D., Rees, A.J., and Kluth, D.C. (2005). Inhibition of macrophage nuclear factor-kappaB leads to a dominant anti-inflammatory phenotype that attenuates glomerular inflammation in vivo. Am. J. Pathol. *167*: 27–37.

Winearls, C.G., and Glassock, R.J. (2011). Classification of chronic kidney disease in the elderly: pitfalls and errors. Nephron Clin Pr. *119 Suppl* : c2–4.

Wing, M.R., Ramezani, A., Gill, H.S., Devaney, J.M., and Raj, D.S. (2013). Epigenetics of progression of chronic kidney disease: fact or fantasy? Semin Nephrol *33*: 363–374.

Wu, C.-F., Chiang, W.-C., Lai, C.-F., Chang, F.-C., Chen, Y.-T., Chou, Y.-H., et al. (2013). Transforming growth factor β-1 stimulates profibrotic epithelial signaling to activate pericyte-myofibroblast transition in obstructive kidney fibrosis. Am. J. Pathol. *182*: 118–31.

Wu, H., Chen, G., Wyburn, K.R., Yin, J., Bertolino, P., Eris, J.M., et al. (2007). TLR4 activation mediates kidney ischemia/reperfusion injury. J Clin Invest *117*: 2847–2859.

Wynn, T.A. (2008). Cellular and molecular mechanisms of fibrosis. J. Pathol. *214*: 199–210.

Yamanobe, T., Okada, F., Iuchi, Y., Onuma, K., Tomita, Y., and Fujii, J. (2007). Deterioration of ischemia/reperfusion-induced acute renal failure in SOD1-deficient

mice. Free Radic Res *41*: 200–207.

Yang, L., Besschetnova, T.Y., Brooks, C.R., Shah, J. V, and Bonventre, J. V (2010). Epithelial cell cycle arrest in G2/M mediates kidney fibrosis after injury. Nat Med *16*: 535–43, 1p following 143.

Yin, M., Wheeler, M.D., Connor, H.D., Zhong, Z., Bunzendahl, H., Dikalova, A., et al. (2001). Cu/Zn-superoxide dismutase gene attenuates ischemia-reperfusion injury in the rat kidney. J Am Soc Nephrol *12*: 2691–2700.

Yoshida, H., Murachi, T., and Tsukahara, I. (1984). Degradation of actin and vimentin by calpain II, a Ca2+-dependent cysteine proteinase, in bovine lens. FEBS Lett. *170*: 259–62.

Young, B., and Heath, J. (2000). Wheater's Functional Histology: A Text and Colour Atlas (Churchill Livingstone). *5th edition*: 202-204

Ysebaert, D.K., Greef, K.E. De, Vercauteren, S.R., Ghielli, M., Verpooten, G.A., Eyskens, E.J., et al. (2000). Identification and kinetics of leukocytes after severe ischaemia/reperfusion renal injury. Nephrol Dial Transpl. *15*: 1562–1574.

Zager, R.A., and Johnson, A.C. (2009). Renal ischemia-reperfusion injury upregulates histone-modifying enzyme systems and alters histone expression at proinflammatory/profibrotic genes. Am J Physiol Ren. Physiol *296*: F1032–41.

Zhang, F., Tsai, S., Kato, K., Yamanouchi, D., Wang, C., Rafii, S., et al. (2009). Transforming growth factor-beta promotes recruitment of bone marrow cells and bone marrow-derived mesenchymal stem cells through stimulation of MCP-1 production in vascular smooth muscle cells. J. Biol. Chem. *284*: 17564–74.

Zhang, J., Li, J., Wang, L., Han, M., Xiao, F., Lan, X., et al. (2014). Glucocorticoid receptor agonist dexamethasone attenuates renal ischemia/reperfusion injury by up-regulating eNOS/iNOS. J. Huazhong Univ. Sci. Technolog. Med. Sci. *34*: 516–20.

Zhou, Y., Zhang, X., Tan, M., Zheng, R., and Zhao, L. (2014). The effect of NF-κB antisense oligonucleotide on transdifferentiation of fibroblast in lung tissue of mice injured by bleomycin. Mol. Biol. Rep. *41*: 4043–51.

Zorov, D.B., Juhaszova, M., and Sollott, S.J. (2014). Mitochondrial reactive oxygen species (ROS) and ROS-induced ROS release. Physiol Rev *94*: 909–950.